INTERIM REPORT

O.R.A. 155-421

Contract # 702930013

A HYDROLOGIC STUDY OF THE SULPHUR ARTESIAN GROUNDWATER SYSTEM AND ASSOCIATED WATERS AT CHICKASAW NATIONAL RECREATIONAL AREA, SULPHUR, OKLAHOMA

Prepared By:

Jim F. Harp, Ph.D., Professor
Joakim G. Laguros, Ph.D., Professor
Stephen S. McLin, Ph.D., Assoc. Professor
Leonard B. West, Ph.D., Assoc. Professor
Charles John Barthel, Jr.

Civil Engineering and Environmental Science Dept.
202 West Boyd, Room 334, Carson Engineering Center
The University of Oklahoma, Norman, Oklahoma 73019

Submitted To:

The United States Department of the Interior
National Park Service

Submitted By:

The Bureau of Water Resources Research,
Oklahoma Research Administration
The University of Oklahoma
Norman, Oklahoma

June 1985

TABLE OF CONTENTS

TABLE OF CONTENTS (continued)

TABLE OF CONTENTS (continued)

LIST OF TABLES

LIST OF TABLES (continued)

LIST OF TABLES (continued)

LIST OF FIGURES

LIST OF FIGURES (continued)

LIST OF FIGURES (continued)

LIST OF FIGURES (continued)

LIST OF PLATES

ABSTRACT

Increasing cessation of fresh water artesian spring flow in the Travertine District, Chickasaw National Recreation Area, prompted this investigation to address the parameters that define subsurface flow in the Sulphur, Oklahoma area.

The Sulphur Fault is responsible for the origin of the fresh water artesian springs, Buffalo and Antelope, and controls groundwater movement from the recharge area downdip to the springs. Buffalo and Antelope Springs derive their water from the confined Arbuckle Aquifer. The intensely fractured dolomites of the Arbuckle group outcrop east of Sulphur, constituting the recharge area of approximately 5 mi^2 for the fresh water springs.

Observation wells and spring hydrograph analysis help to establish a relationship between discharge, piezometric elevation of the confined Arbuckle Aquifer, and seasonal precipitation events. The long-term trend of the hydrographs reveal that the piezometric elevation of the Sulphur artesian basin is declining at a rate of .65ft/year. If this trend continues, permanent cessation of spring flows will occur in about 40 years.

Statistical and spring hydrograph analysis have provided the basis for the classification scheme of Antelope and Buffalo Springs. As a result, Antelope and Buffalo are classified as third-magnitude, intermediate-response, diffuse-flow, fresh water artesian springs.

Finally, a hydrologic budget was developed for the Sulphur, Oklahoma area. The recharge area for the City of Sulphur is approximately 15 mi^2 with an average annual recharge rate of about 4.6 inches per year; the total amount of water available on a yearly basis is approximately 1.2×10^9 gallons per year. However, current analysis reveals that in excess of 1.4×10^9 gallons per year is withdrawn from the Sulphur artesian basin.

CHAPTER I

INTRODUCTION

1.1 The Meaning of Hydrogeology

Hydrogeology is a discipline that is primarily concerned with the flow of water that is influenced by geologic processes (Narasimhan, 1982). Specifically, hydrogeology entails surface water and groundwater interactions governed by the geometry, material distributions, and boundary and initial conditions of the porous media.

Occasionally, geohydrology and hydrogeology are used synonymously in the literature. Interestingly enough, the term, hydrogeology, does not appear in the 1981 edition of the Websters New Collegiate Dictionary. Yet, geohydrology does, and the definition is as follows: "Science that deals with the character, source, and mode of occurrence of underground water". However, for the purpose of this study, hydrogeology connotes an emphasis on groundwater flow governed by geological parameters.

1.2 Man and Springs

Mankind, throughout recorded history, has been fascinated and attracted to springs. Ancient civilizations

settled in close proximity to springs in arid regions (Davis and DeWiest, 1966). Mineral springs and thermal springs of reputed medicinal and therapeutic value were exploited by vigorous commercial ventures that resulted in the establishment of permanent settlements in the United States. The city of Sulphur in south-central Oklahoma owes its origins to the commercialism of the mineral springs and the life-sustaining, freshwater artesian springs.

The land encompassing these springs were given to the Choctaw and Chickasaw Indian Tribes in 1835 by the U.S. Government (Barker and Jameson, 1975). By 1880 white ranchers had moved in by intermarriage and leases, and began to take over the economic and political aspects of the region. The Chickasaws were fearful that they would lose these springs to private interests pending statehood. So, they relinquished control of the springs back to the U.S. Government in 1902. This was accomplished so that all people could enjoy the use of these springs for years to come.

The small tract of land, approximately 1.5 square miles, along the southern periphery of the city of Sulphur, became a national park in 1906. The federal land was named Platt National Park in commemoration of a United States Senator, Orville H. Platt, who served on

the Committee of Indian Affairs.

The park was enlarged to 15 square miles in 1976 and subsequently renamed, Chickasaw National Recreation Area. Additions to the park system included Arbuckle Reservoir, Veterans Lake, and the Vendome Well.

Charles Gould, a geologist, forwarded a report to the Secretary of the Interior in 1906 that stated that there were 33 springs in the park. To date, there are only 5 springs that flow with any degree of regularity. A strong possibility exists that all springs will cease flowing in the next 40 years unless groundwater conservation measures are taken. The increasing frequency of cessation of springflow can be attributed to deprivational effects of production wells in close vicinity to the park.

1.3 Scope of the Project

The primary thrust of the project will be confined to the hydrogeologic investigation of the two freshwater artesian springs in the park, Antelope and Buffalo. The mineralized springs will be included as a supplementary analysis of the structural and lithological parameters that govern groundwater movement in the Sulphur, Oklahoma, area.

The intentions of this study are to accurately address the two artesian springs in the form of data analy-

sis and provide a concise, descriptive narrative of the same.

The principal objectives of this investigation are: (1) review previous findings and literature pertinent to the study; (2) deduce the origin of the two artesian springs; (3) assign concise nomenclature to the springs; (4) assess the geologic characteristics of the aquifer responsible for spring discharge; (5) determine the recharge area; and (6) utilize the Prickett-Lonnquist groundwater model to approximate aquifer properties, at selected points.

CHAPTER II

BACKGROUND

2.1 Geography and Hydrology at the Project Area

The area of investigation is located in and adjacent to Sulphur, Murray County, Oklahoma (Figure 1). South and east of the city of Sulphur is the Arbuckle Mountains (Figure 2). Reference to the Arbuckle Mountains in south-central Oklahoma is somewhat misleading, since 80 percent of the roughly triangular area of 1,000 square miles is rolling plains (Ham, 1978). The Arbuckle Mountains can be further subdivided into western and eastern regions (Figure 3). The study area is located in the western portion of the eastern part of the Arbuckle Mountains.

Buffalo and Antelope Springs are located at the east end of Travertine District, Chicasaw National Recreational Area (Figure 4). The remainder of the flowing springs are located in the central portion of the park and are somewhat mineralized. Surface elevations of Buffalo and Antelope are 1078 feet and 1080 feet, respectively (Table 1). The maximum surface elevation in the park is 1160

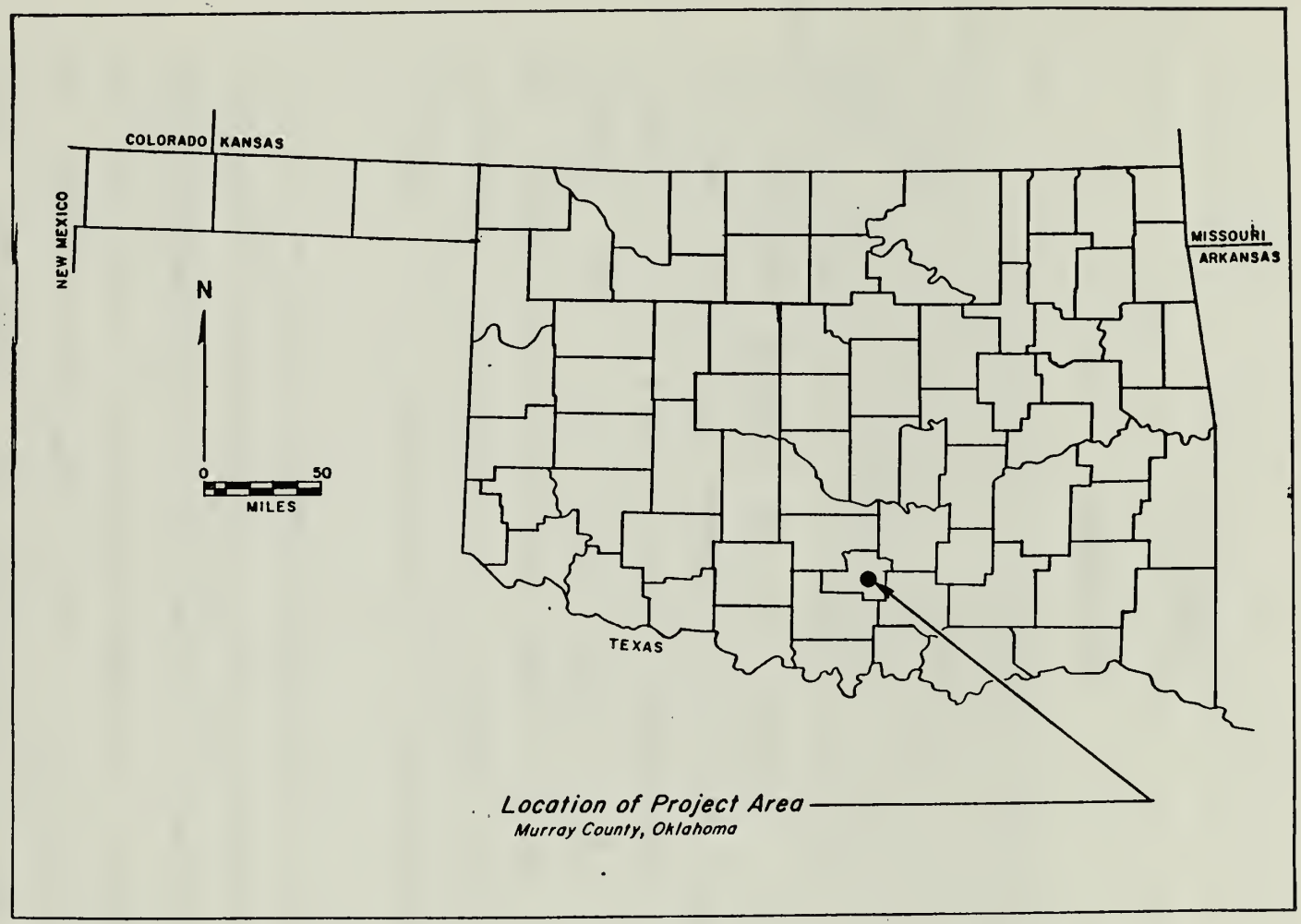

Figure 1. Location of project area, Murray County, Oklahoma (After Harp et al., 1976).

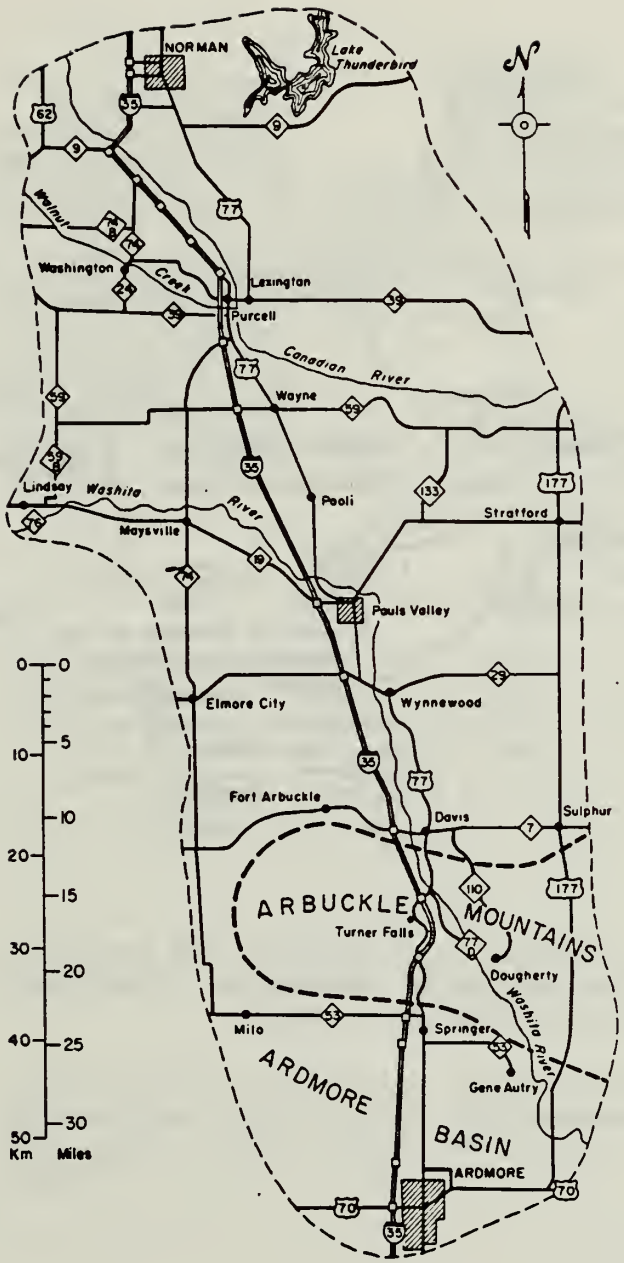

Figure 2. Location of Sulphur in relation to the Arbuckle Mountains (After Johnson, 1984).

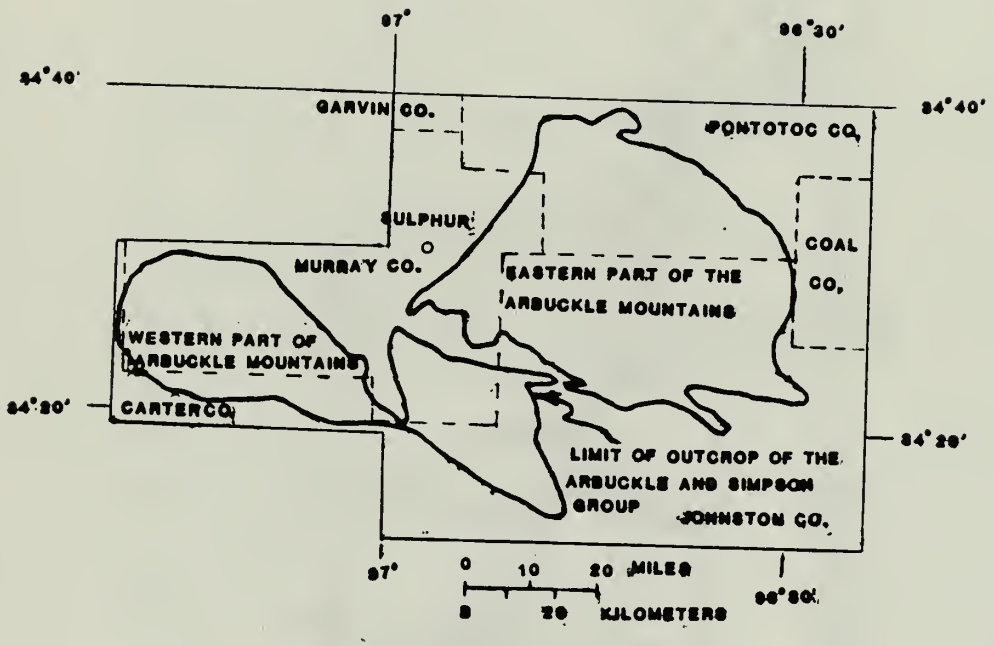

Figure 3. Map showing the eastern and western regions of the Arbuckle Mountains (Modified after Fairchild et al., 1983).

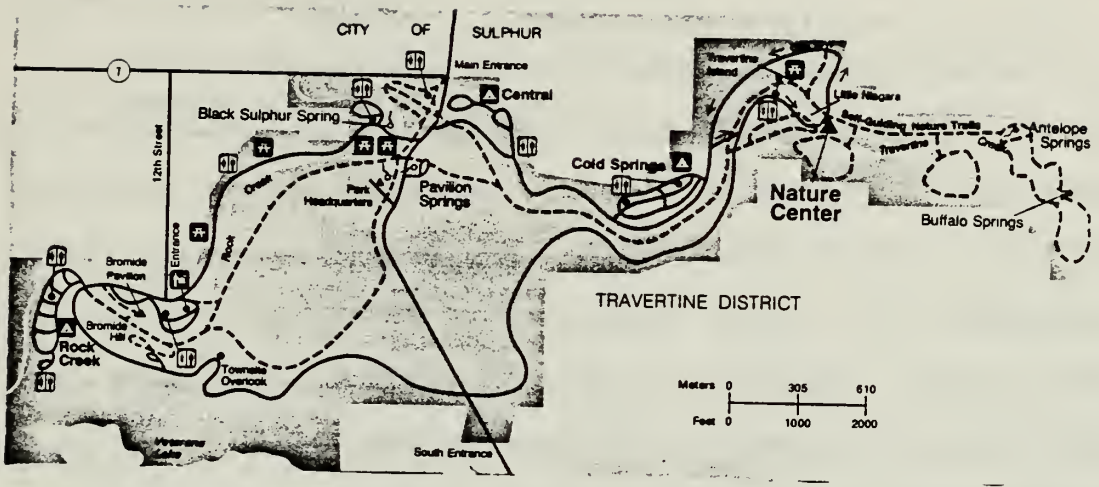

Figure 4. Map depicting location of springs in the Travertine District of Chickasaw National Recreation Area (After National Park Service, 1984).

Table 1. Surface Elevations of Springs

Spring	Surface Elevation (feet)
Antelope	1080
Buffalo	1078
Black Sulphur	942
Pavillion	938
[+]Hillside	960
Bromide/Medicine	925

[+] Hillside Spring is now considered to be one of the Pavillion Springs by the National Park Service. For the purpose of this study, the original nomenclature of the spring will be retained.

Data obtained from the 1984 United States Department of the Interior, National Park Service, Topographic Map. Contour interval is 2 feet.

feet, at the northeast corner. The minimum surface elevation is 915 feet, along Rock Creek at the southwest corner of the park.

The Travertine District is comprised primarily of a vibrant growth of hardwoods. This particular ecotone is sustained by the springs, and by the perennial streams, Travertine and Rock Creek. Travertine Creek traverses the park in a westerly direction until its confluence with Rock Creek at the center of the park. Then, Rock Creek flows in a southwesterly direction and reaches its base level at Arbuckle Lake, surface elevation of 872 feet.

Outside the park, to the north, the terrain consists of rolling hills heavily dissected with numerous ravines and intermittent streams. Riparian vegetation abounds in the stream bottoms, and grasses grow mainly on the hills. The maximum surface elevation is approximately 1130 feet. Rock Creek is the major stream, and flows in a southerly direction.

To the northeast and east of the park, within a 7-mile radius, the terrain consists of a plains topography, moderately dissected with intermittent streams. The maximum surface elevation is 1309 feet. Numerous low-lying rock outcrops of the Arbuckle Group appear in this area. Mill Creek is the largest intermittent stream in this area and flows in a southerly direction.

South of the park within a 2-mile radius, the terrain is hilly, heavily dissected with numerous ravines and intermittent streams. The maximum topographic relief in the entire study area outside the park boundary occurs along U.S. Highway 177, with a differential elevation of 156 feet for a distance of one mile. Riparian vegetation exists along the stream bottoms, cacti and grasses grow on the rocky ridges and hilltops. A major intermittent stream, Wilson Creek, flows in a westerly direction before reaching its base level, Veterans Lake. The maximum surface elevation is 1238 feet.

Southeast of the park within a 5-mile radius, the terrain is characterized by comparatively wider valleys and gently rolling hills. The south-flowing Mill Creek is the major intermittent stream. The maximum surface elevation is 1160 feet.

Generally, the terrain in the study area is characterized by a gently rolling topography overlying relatively flat-lying, fractured and faulted carbonates (Fairchild et al., 1983). However, the topographic relief in the park is comparitively greater than that of the surrounding study area. Also, just south of the park are northwest-trending ridges that are relatively pronounced. Both of these topographic expressions can be attributed to synclinal deformation and faulting. In addition, karst topography is not well developed in the

project area (Fairchild et al., 1983).

The study area is located in a moist subhumid zone. The climate is generally characterized by long summers and relatively mild winters of short duration. The mean annual air temperature for Sulphur is 62.5°F for the time period of 1941 to 1970 (Fairchild et al., 1983). The mean annual precipitation is 37.96 inches for the time period of 1919 to 1984 (Table 2).

Maximum temperatures commonly occur during the months of July and August (Fairchild et al., 1983). Minimum temperatures occur during the months of December and January. Maximum precipitation generally occurs during the spring months, from April through June (Table 2). Another wet season of lesser magnitude takes place during September and October. The dry season normally occurs from November through February.

2.2 Geology of the Area

The Arbuckle Mountains consist mostly of Paleozoic carbonates and Late Paleozoic clastics deposited partly upon a craton of Precambrian granite and partly in a geosyncline where the basement rocks are Middle Cambrian Volcanics (Figure 5). The western part of the Arbuckle Mountains, named the Arbuckle Anticline, represents an intense orogenic event of the geosyncline, composed of 34,000 feet of Paleozoic sediments. The eastern portion

Table 2. Rainfall Record

Chickasaw National Recreation Area
Sulphur, Okla.

For the Years 1917-1984

Year	Jan	Feb	Mar	Apr	May	June	July	Aug	Sept	Oct	Nov	Dec	TOTAL
1917		.62	.17	4.68	2.28	3.04	3.12	2.15	3.09	T	1.72	T	
1918	.62								4.15	4.37	2.56	3.92	
1919	1.21	2.39	2.18	3.40	5.35	3.67	3.81	7.25	.79	8.04	3.86	1.10	43.04
1920	2.65	.14	1.45	3.22	6.08	4.88	1.64	2.15	5.38	5.64	1.18	1.48	35.89
1921	1.66	2.17	4.91	4.27	2.80	8.00	3.90	2.83	.78	.05	1.11	1.06	33.54
1922	1.40	1.36	3.09	8.31	6.08	1.11	2.58	.79	.04	2.33	4.50	.40	31.99
1923	2.51	1.28	1.80	5.30	8.88	3.87	T	2.51	6.54	10.75	2.81	4.26	50.51
1924	.89	.79	3.42	5.88	3.10	3.63	.35	.72	1.98	.14	.49	2.85	24.24
1925	.99	.78	.08	2.19	4.83	.02	2.95	1.32	5.08	3.63	1.48	.32	23.67
1926	3.47	.72	2.56	2.56	4.40	3.17	6.19	8.28	5.84	5.39	.66	3.31	46.55
1927	4.78	2.97	1.95	9.99	.76	6.44	7.70	2.93	5.00	3.19	.77	3.65	50.13
1928	3.30	2.99	1.10	7.86	3.20	9.77	4.97	3.06	.76	3.55	2.68	1.74	44.98
1929	2.04	1.22	3.52	1.87	10.46	2.49	1.84	.14	5.05	6.76	2.36	2.78	40.53
1930	2.10	2.76	1.23	3.73	7.99	2.57	1.18	3.42	1.73	2.47	4.02	2.34	35.54
1931	.35	7.20	4.30	2.02	1.83	1.63	2.95	.72	.14	6.22	6.03	1.44	34.83
1932	7.33	3.41	1.73	3.71	2.11	4.06	1.48	1.76	.44	2.54	.22	9.30	38.09
1933	2.50	2.02	4.40	2.25	13.78	.54	2.22	5.95	4.96	.46	1.82	1.44	42.34
1934	2.40	2.72	3.80	2.97	3.00	2.81	.00	.87	6.38	1.06	5.98	.48	32.47
1935	1.89	.85	5.38	4.31	12.54	7.48	2.34	4.14	5.45	3.84	3.09	3.05	54.36
1936	.43	.40	1.61	1.07	8.38	.60	2.52	T	12.68	3.56	.31	1.62	33.17
1937	2.47	.18	4.06	3.68	2.22	2.79	4.63	4.38	.05	3.27	2.10	2.93	32.76
1938	2.60	9.55	4.61	2.35	6.05	4.83	2.57	1.43	2.44	.50	2.80	.68	40.41
1939	3.07	1.73	1.96	2.78	2.70	4.35	1.26	2.67	.59	2.91	2.28	1.20	27.50
1940	.45	2.87	T	6.82	9.33	6.58	6.83	2.47	.22	3.28	6.67	2.87	48.39
1941	2.88	3.18	.47	6.89	4.62	7.71	1.06	6.63	4.02	14.89	1.59	1.58	55.52
1942	.46	2.30	1.70	10.60	4.28	8.18	.77	4.76	3.68	5.41	2.24	2.53	46.93
1943	.15	.74	3.14	4.23	7.81	2.73	1.21	T	1.21	1.63	.12	3.87	26.84
1944	2.78	4.76	4.63	2.75	5.86	2.54	3.12	2.77	.85	4.44	3.82	2.65	38.97
1945	1.70	4.44	9.76	8.61	1.41	10.99	4.58	6.13	11.13	.78	.72	.08	60.33
1946	6.42	3.66	4.01	2.83	5.66	3.43	.84	6.17	2.72	.14	6.80	8.42	51.64
1947	.32	.34	1.21	9.04	8.04	4.28	1.57	1.13	3.33	1.61	2.87	2.70	39.34
1948	.98	4.19	2.51	.70	7.59	6.64	3.62	1.32	.12	.78	.48	1.27	30.20
1949	5.97	2.69	3.38	2.18	6.14	4.90	.58	2.75	6.28	4.54	.00	1.48	40.84
1950	3.02	1.86	.35	2.03	6.44	3.39	5.91	7.94	2.48	.71	.22	.10	34.45

(continued)

Table 2. Rainfall Record (continued)

Chickasaw National Recreation Area
Sulphur, Okla.

For the Years 1917-1984

Year	Jan	Feb	Mar	Apr	May	June	July	Aug	Sept	Oct	Nov	Dec	TOTAL
1951	1.14	3.61	1.35	1.43	5.88	6.87	5.54	2.92	1.78	3.15	1.84	.31	35.82
1952	.31	1.23	3.33	4.72	4.86	.50	2.85	.90	.10	.03	4.47	1.45	24.75
1953	.55	.97	3.14	4.36	4.51	2.28	7.72	1.44	1.16	5.15	2.22	1.05	34.55
1954	1.49	.55	.93	5.45	8.21	4.34	.15	.83	.36	5.72	.36	3.08	31.47
1955	1.47	2.18	2.45	1.81	4.77	1.79	2.09	1.08	7.37	.21	.02	.40	25.64
1956	1.47	2.14	.39	2.89	4.81	1.55	1.43	1.39	.04	3.73	3.93	3.15	26.92
1957	2.13	2.09	4.37	9.14	13.24	6.09	2.34	1.68	11.41	2.25	4.86	1.46	61.06
1958	2.44	.51	4.15	2.06	4.85	3.52	4.30	1.91	.78	.33	1.94	.86	27.65
1959	.45	.79	3.36	2.74	4.45	2.87	3.04	2.07	1.81	8.96	2.50	2.77	35.81
1960	2.74	3.08	2.10	2.76	6.89	1.84	3.59	3.16	5.33	4.38	.21	4.95	41.11
1961	.10	2.00	3.62	.92	3.75	3.51	3.70	.64	6.87	3.72	3.20	1.74	33.67
1962	.34	.35	2.55	2.97	1.91	8.91	4.13	1.19	4.69	4.85	2.75	1.79	36.43
1963	.07	.04	5.02	3.22	.81	.56	2.28	1.99	1.77	.04	2.29	1.45	19.54
1964	.96	1.59	2.89	1.79	8.52	.98	.70	4.98	6.33	.47	6.70	.72	36.63
1965	2.14	1.55	1.65	2.60	5.90	1.69	1.58	2.48	2.04	1.95	.83	1.32	25.73
1966	1.26	1.87	1.26	5.09	.71	2.18	4.65	5.36	2.04	1.86	.94	.69	27.91
1967	.34	.80	1.05	8.17	6.68	6.73	3.89	.20	5.81	5.37	.79	2.13	41.96
1968	4.13	1.27	3.82	2.35	9.47	4.02	5.75	.97	4.43	2.87	5.73	2.04	46.85
1969	1.25	2.97	2.55	5.21	5.05	3.30	1.74	1.61	2.65	7.92	.51	3.47	38.23
1970	.18	1.74	3.90	4.97	2.26	4.82	1.68	.80	11.73	16.43	.79	.77	50.07
1971	1.89	1.15	.68	2.76	2.83	2.63	4.05	4.92	2.79	6.62	.57	5.46	36.35
1972	.36	.56	.61	3.95	4.05	2.39	1.41	3.56	2.52	7.69	3.87	.88	31.85
1973	3.01	3.00	6.44	6.04	2.72	8.12	3.94	.99	10.90	4.89	8.02	.86	58.93
1974	.90	1.76	1.45	4.91	3.64	3.47	2.10	5.49	8.65	7.10	2.48	1.53	43.48
1975	1.98	4.26	4.71	3.05	6.85	2.43	4.73	1.98	3.55	1.24	2.05	1.50	38.33
1976	.07	.29	3.70	3.88	7.78	1.33	1.90	1.18	1.36	4.71	.90	1.57	28.67
1977	1.91	1.39	6.39	3.51	5.29	2.48	2.04	2.83	1.89	1.73	1.29	.34	31.09
1978	1.15	2.82	3.69	3.00	8.12	3.33	2.13	1.95	2.37	1.31	4.46	.58	34.91
1979	2.33	1.31	4.56	3.68	4.75	6.83	.80	2.72	2.63	3.18	.95	1.69	35.43
1980	1.44	1.26	.91	.56	9.58	2.50	.18	.00	10.73	1.74	1.79	2.29	32.98
1981	.29	2.61	2.52	2.29	8.51	3.46	3.95	1.81	2.10	16.26	1.71	.26	45.77
1982	1.75	2.29	1.60	1.04	15.71	6.21	2.95	1.04	1.02	2.84	3.43	1.77	41.65
1983	2.57	3.70	2.95	2.95	10.67	3.64	.90	3.28	2.11	4.53	2.61	.57	40.48
1984	.98	1.98	3.97	3.86	2.83	4.29	3.51	2.52	1.62	7.55	4.58	5.10	42.59
Avg.	2.08	2.10	2.80	3.94	5.62	3.95	2.79	2.61	3.62	4.02	2.43	2.02	37.96

(modified after Harp et al., 1976)

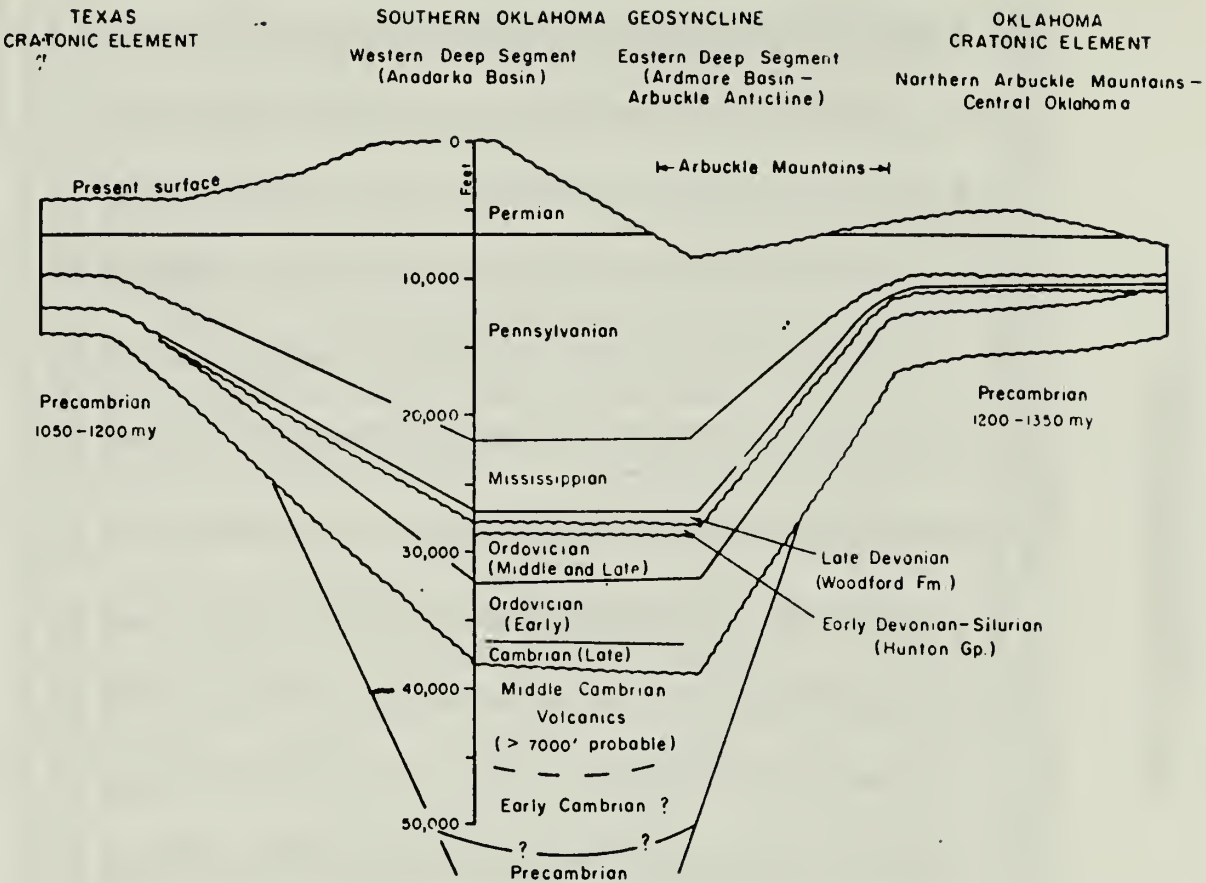

Figure 5. Regional stratigraphic section across the Southern Oklahoma geosyncline. Note, thickness change of paleozoic sediments in the Arbuckle Mountain sequence (After Ham, 1978).

of the Arbuckle Mountains consists of Paleozoic sediments of a thickness of 10,000 feet upon the relatively more stable craton (Ham, 1978). Besides the marked differences in thickness of sediments between the two provinces, major facies changes also occur (Figure 6). The most notable facies change occurs in the Arbuckle Group, predominantly limestone in the geosyncline and dolomite on the craton.

The structural and depositional history of the Arbuckles can be summarized chronologically as follows (Ham, 1978).

1. The geosyncline was filled with volcanics during the Cambrian.
2. Marine sedimentation in the form of carbonates, sandstones, and shales continued from Late Cambrian through Mississippian.
3. The early Pennsylvanian marked the inception of the emergence of the craton, sedimentation of clastics continued on the geosyncline, and conglomerates were deposited along the margins of the craton.
4. The uplifted craton remained distinct from the geosyncline through Middle Pennsylvanian.
5. The comparitively thinner sediments of pre Pennsylvanian continued to erode on the craton during Middle and Late Pennsylvanian (the

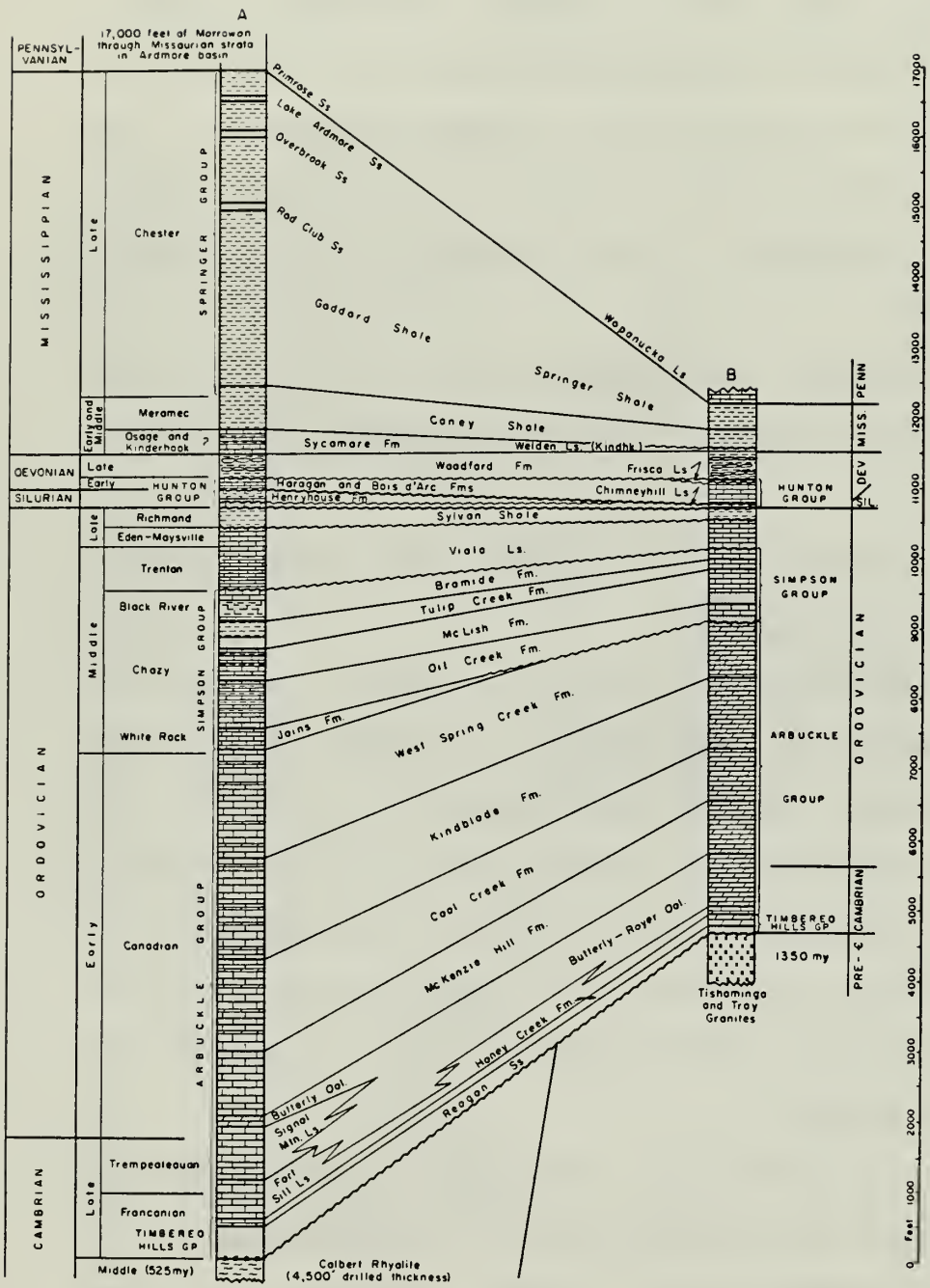

Figure 6. Stratigraphic columns (pre-Pennsylvanian) of the Arbuckle Mountains. Column A is the geosyncline, Western Arbuckles, and Column B is the craton, Eastern Arbuckles. Note facies and thickness variation between the two provinces (After Ham, 1978).

basement rock of the craton was 6 miles above the floor of the geosyncline).

6. Compressional forces during the Upper Pennsylvanian produced close folding and high-angle thrust faulting of the thick prism of sediments in the geosyncline against the relatively immovable craton. The orogeny slightly affected elements of the craton.
7. Two orogenic pulses yielded the older Ada Conglomerate and the younger Vanoss Conglomerate (Hart, 1974 and Ham, 1978).
8. Additional, less pronounced orogenic pulses continued through Lower Permian, marking the close of the Arbuckle Orogeny.

Erosional processes during and after the orogeny have morphologically produced the surface geology of the present-day Arbuckle Mountains (Figure 7). In addition, Figure 7 depicts the areal extent of this hydrogeologic investigation. The surficial and structural geology of the project area is depicted in greater detail in Plate I (Ham, 1954). Included is a geologic section of the subsurface geology; based on known stratigraphic thickness and sequence of geologic units, and observed surface structure.

The following geologic units in chronological order appear as surface outcrops in the project area: (1) the

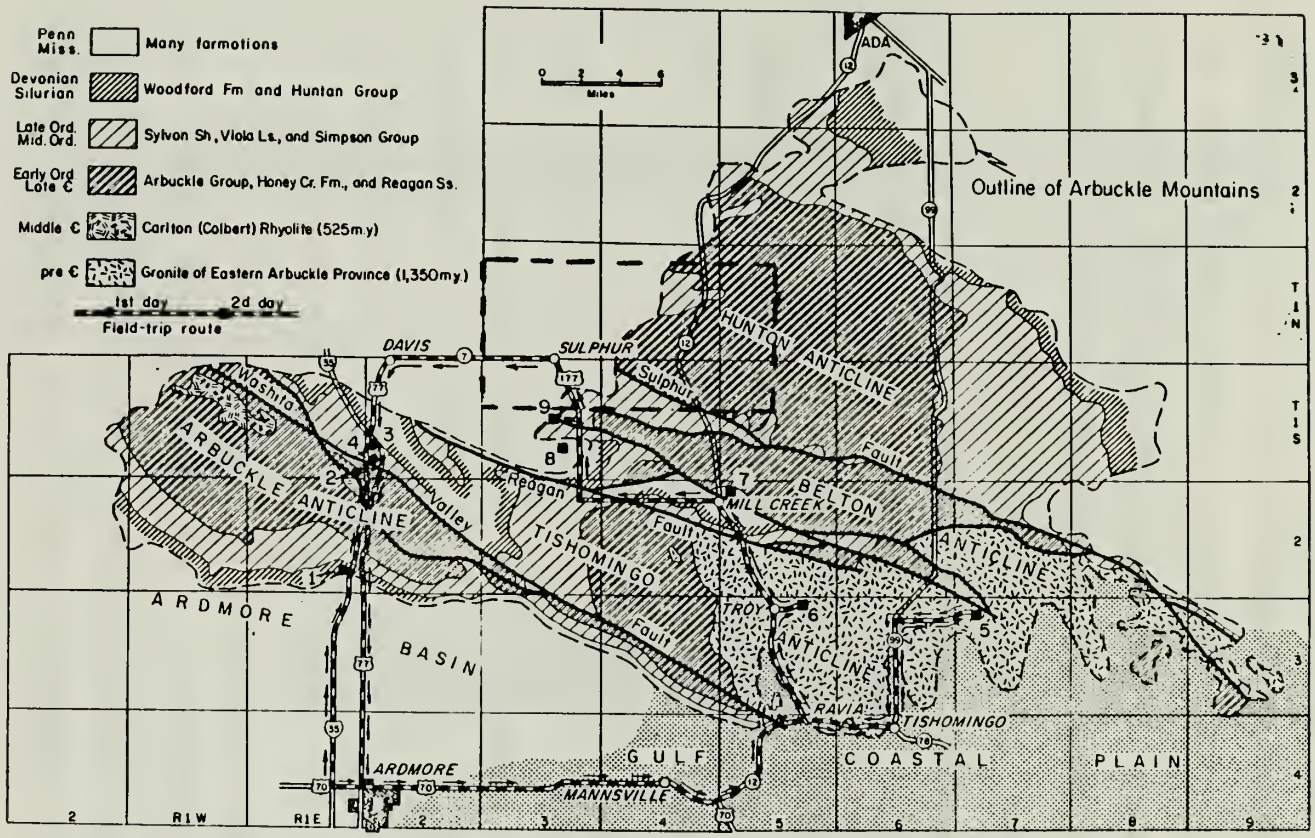

Figure 7. Geologic map of the Arbuckle Mountains. Superimposed on the map are dashed lines, rectangular in configuration, depicting the areal extent of the hydrogeologic investigation of the Sulphur, Oklahoma, area (Modified after Ham, 1978).

Arbuckle Group (Upper Cambrian to Lower Ordovician), (2) the Simpson Group (Middle Ordovician), (3) the Viola Limestone (Upper Ordovician), (4) the Sylvan Shale (Upper Ordovician), (5) the Ada Formation (Upper Pennsylvania), and (6) the Vanoss Formation of the Pontotoc Group (Upper Pennsylvanian). The remainder of the geologic units in the study area, the Tishomingo Granite (Precambrian) and the Timbered Hills Group (Upper Cambrian), are situated at considerable depth below the surface.

The Tishomingo Granite is the local basement rock of the study area, estimated thickness of 10 miles. The Tishomingo Granite is generally coarse crystalline, pink, with much microcline and biotite (Ham et al., 1964).

The Timbered Hills Group is comprised of the Reagan Sandstone and the Honey Creek Formations (Col. B, Figure 6). The Reagan Sandstone is a feldspathic, glauconitic sequence deposited on the Tishomingo Granite (craton) during Late Cambrian, 75 to 450 feet thick (Ham, 1978). The Honey Creek formation is a fossiliferous, sandy dolomite, about 225 feet thick, that lies conformably over the Reagan Sandstone. The Timbered Hills Group was determined to be deposited in a shallow marine environment on a slowly subsiding craton.

The Arbuckle Group consists of the following formations in chronological order: (1) Butterly-Royer Dolomite (Late Cambrian), 750 feet thick; (2) McKenzie

Hill Formation (Early Ordovician), 750 feet thick; (3) Cool Creek Formation (Early Ordovician), 750 feet thick; (4) Kinblade Formation (Early Ordovician), 1,000 feet thick; and (5) West Spring Creek Formation (Early Ordovician), 750 feet thick (Col. B, Figure 6).

The highly resistant Arbuckle Group, of shallow water marine deposition, approximate thickness of 4,000 feet is primarily dense, crystalline dolomite with some thin beds of white friable sandstones (up to 10 feet thick) and shales (Col. B, Figure 6). The Arbuckle rocks are in part, richly fossiliferous in the Arbuckle anticline. Yet, there is poor faunal preservation on the craton (shelf) because of dolomitization.

The Simpson Group (Middle Ordovician), 600 to 1,600 feet thick, is divided into the following five formations in chronological order: Joins Formation, Oil Creek Formation, McLish Formation, Tulip Creek Formation, and Bromide Formation (Col. B, Figure 6). The five formations represent five complete sedimentary cycles in a marine environment with a basal sand in each of the four upper ones (Decker et al., 1931). The Tulip Creek and Joins are very thin or lacking in the study area and have been incorporated into the Bromide and Oil Creek formations, respectively, by previous investigators (Ham et al., 1954). Each formation of the Simpson Group in the study area basically contains greenish-gray shale,

skeletal calcarenites or algal-mat carbonates; and a friable, basal sand of varying thickness, 50 to 350 feet. The basal sand is composed of well sorted, rounded, fine-grained frosted quartz.

The Viola Limestone (Upper Ordovician) of marine environment is gray, fine to coarse grained limestone, 350 feet thick. The Viola lies unconformably on the Bromide Formation of the Simpson Group (Col. B, Figure 6). The Sylvan shale (Upper Ordovician), 150 feet thick, lies disconformably on the Viola. The Sylvan is a dark greenish-gray shale, well laminated, with numerous bedding surfaces that are crowded with graptolites.

In ascending chronological order, the Ada Formation and the Vanoss Group (both units, Upper Pennsylvanian) represent two distinct, depositional and deformational episodes during the Arbuckle Orogeny (Upper Pennsylvanian). The Ada Formation primarily consists of a well-cemented conglomerate of limestone cobbles, red shales, and bituminous sandstone. Thickness of the Ada Formation varies from 0 to 500 feet in the project area. The Ada lies upon older rocks as an angular unconformity, deformation of this strata occurs locally. The Vanoss Group consists of maroon shales, arkoses, and limestone conglomerates. The Vanoss, 0-500 feet thick, is undeformed, and lies upon older rocks as an angular unconformity. For the purpose of this study only and for simpli-

fication, the Ada and the Vanoss will be summarily joined; to be called the following hydrogeologic unit, the Pontotoc Group.

The central part of the Arbuckle Mountains, covered by this investigation, encompasses the following major structural features: (1) the Hunton Anticline, (2) the Hickory Syncline, and (3) the Sulphur Syncline (Figure 7 and Plate I). The Hickory Syncline is a localized structural unit and subsidiary to the Hunton Anticline, vicinity of Hickory, Oklahoma. In actuality, the Hickory Syncline is composed of two synclinal structures, one north of Hickory and one south of Hickory (Section, Plate I). A major fault, trending in a west, southwest direction, subtends both synclines. The Simpson Group has been preserved in both synclines from erosion by down faulting and accompanying drag folds (Ham, 1945). East of Sulphur at the eastern fringe of the project area, is the northwest-trending Hunton Anticline (Figure 7). The basement rock is approximately 3,200 feet below the surface in this area (Figure 8). The relatively flat-lying, highly-resistant, Upper Arbuckle Group outcrops 1 mile east of the Travertine District boundary and continues eastward.

The west, northwest-trending Sulphur Fault, southeast of Sulphur, is the major fault in the project area. The fault is the northern boundary of the Sulphur

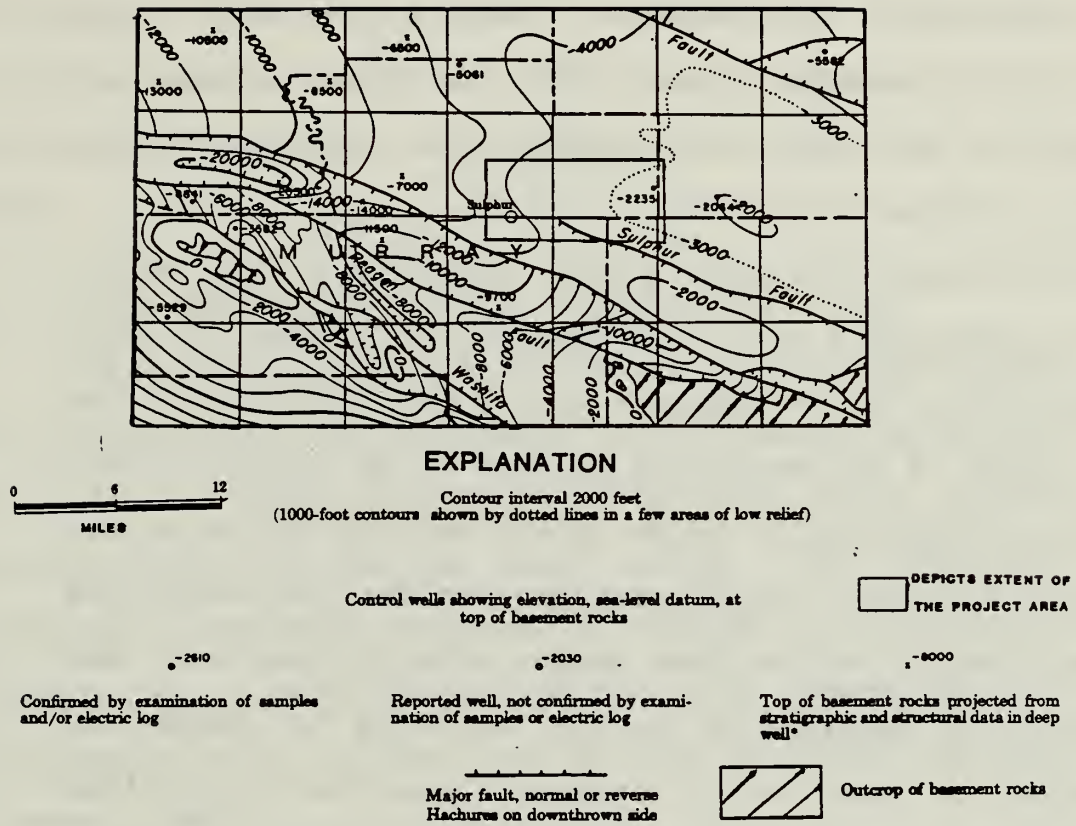

Figure 8. Surface contour map of the basement rock of the Arbuckle Mountain area. The solid lines, rectangular in shape, outline the general extent of the project area, vicintiy Sulphur, Oklahoma (Modified after Ham, 1964).

Syncline, and delineates the Arbuckle Group to the north (upthrown side), from the Simpson Group preserved in the synclinal graben to the south (Section, Plate I). The amount of high-angle throw along the Sulphur Fault increases in the same direction as the west, northwest plunging Sulphur Syncline.

The Sulphur Syncline begins plunging to the northwest in Sections 8 and 17 of Township 1S, Range 3E; with moderate dips of 10 degrees northwest (Plate I). The south limit of the graben is bounded by an unnamed fault. The fault decreases in throw in the same direction as the plunging syncline. This would account for the steep dips of the Simpson on the down thrown side to the north and northeast in Sections 11 and 12, Township 1S, Range 3E. According to Ham (1945), strictly synclinal conditions prevail just south and southeast of Sulphur. The syncline plunges under the Upper Pennsylvanian cap rock towards Sulphur, completely encompassing the Travertine District. The graben is flanked to the north by the west-northwest trending Sulphur Fault, exact location unknown.

In general, the major structural features of the project area trend in a west, northwest direction. The major faults parallel the synclinal and anticlinal axes. The resistant Arbuckle Group, relatively flat lying, outcrops to the northeast and east of Sulphur. The Simpson

Group is preserved in grabens, the Sulphur Syncline and the Hickory Syncline. The Pontotoc Group, outcrops throughout the entire park, capping the northwest-plunging Sulphur Syncline. The Pontotoc covers the remainder of the project area, gently dipping to the northwest.

2.3 Groundwater Flow Through Geologic Materials

Introduction of the hydrologic cycle is instrumental in understanding the processes to the mode, occurrence, and origin of water (Figure 9). The word, cycle, explicitly connotes no end or start point. The hydrologic equation, a succinct statement of the law of mass conservation, for a specific period of time, quantifies the hydrologic cycle in the form of the following equation (Fetter, 1980).

Inflow = Outflow ± Changes in Storage

$$I' = O' \pm S' \qquad (2.1)$$

For example, inflow, I', could be represented by precipitation, surface flow, groundwater, seepage, and overland flow. Storage, S', could be in the form of a lake or reservoir. Outflow, O', could be evapotranspiration, an outlet stream, and seepage from the reservoir or lake. If outflow exceeds inflow, storage will decrease. Conversely, if inflow exceeds outflow, storage will increase. The hydrologic equation can be applied to any

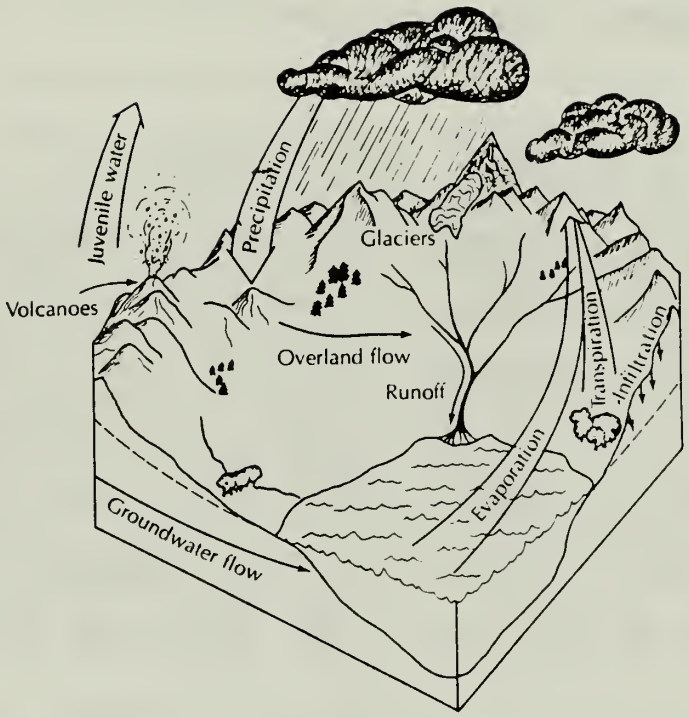

Figure 9. Hydrologic cycle (After Fetter, 1980).

size system and is time dependent (Fetter, 1980).

For the purpose of this investigation, the hydrologic budget will be defined as inflow equals outflow (Fairchild et al., 1983). Inflow is the amount of annual rainfall that falls on a specific area. Outflow entails evapotranspiration, surface flow, and groundwater; all of which result from precipitation events for the calendar year (a set period of time).

The outflow element of the hydrologic budget, groundwater, becomes the inflow parameter of the subsurface hydrologic equation. The groundwater (units in length^3) introduced to the aquifer is called recharge. Recharge is the fractional amount of the annual rainfall (units in length) that infiltrates to a water table, distributed over an identified area (units in length^2). The aquifer, which stores and transmits groundwater, is the storage element of the hydrologic equation. Changes in the potentiometric level of the aquifer for a specified time and area are functions of inflow and outflow. Outflow entails natural and artifical discharge. Natural discharge includes springs and seeps, and subsurface flow from the local system into a regional one. Artifical discharge consists of domestic, municipal, and industrial production wells.

Darcy's Law and the continuity principle (law of mass conservation) are fundamental in the development of

the physics of groundwater flow (Wang et al., 1982). The continuity principle is a mathematical formulation (a partial differential equation) of the hydrologic equation for aquifers, confined or unconfined. Darcy's Law relates the specific discharge vector to the gradient of the potential, and is normally valid for a Newtonian fluid (such as water) and nonturbulent flow (Narasimhan, 1982). Laminar or nonturbulent flow for a porous media is generally considered to be less than a Reynolds Number of 1 (Collins, 1961).

Henry Darcy, a French engineer, in 1856, conducted an experiment (Figure 10) of water flow through a vertical column of sand and arrived at the following equation:

$$Q = -KA \frac{h_2 - h_1}{L_2 - L_1} \qquad (2.2)$$

Where volume discharge rate, Q, is proportional to the head drop $(h_2 - h_1)$ to a cross-sectional area, A, and inversely proportional to the length difference $(L_2 - L_1)$.

The negative sign indicates that groundwater flows in the direction of head loss (Wang et al., 1982). Finally, a proportionality constant of a geologic material, K, known as hydraulic conductivity, is included in the right side of Equation 1.1. Dimensional analysis of K reveals units of LT^{-1}. The general form of Darcy's Law is given by the following differential equation:

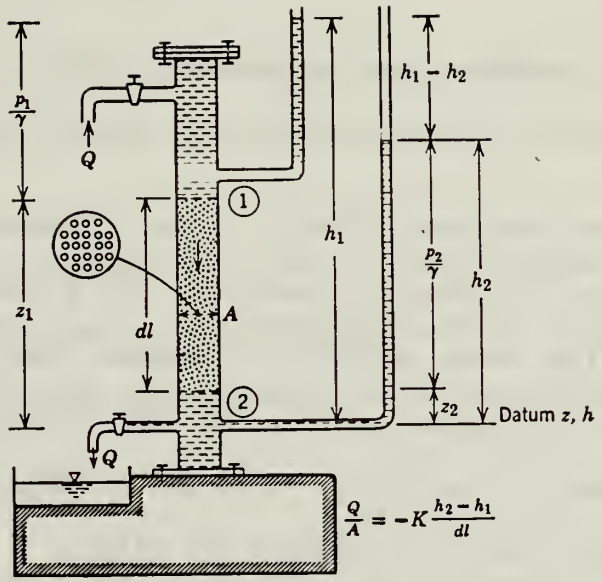

Figure 10. A sketch of an apparatus to demonstrate Darcy's Law (After Davis and DeWiest, 1966).

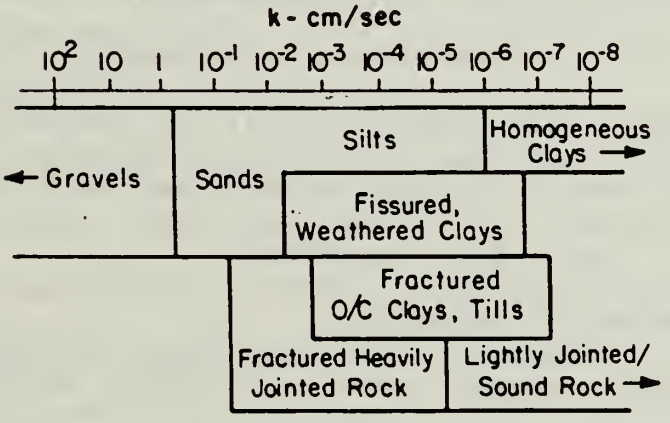

Figure 11. Approximate range of hydraulic conductivity in soil and rock (After Houstin et al., 1982).

$$q = \frac{Q}{A} = -K \frac{dh}{dl} \qquad (2.3)$$

Where specific discharge or apparent velocity, q, is equal to the hydraulic conductivity, K, times the gradient, $\frac{dh}{dl}$ (Davis and DeWiest, 1966). Also, Figure 10 pictorially shows that hydraulic head, h, is a function of elevation , z, from some arbitrary datum, and pressure head, P/γ, where the pressure, P, is the pore pressure, and γ, is the specific weight. Hydraulic head in these equations is energy per unit weight of water.

The total energy of an incremental volume of fluid in motion is equal to the sum of kinetic, gravitational, and fluid-pressure energy:

$$E_{tv} = 1/2\ \rho v^2 + \rho g z + P \qquad (2.4)$$

where E_{tv} is total energy per incremental volume, ρ is density, g is the gravitational acceleration constant, and P is pressure. If equation (1.3) is divided through by density, the result is total energy per unit mass:

$$E_{tm} = v^2/_2 + gz + p/\rho = \text{constant} \qquad (2.5)$$

which is the Bernoulli equation.

The kinetic energy term, velocity squared, is generally considered to be negligible in flow through porous media and is dropped from the above equation. The force potential is expressed in terms of energy per unit mass (Fetter, 1980):

$$\Phi = gz + P/\rho = gz + \frac{\rho gz}{\rho} \tag{2.6}$$

and $h = z + h_p$, the hydraulic head, and h_p is feet of pressure, then

$$\Phi = gh \tag{2.6}$$

Both force potential and hydraulic head are potentials. Darcy's Law can be expressed in hydraulic head and also in force potential for one dimensional flow:

$$q = \frac{Q}{A} = - K \frac{dh}{dL} \tag{2.7}$$

$$q = \frac{Q}{A} = - \frac{K}{g} \frac{d\Phi}{dL} \tag{2.8}$$

Hydraulic conductivity is not only a function of characteristics of the medium, it depends on the properties of the fluid as well. The hydraulic conductivity is given by the following equation:

$$K = K_1 \rho g/\mu \tag{2.9}$$

where K_1 is intrinsic permeability and is characteristic of the medium only, and μ is the dynamic viscosity of the fluid (Davis and DeWiest, 1966). Intrinsic permeability is proportional to the average pore diameter:

$$K_1 = cd^2 \tag{2.10}$$

where c (dimensionless units) is a shape factor which accounts for stratification, packing, arrangement of grains, size distribution, and porosity.

Porosity of a porous media, n, is a fraction of the

bulk volume, V_B, occupied by voids (Collins, 1961)

$$n = \frac{V_P}{V_B} = \frac{\text{Volume of Pores}}{\text{Bulk Volume}} = 1 - \frac{V_S}{V_B} = 1 - \frac{\text{Volume of Solids}}{\text{Bulk Volume}} \qquad (2.11)$$

where bulk volume is equal to the sum of the volume of pores, V_P, and the volume of solids, V_S.

Porosity of a porous material is a function of grain size distribution, grain configuration, and diagenetic processes. Primary porosity is related to pore spaces between grains. Secondary porosity is related to fractured media and subsequent enlargement by solution activities of groundwater. Effective porosity is the fractional amount of interconnected pores for a given bulk volume through which groundwater can be transmitted. Absolute porosity is the total fractional amount of voids for a given bulk volume, regardless of its ability to transmit fluids (Chilingarian et al., 1975).

In general, hydraulic conductivity is a measure of the ability of porous media to transmit groundwater and is related to effective porosity. As interconnected pore diameters become smaller, resistance to flow increases, resulting in a decrease in hydraulic conductivity and a corresponding increase in hydraulic gradient. Conversely, hydraulic conductivity approaches infinity in large solution cavities and fractures (Chilingarian et al., 1975). A wide spectrum of values for hydraulic conductivity of soil and rock are shown in Figure 11 (Houstin

et al., 1982).

Values of porosity vary considerably for sedimentary rocks. Clastics generally range from .03 to .30. Carbonates range from less than .01 to about .30 (Fetter, 1980). Table 3 lists typical porosities of porous materials (Houstin et al., 1982). Indurated sediments at depths of several thousand feet might have porosities that are only half to one-third the porosities of the same lithology of the surface or at shallow depths (Goodman, 1979).

The ensuing discussion of aquifer characteristics is necessary prior to the development of the continuity equation, and subsequent methodology of hydrogeologic exploration.

An aquifer is a geologic unit that stores and transmits water rapidly enough to supply adequate amounts to wells. Also, a porous media with at least an intrinsic permeability of 10^{-2} darcy constitutes an aquifer (Fetter, 1980).

The intrinsic permeability of a confining layer is generally less than 10^{-2} darcy. The confining layer can be further subdivided into aquifuges (impermeable), aquitards (low permeability), and aquicludes (upper boundary or a lower boundary to a flow system, low permeability). Confining layers of large aerial extent, hundreds of square miles, can provide significant amounts

Table 3. Typical Porosities for Porous Materials

	Material	Range in n (%)	Commonly encountered values of n (%)
Soft skeleton	Sand	25 - 50	40 ± 8
	Silt	40 - 63	52 ± 8
	Clay	40 - 94	62 ± 12
Stiff skeleton	Marble	0.3 - 1.1	0.7 ± 0.4
	Granite	0.1 - 20	2 ± 1
	Limestone	0.4 - 43	10 ± 20
	Sandstone	0.7 - 34	15 ± 79
	Shale	1.6 - 25	15 ± 7
	Tuff	14 - 40	25 ± 6
	Chalk	25 - 50	35 ± 7

(after Houstin, 1982; and originally from Clark, 1966; Riley, 1972; and Goodman, 1979)

of recharge to the underlying aquifer.

Water-table aquifer (also referred to as phreatic or unconfined aquifer) is defined as a continuous geologic material of high intrinsic permeability from the land surface to the base (Figure 12). Recharge is normally downward seepage from the unsaturated zone.

Confined aquifers or artesian aquifers are overlain by confining layers. Recharge occurs from confining layers or where the aquifer outcrops (Figure 12). The piezometric level of an artesian aquifer is above the base level of the overlying, confining layer. The distance above the base level of the confining layer to which water will rise is the pressure head of the force potential.

Transmissivity is the measure of the amount of water that is transmitted laterally by the full saturated thickness of an aquifer. Transmissivity, T, is the product of hydraulic conductivity, K, and saturated thickness, h':

$$T = Kh' \qquad (2.12)$$

For this study, units for transmissivity are ft^2/day.

Storage coefficient, S_c, is the volume of water than an aquifer can expel or absorb from storage per unit area per unit change in head (Fetter, 1980). Water is stored or withdrawn from a confined aquifer by elastic behavior of the media. Water extracted or absorbed in a phreatic

aquifer is a function of gravity and elastic mechanisms. Specific storage, S_S, is the amount of water released per unit volume of aquifer due to compressibility of the geologic unit and compressibility of the water:

$$S_S = \gamma(\alpha + n\beta) \tag{2.13a}$$

$$\gamma = \rho g \tag{2.13b}$$

and

$$S_S = \rho g\ (\alpha + n\beta) \tag{2.14}$$

where ρ = density of water,

g = acceleration of gravity,

γ = specific weight of water,

α = matrix compressibility of the aquifer,

n = porosity,

β = compressibility of the water.

The storage coefficient of a confined aquifer is the product of specific storage, S_c, and the aquifer for thickness, b':

$$S_c = b'\ S_S \tag{2.15}$$

The storage coefficient of a phreatic aquifer is sum of the specific yield, S_y, and the specific storage, S_c:

$$S_c = S_y + h'S_S \tag{2.16}$$

where h' is the saturated thickness of a phreatic aquifer. It is customary to set the storage coefficient equivalent to the specific yield, because specific storage is at least two orders of magnitude less than specific yield (Fetter, 1980). Values of specific yield

for an unconfined aquifer range from .02 to .30. Storage coefficients of a confined aquifer are usually less than .005.

A homogeneous aquifer has the same rock properties throughout the porous media. Narasimhan (1982) stated that homogeneity is a frequency distribution of rock properties that does not vary spatially for a geologic unit. Conversely, a heterogeneous media is characterized by frequency distributions of rock properties that vary spatially.

If all measurable properties of a media at some finite element or point are spatially equal the unit is isotropic. If a certain property of the media at some finite element has a preferred orientation and is not spatially equal, the unit is anisotropic. Examples of anisotropic behavior of intrinsic permeability of a media are: (1) fractured carbonates, and (2) preferred grain orientation in clastics.

The derivation of the law of mass conservation (the continuity principle) for an isotropic, homogeneous, elemental volume (Figure 13) of a confined aquifer is given in Appendix I. The resultant continuity equation of two-dimensional transient flow is:

$$\frac{\partial^2 h}{\partial x^2} + \frac{\partial^2 h}{\partial y^2} = \frac{S_c}{T} \frac{\partial h}{\partial t} \qquad (2.17)$$

If the confined aquifer is anisotropic, (where $T_x \neq$

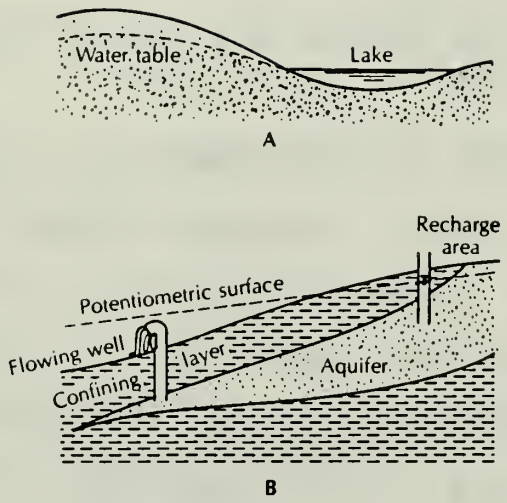

Figure 12. A. Water-table aquifer
B. Artesian aquifer
(After Fetter, 1980).

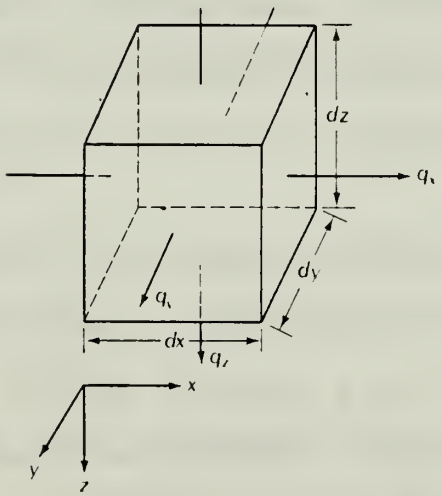

Figure 13. Elemental volume of flow through a confined aquifer (After Fetter, 1980).

T_y), and heterogeneous (where T_x and T_y vary spatially within the aquifer) then, the following two-dimensional, transient flow equation applies:

$$\frac{\partial}{\partial x} T_x \frac{\partial h}{\partial x} + \frac{\partial}{\partial y} T_y \frac{\partial h}{\partial y} = S_c \frac{\partial h}{\partial t} \pm Q_n(x,y,t) \qquad (2.18)$$

where $+Q_n$ per unit area denotes a sink, and $-Q_n$ represents recharge per unit area (Wang et al., 1982). There is no known analytic solution to Equation (2.18). As a result, numerical methods are necessary to solve the preceding equation. A well documented and widely used groundwater model, Prickett and Lonnquist (1971), can be utilized to solve Equation 2.18. In addition, the Prickett-Lonnquist model can solve phreatic, two-dimensional transient flow:

$$\frac{\partial}{\partial x} h \frac{\partial h}{\partial x} + \frac{\partial}{\partial y} h \frac{\partial h}{\partial y} = S_y \frac{\partial h}{\partial t} \qquad (2.19)$$

which is the Boussinesq equation (Fetter, 1980). Appendix 2 contains the Prickett-Lonnquist model, and an accompanying flow chart and discussion.

The remainder of this section will be devoted to anisotropic flow behavior. Before proceeding into this topic, an understanding of isotropic flow is necessary.

For isotropic porous media and steady state conditions, the specific discharge, q, flows parallel to the gradient, and normal to the equipotential lines

(Figure 14*). A potentiometric map constructed from field data, consists of isobars of equipotential points that depict water surface contour elevations (force potential, Φ). If hydraulic conductivity varies in the three principal axes, then specific discharge will flow obliquely to the equipotential lines (Davis and DeWiest, 1966).

For this study, anisotropic flow behavior will be specifically focused on fractured media. J.E. Gale (1982) states that fracture hydrogeology is poorly nurtured and not well understood when compared to fluid movement through porous media.

Gale (1982) maintained that the hydraulic characteristics of fractured media should be a function of: the permeability tensor, K_{ij}, which reflects the nature of the aperture distribution; the effects of the stress tensor, σ_{ij}, on fracture permeability; and the geometry of the different fracture sets and the degree of interconnection. He also agreed with Castillo (1972) that the concept of flow through porous media is inadequate to describe flow behavior in jointed rock.

Hydraulic conductivity, K_f, of a single fracture through parallel plates for a single-phase, laminar flow

---

* Figure 14 is a graphical solution to the Laplace equation, $\nabla^2 h = 0$.

of a viscous incompressible fluid is:

$$K_f = \frac{\rho g}{12\mu} (2b)^2 \qquad (2.20)$$

where 2b is the fracture aperture (Gale, 1982). The specific discharge, q, and continuity equations for interconnected, continuous fractures are, respectively:

$$q = - K_f \frac{\partial h}{\partial \ell} \qquad (2.21)$$

and

$$\frac{\partial}{\partial \ell} K_f \frac{\partial h}{\partial \ell} = 0 \qquad (2.22)$$

where h is the hydraulic head and steady state conditions prevail.

In addition, empirical models were developed to describe variations of fracture permeability with normal stress. One such model by Snow (1968), that accounts for normal stress phenomena of hydraulic conductivity of parallel plate flow is (Gale, 1982):

$$K_h = K_o + [K_n (2b)^2/S_f] (P - P_o) \qquad (2.23)$$

where

K_h = horizontal hydraulic conductivity of fractures,

K_o = hydraulic conductivity at initial pressure P_o,

K_n = normal stiffness factor of the fracture,

S_f = fracture spacing,

P = pressure.

Another empirical model that accounts for pressure, by P.

Jones (1975), for carbonate rocks is:

$$K = K_o \left[\log (P_h/P)\right]^3$$

where K_o is a constant, and K, hydraulic conductivity, is equal to zero at P_h, the "healing" effective pressure (Gale, 1982).

A basic flow equation for multiple fracture systems was developed by Snow (1965). The flow of a single fracture is:

$$q_j = - \frac{(2b)^3}{12\mu} \rho g \, (\delta_{ij} - M_{ij}) \, I_i \qquad (2.24)$$

where q_j = fracture-flux vector per unit width of fracture $[L^3/T]$,

δ_{ij} = Kronecker delta,

M_{ij} = $n_i \, n_j$, a matrix formed by direction cosines of the normal to the fracture,

I_i = potential gradient vector.

Snow maintains that for each fracture that intersects a sample line has it image at a distance L equal to the length of the sample line and in the same direction as that of the sample line. Hence, the spacing between the fracture and its repetition is as follows:

$$w = L \, |n_i D_i| \qquad (2.25)$$

where w = spacing between the fractures,

L = length of the sample line,

n_i = direction cosines of normal to fracture plane,

D_i = direction cosines of sampling line.

Thus, the permeability of a medium for a single fracture is given by:

$$K_{ij} = \frac{1}{3L} \frac{b^3}{|n_i D_i|} (\delta_{ij} - M_{ij}) \qquad (2.26)$$

where K_{ij} is the intrinsic permeability tensor (L^2). The permeability of a given station is the sum total of each individual fracture (Gale, 1982).

Other important factors put forth by Gale (1982) are: (1) a strong correlation exists between surface fracture geometry and subsurface fracture geometry; (2) fracture porosity decreases logarithmically with depth; (3) fractures have highly nonlinear deformation characteristics; and (4) fracture interconnection with other fractures determines to a great extent the rock mass permeability.

Gale (1982) intentionally restricted his discussion on fracture-flow phenomenon to crystalline rock (igneous and metamorphic rocks). He cited at the beginning of his article that fractured carbonates are hydrologically distinct from other fractured rocks, because fluid flow is dominated by solution channels.

Duguid (1973) developed a system of equations that is coupled by the interaction of the fluid out of the primary pores and into the fractures. The interaction term describes the mass flux from the pores into frac-

tures by a pressure differential. Gale (1982) asserts that Duguid's theoretical approach to non-steady, fractured porous media flow is the most promising development as of late. The system of equations derived by Duguid (1973) are:

$$(1 - n_2)\, n_1\, \beta\, \frac{\partial P_1}{\partial t} + (1 - n_2)\, n_2\, \beta\, \frac{\partial P_2}{\partial t} + \frac{\Gamma}{\rho} - \frac{K_1}{\mu}\, \nabla^2 P_1 = 0$$

$$(1 - n_1)\, n_1\, \beta\, \frac{\partial P_1}{\partial t} + (1 - n_1)\, n_2\, \beta\, \frac{\partial P_2}{\partial t} - \frac{\Gamma}{\rho} + \nabla \cdot (q_{2S}) = 0$$

$$(q_{2S}) = -(K_2/\mu) \cdot [\rho\, (\partial (q_{2S})/\partial t) + \nabla P_2] \qquad (2.27)$$

where

n_1 = primary porosity or matrix porosity,

n_2 = fracture porosity,

β = coefficient of compressibility of water,

P_1 = pore pressure in the matrix,

P_2 = pore pressure in the fracture,

Γ = mass flow rate from block to fracture,

K_1 = intrinsic permeability of the matrix,

K_2 = intrinsic permeability along the fracture,

q_{2S} = space-averaged velocity over the fractures relative to the matrix,

Duguid developed a numerical solution to the preced-

ing equations by using the Galerkin finite element method (Duguid et al., 1974). Duguid et al. (1977), used the preceding numerical method to solve a hypothetical, leaky, confined aquifer. A very interesting result reported by Duguid et al. (1977), was that discharge (constant discharge problem) is divided between the primary pores and fractures in the ratio of matrix permeability to fracture permeability.

Gringarten (1982) summed it up quite well as to when usage of deterministic models and homogeneous models are appropriate. He states that deterministic models are based on duplication of the geometry, and discontinuous behavior of the fracture system; and are useful for small-scale geotechnical investigations. Whereas, homogeneous models that incorporate anisotropic behavior, are useful for a continuum of fractured media on a regional basis, such that fracture distributions are not too dispersed.

Karst hydrogeology is somewhat more complicated than fracture flow because conduits are introduced into the overall flow regime. Basmaci (1977) maintains that solution cavities and the like, constitute another class of porosity, and should be differentiated from primary and fracture porosities. In addition, he states that solution cavities behave as pressure conduits or seepage faces, and should be treated as boundaries to flow of wa-

ter in karst regions.

Figure 15 depicts the mean hydraulic conductivity and corresponding distribution for a given volume (after Basmaci, 1977). Mean values of hydraulic conductivity of laboratory samples are the smallest. Mean values obtained from drilled holes are 2 orders of magnitude larger than laboratory samples. Mean values for a basin are 3 orders of magnitude larger than drilled-hole values. The high values for a basin are a function of the karstification (development of solution cavities).

In summary, an understanding of the physics of groundwater flow is crucial in properly assessing groundwater regimes. In addition, the rate of water flow and skeletal deformation of porous materials are contingent on the mechanical behavior of the following main parameters: (1) porosity, (2) permeability, and (3) compressibility (Houstin et al., 1982).

2.4 Spring Flow Assessment and Related Methodology

Natural discharge from groundwater occurs in the form of springs and seeps. A classification based on spring discharge is given in Table 3 (after Davis and DeWiest, 1966). A spring can be further defined by the following parameters: type of aquifer, chemical characteristics, water temperature, direction of water migration, relation to topography, and geologic structure.

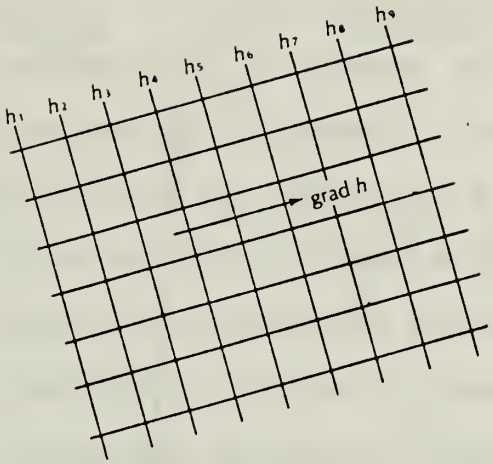

Figure 14. Equipotential lines, h_1 through h_9, in a two-dimensional flow field and the gradient of h (After Fetter, 1980).

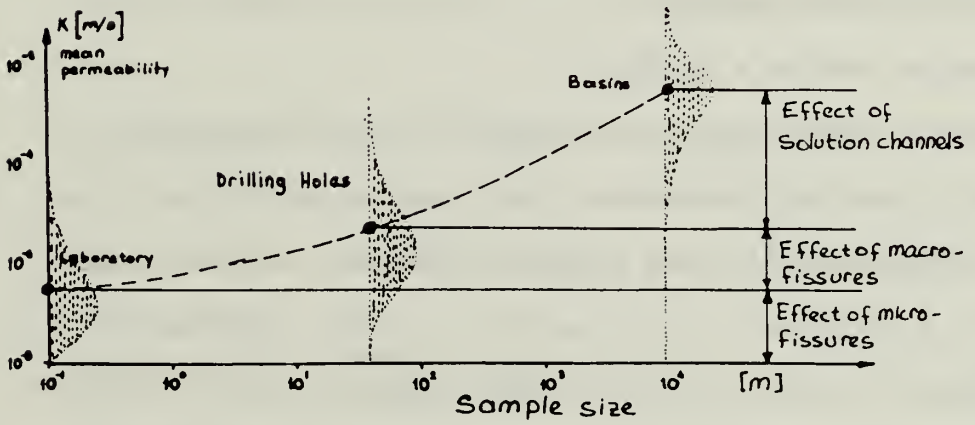

Figure 15. A schematic representation of the scale on karst permeability or hydraulic conductivity (After Basmaci et al., 1977).

A spring is any natural discharge of groundwater on the surface that is large enough to flow into a rivulet (Davis and DeWiest, 1966). Seeps discharge in the form of surface flow, and as a result do not form rivulets.

Spring discharge is a function of the aquifer permeability, area contributing recharge to the aquifer, and the quantity of recharge. A useful analytical tool in aquifer assessment, related to spring discharge, is presented by White et al. (1974). The authors assert that spring hydrographs should provide information on response of aquifers to precipitation events. The spring hydrograph, Figure 16, depicts two key parameters than can be obtained. The first parameter, the discharge ratio, is defined as the ratio of maximum discharge, Q_m, to base flow discharge, Q_B,

$$\text{Discharge Ratio} = Q_M/Q_B \tag{2.28}$$

The discharge ratio is a measure of the "flashiness" of an aquifer. Another parameter that can be extracted from a spring hydrograph is the characteristic response time, t_r, which is defined as the length of time necessary for the discharge to fall to $1/\varepsilon$ (approximately -37%) of Q_o. The exhaustion coefficient, ε, is also related to Burdon's (1963) exhaustion coefficient by

$$t_r = \frac{1}{\varepsilon} = \exp(1) = 0.368 \tag{2.29}$$

The recession limb of the hydrograph provides the follow-

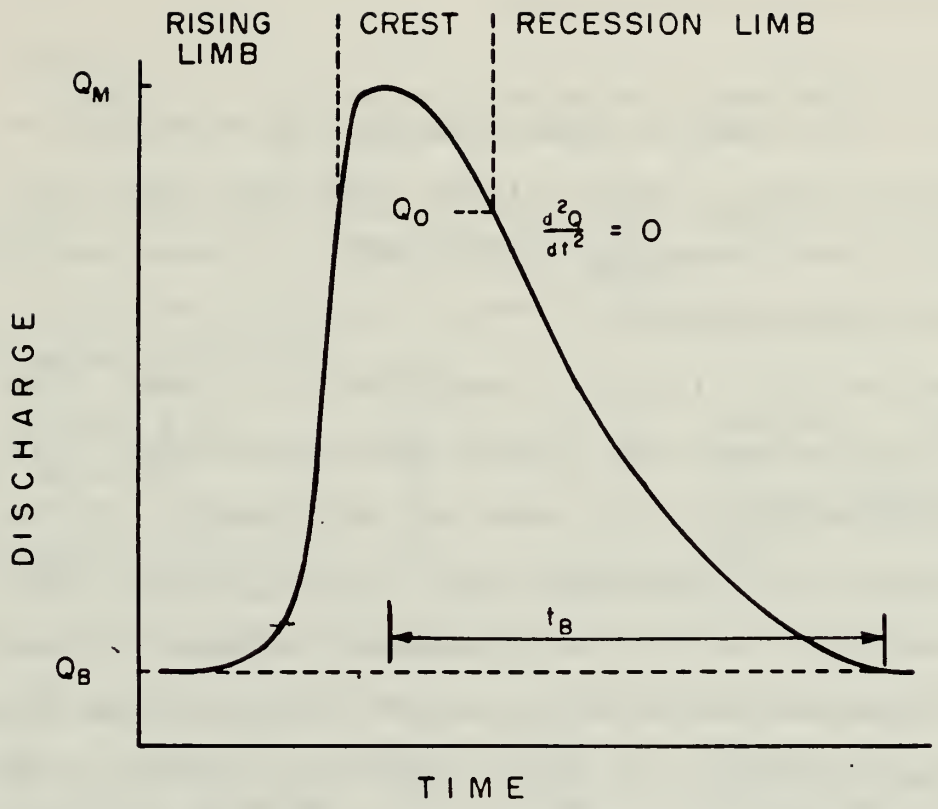

$Q = Q_O K^{-t}$ (LINDSLEY, KOHLER, & PAULUS)

$Q = Q_O e^{-\epsilon t}$ (BURDON)

DISCHARGE RATIO = $\frac{Q_M}{Q_B}$ (dimensionless)

EXHAUSTION COEFFICIENT = $\epsilon = \ln K$ ($time^{-1}$)

RECOVERY TIME = t_B

RESPONSE TIME = $t_R = \frac{1}{\epsilon}$

Figure 16. Schematic hydrograph for high discharge from a carbonate spring (After White et al., 1974).

ing exponential decay function:

$$Q = Q_o \exp(-\varepsilon t) \tag{2.30}$$

where Q is discharged at time t, and Q_o is discharge at time equal to zero. White (1974) maintains that discharges near the hydrograph crest don't fit the simple exponential form very well.

White et al. (1974), identified at least four hydrogeologic factors that control spring response: (1) aquifer hydrogeology, (2) stage of development of the conduit system, (3) catchment area for the springs, and (4) piezometric level of the groundwater. Table 4 lists typical values of discharge ratio and response time for fast, intermediate, and slow response springs. In addition, the rate of recovery, t_B, for springs is a function of the remaining storage of groundwater (Figure 16).

The variability, V'_a, of a spring can be determined by the following formula:

$$V'_a = \frac{Q_{max} - Q_{min}}{Q_{md}} \tag{2.31}$$

where Q_{max} is the maximum discharge, Q_{min} is the minimum discharge, and Q_{md} is the median discharge (Davis and DeWiest, 1966). The time period for calculation of variability must be specified. Variability is a key indicator of the storage capacity of an aquifer. For example, aquifers of large storage capacity may have only a

Table 4. Calculated Discharge Parameters for Selected Karst Springs

Springs	Q_{max}/Q_{base}	t_R (days)	Source of Data
Fast-Response Springs			
Rock Spring, Pa.	42	7.3	Jacobson (1973),
Penns Cave, Pa.	96	19.0	White and mack (1968)
Davis Spring, W.Va.	91	4.1	USGS
Intermediate-Response Springs			
Thompson Spring, PA	9.5	70	Jacobson (1973
Tuscumbia Spring, AL	7.0	65	USGS
Aghia Eleousa (Greece)	7.5	86	Aronis et al., (1961)
Slow-Response Springs			
San Marcos Springs, TX	1.6		Garza (1962)
Silver Spring, FL	1.5		Ferguson et al., (1947)
Ras-el-Ain Spring, Syria	1.16	2,070 (5.67 years)	Burdon and Safadi (1963)

(after White, 1974)

slight fluctuation in discharge, and as a result, a low variability (less than one).

Almost all first magnitude springs eminate from basalt, carbonate, boulder or gravel aquifers (Table 5). Other aquifers such as sandstones, conglomerates, and alluvial sand lack sufficient transmissivity to form first- or second-magnitude springs.

The most common cause of spring occurrence is lateral or vertical variation of permeability. Vertical variation would include a permeable unit overlying an impermeable one. Lateral variation could be structurally controlled by faulting where a permeable unit is offset next to an impermeable one. Other examples of spring occurrence are: (1) intensely fractured zones of brittle rock caused by faulting; (2) granular or unconsolidated rocks crossed by faults that become an impediment to groundwater flow; and (3) folded and tilted geologic units, permeable or impermeable or both, exposed at the surface (Davis and DeWiest, 1966).

The remainder of this section will discuss methodology to properly assess spring flow parameters. The primary emphasis is on carbonate rocks, since this particular lithology is the dominant rock type in the study area.

To determine the recharge area for a spring requires an extensive amount of data collection. Preliminary in-

Table 5. Meinzer's Classification of Spring Discharge

Magnitude	English Units	Metric Units
First	Greater than 100 ft^3/sec	Greater than 2.83 m^3/sec
Second	10 to 100 ft^3/sec	0.283 to 2.83 m^3/sec
Third	1 to 10 ft^3/sec	28.3 to 283 liters/sec
Fourth	100 gal/min to 1 ft^3/sec	6.31 to 28.3 liters/sec
Fifth	10 to 100 gal/min	0.631 to 6.31 liters/sec
Sixth	1 to 10 gal/min	63.1 to 631 ml/sec
Seventh	1 pt/min to 1 gal/min	7.9 to 63.1 ml/sec
Eighth	less than 1 pt/min	less than 7.9 ml/sec

(after Davis and DeWiest, 1966)

formation gathering includes acquisition of: black and white aerial photographs of the study area, geologic maps and hydrogeologic maps (if available), and previous hydrogeologic findings. Information obtained from aerial photographs include: geomorphology; lineaments traces, such as fractures and faults; formation contacts; and attitudes of formations (direction of dip and strike).

The next phase of the investigation entails on-site reconnaissance that substantiates or refutes previous geologic investigations. Fracture measurements are taken at certain locations to determine orientation and intensity. In addition, observation of soil cover, vegetation cover, and landforms are recorded.

Fracture measurements could conceivably lend insight to flow direction and deformational behavior of the rock. If a strong fracture orientation exists in a given locale, combined with known potentiometric levels, direction of flow can be reasonably ascertained (Figure 17). Also, strong correlation exists between orientations of lineations observed from aerial photographs versus measurements of fractures in the field (Hanson, 1973). Hanson (1973) concluded that 96% of the springs in his study area are associated with mapped linear trends.

Stearns (1967) demonstrated that the frequency of fractures is a function of lithology (Figure 18). Fracture frequency is approximately four times higher for

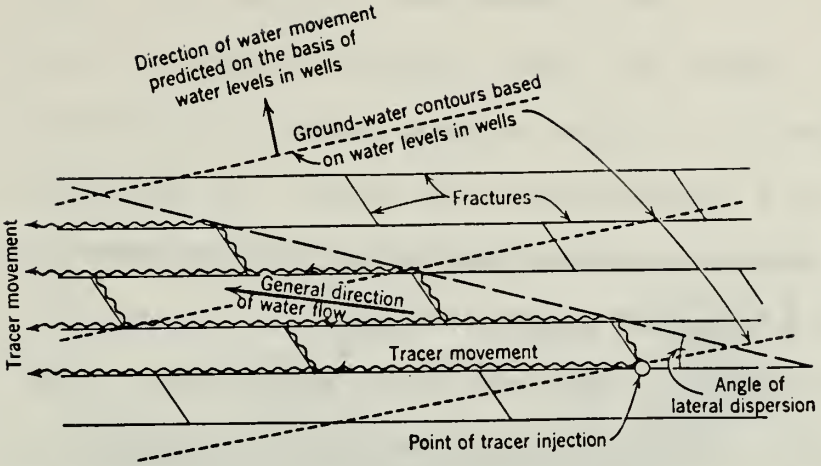

Figure 17. Two-dimensional fracture pattern showing the relation between true flow and direction inferred by drawing orthogonal lines to the potentiometric contours (After Davis and DeWiest, 1966).

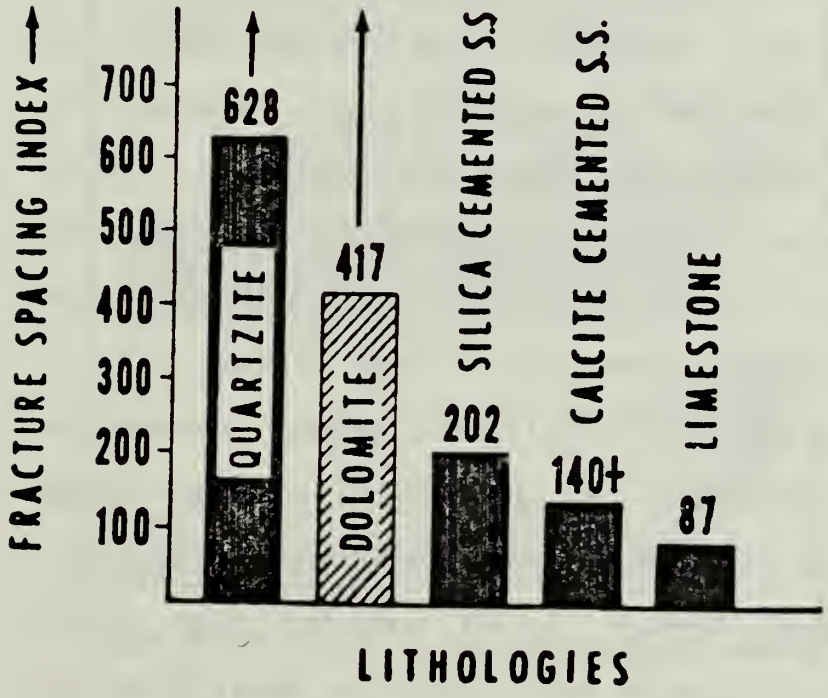

Figure 18. Histogram depicting frequencies of fractures for various lithologies (After Stearns, 1967).

dolomites than it is for limestones (Figure 18). The fracture space index on the vertical scale of the histogram, Figure 18, is the average number of fracture planes normal to a traverse of 100 feet. In addition, Stearns (1967) maintains that fractures can be used to predict attitude of faults and fault types.

Morphogenetic development of karst topography is dependent on solubility of the carbonate and the amount of rainfall (Tuttle, 1975). Figure 19 depicts the four stages of karst development of a soluble carbonate rock. Usually, dolomites are more resistant to dissolution activities than are limestones (Jakucs, 1977). Jakucs (1977), asserts that dolomites very rarely duplicate textbook karst forms, and in actuality are semi-karstic only. Another interesting item put forth by Jakucs (1977), open fissure (fracture) density and permeability of Lower Paleozoic limestone rocks are quite low, even though aggregate fracture density is high (Figure 20).

According to Dreiss (1974), the extent of conduit development in dolomites is a function of increasing amounts of calcium carbonate, opaque minerals, and porosity. In addition, Dreiss (1974) asserts that fine-grained carbonates are more susceptible to karstification than coarse-grained carbonates; attributing this to increased surface area in fine grained carbonates. Also, she maintains that bedding planes rather than fractures

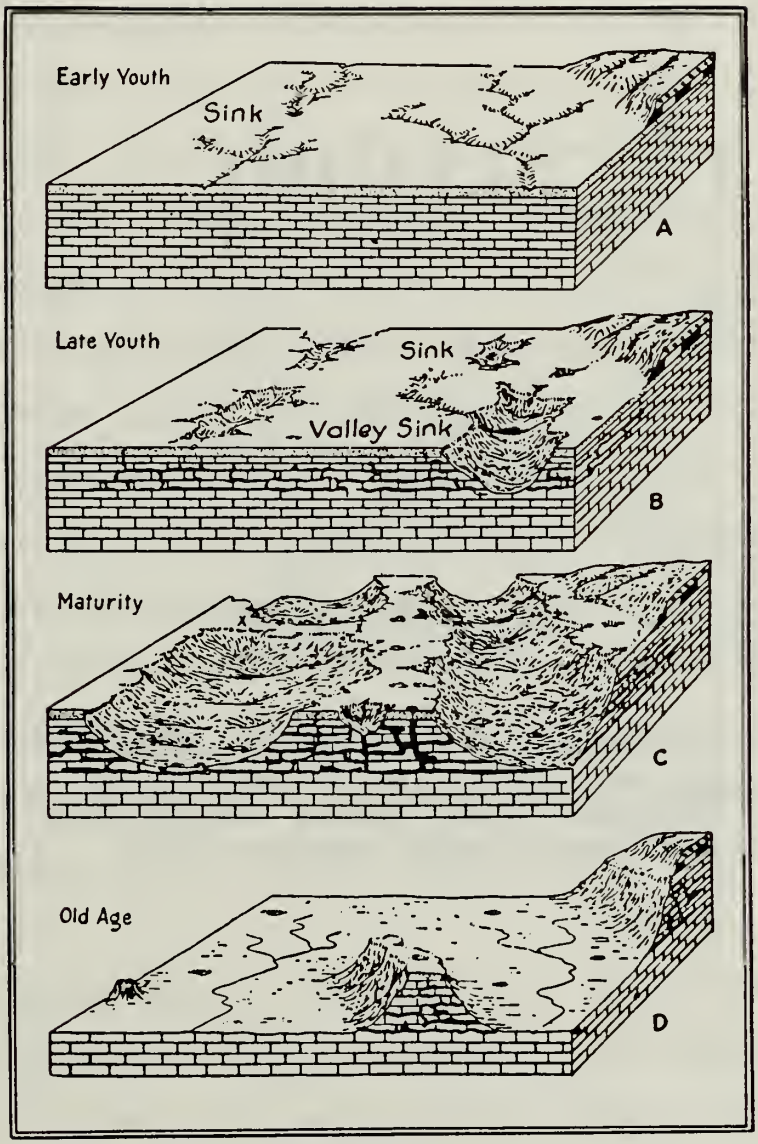

Figure 19. Four stages of karstic landform development (After Tuttle, 1975).

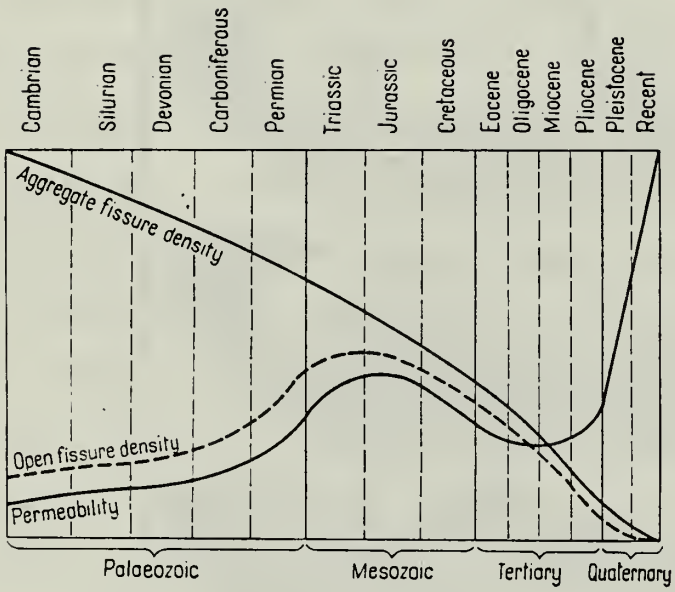

Figure 20. Permeability, open fissure density, and aggregate fissure density of limestone rocks versus the geologic time scale (After Jakucs, 1977).

in carbonates, control cavern occurrence.

It is important during the field phase that an investigator take note of geomorphological development of carbonates in the outcrop area. Davis and DeWiest (1966) state that a carbonate unit is permeable at depths greater than 1,000 feet if solution openings or swallow shafts and closely spaced joints are present, and shale partings are absent. Increased permeability in carbonates occurs along the crests of anticlines and the troughs of synclines (Davis and DeWiest, 1966). In addition, Davis (1966) maintains that in relatively homogeneous, carbonate rocks, the greatest amount of solution activity occurs at natural discharge points.

The field phase should include data collection and analysis of faults as a structural parameter that governs groundwater flow. Kastning (1977) asserts that no general statement of fault influence on groundwater flow in carbonates cannot be made without some detailed examination.

Tracers such as tritium, and helium can give much needed insight to the groundwater flow system (Davis and DeWiest, 1966). Tracers can be used to delineate the recharge area, determine seepage velocity (Marine, 1967), and determine local or regional flow systems.

Local or regional flow systems (Figure 21) can be deduced from temperature logs, variation of spring dis-

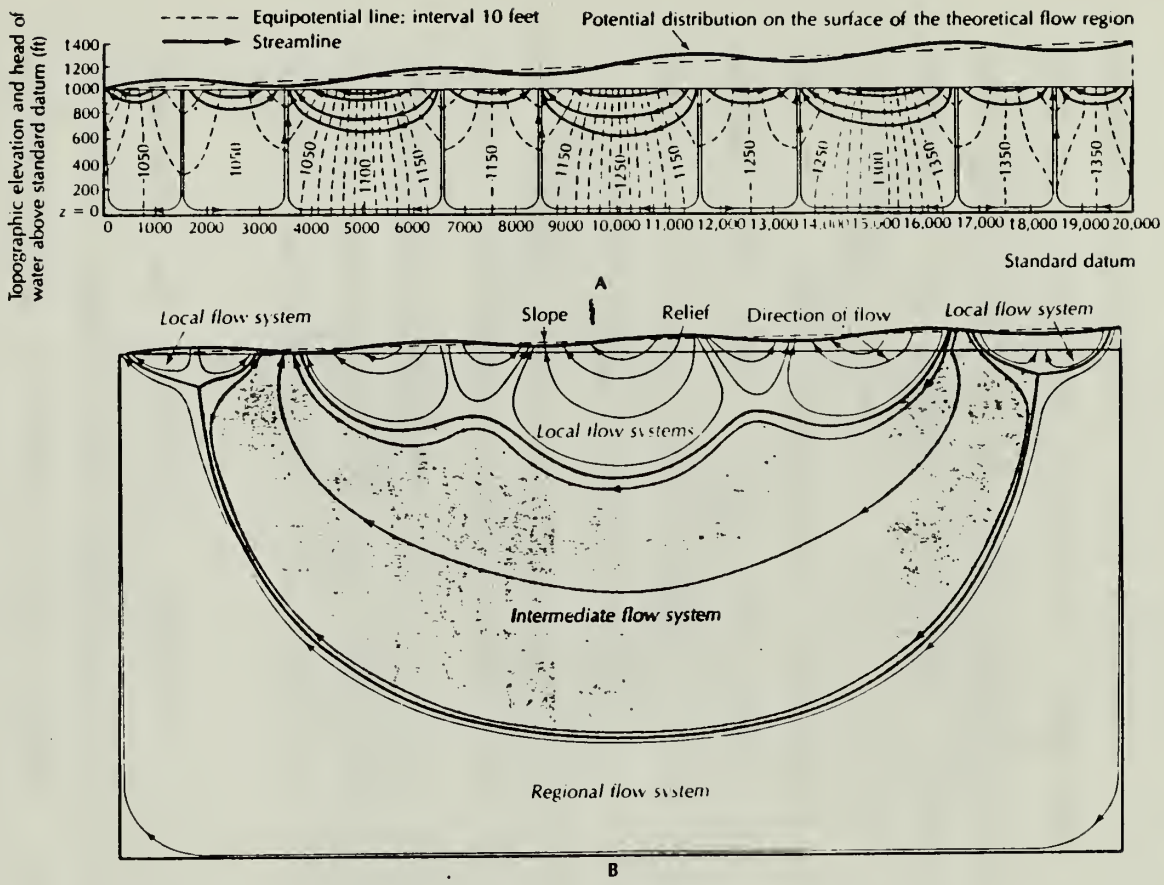

Figure 21. Parts A and B depict flow systems as a function of basin depth, topography, and potential distributions (After Fetter, 1980).

charge, and the degree of mineralization (Fetter, 1980). Temperature gradients within the earth's upper crust increases at about 1°C per 100 meters of depth. Regional systems are generally characterized by a higher degree of mineralization. In addition, water temperatures of local flow systems are close to the mean annual air temperature.

The use of black and white aerial photographs, a form of remote sensing analysis, constitutes a viable preliminary reconnoiter of a project area. Radar imagery is another useful remote sensing technique for geological investigations. SLAR (Side Looking Airborne Radar), is extremely useful in detecting lineations in heavily forested areas (Sabins, 1978).

Observation well hydrographs combined with spring hydrographs provide extremely useful information on aquifer properties (Davis and DeWiest, 1966). Observation wells, located adjacent to springs, provide information on piezometric level versus the amount and periods of spring discharge. In addition, well hydrographs depict long-term deprivation effects due to decreasing amounts of rainfall, and nearby production wells (Figure 22).

Fractures and solution openings, formation contacts, depth of well, and extent and condition of casing in wells; can be ascertained by the use of television logs.

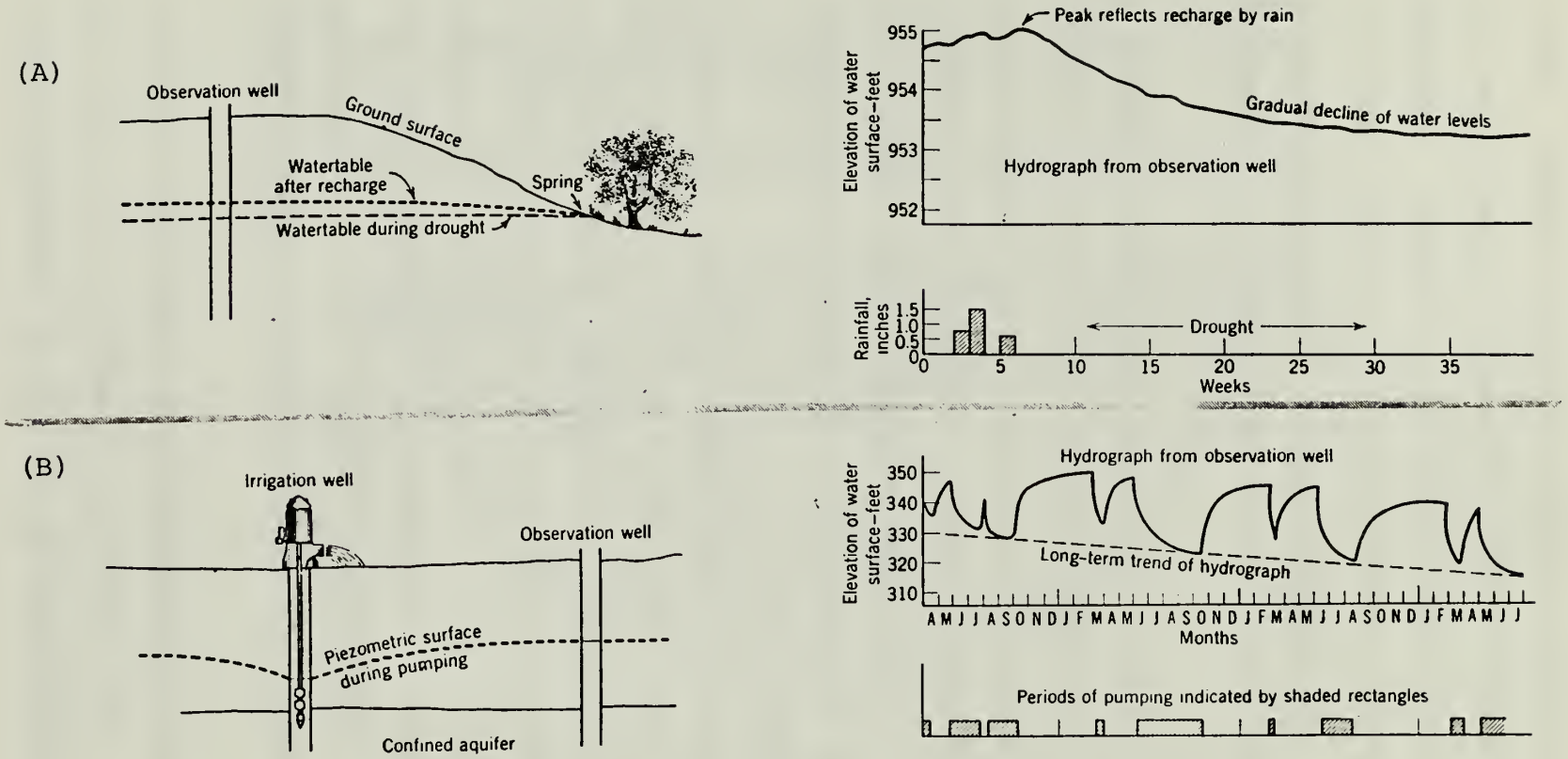

Figure 22. A. Hydrograph of observation well depicting changes in piezometric level in relation to spring discharge;
B. Hydrograph of observation well showing long-term deprivation of irrigation (After Davis and DeWiest, 1966).

Other common borehole geophysical techniques are: caliper logs, resistivity logs, temperature logs, spontaneous potential, and nuclear logs (Fetter, 1980). Information obtained directly from geophysical well logging includes porosity, lithology, temperature, and water zones.

Surficial geophysical methods include seismic, resistivity, and gravimetric surveys. Information obtained from surveys include: vertical variation in lithology, structural disposition of the area, and location of faults.

Petrophysical investigations of rock samples acquired from field recce entail permeability and porosity measurements. Falling-head and constant-head permeameter tests are conducted on unconsolidated or loosely cemented sediments (Davis and DeWiest, 1966). High-pressure gas permeameter tests can measure sample permeability of indurated sediments. Klinkenberg (1941) accounted for slip-flow phenomena associated with gas flow through porous media by the following equation:

$$K_1 = K_\infty \ (1 + b/p) \qquad (2.31)$$

where K_1 is the intrinsic permeability of the media, K_∞ is the intrinsic permeability as observed for an incompressible fluid, p is the average flowing pressure, and b is a constant characteristic of both gas and the medium.

Typical methods to determine porosity of rock samples in the laboratory include: the direct method, the

gas expansion method, the mercury injection method, the imbibition method, and the statistical method (Collins, 1961). The most accurate method to determine porosity is the imbibition technique. The gas expansion method based on Boyles gas law can determine pore volume by the following equation:

$$\text{Volume of pores} = V_p = V_B - V_a - V_b \frac{P_2}{P_2 - P_1} \qquad (2.32)$$

where V_B = bulk volume of the sample,

V_a = volume of sample chamber,

V_b = volume of evacuated chamber,

P_1 = initial pressure,

P_2 = final pressure (Collins, 1961).

This method is not quite as accurate as other techniques, yet it is the most widely used method in industry.

Houstin et al. (1982), assert that the most effective means to assess hydraulic conductivity of an aquifer is to conduct field pump tests of long duration with at least two observation wells, in conjunction with laboratory tests. Also, Houstin et al. (1982), claim the best estimate of insitu hydraulic conductivity is given by the following equation:

$$K = (K_{OUT} \cdot K_{IN})^{1/2} \qquad (2.33)$$

where K_{OUT} is hydraulic conductivity measured from drawdown tests (pump test), and K_{IN} is hydraulic conductivity measured from infiltration tests (rate of rise tests).

Extensive literature exists on well hydraulics for granular media. However, Gringarten (1982) states that there is scant field evidence in the literature that validates the double-porosity approach in fractured media. Yet, Briz-Kishore et al. (1982), conducted extensive pump tests in fracture crystalline rock in India; and concluded that the majority of the drawdown occurred within 10 minutes, and that the drawdown curves behaved very similar to that of porous media. In addition, Briz-Kishore et al. (1982), surmised that the amount of discharge for a given well has no relation with the number of fractures but depends only on the productivity of any single fracture.

Gringarten (1982) conducted pump and build-up tests in a limestone karst aquifer in 1976 (Figure 23). Observation wells, P_4, P_9, and P_2 were located at approximately the same distance from the pumping well; yet all three had distinctively different responses. Gringarten (1982) knew that observation wells P_2 and P_9 were connected to the pumping well by a horizontal fracture. With the use of the packer test and the horizontal model theory (Gringarten et al., 1973) for single fracture flow, he determined the average hydraulic conductivity to be .28 ft/day.

Less costly means to determine hydraulic conductivity include slug tests (Bouwer, 1978). In essence, a

slug test entails instantaneous removal of water with a bucket or bailer, and measuring the corresponding rise of water with a pressure transducer versus time. Another technique commonly used is a closed cylinder filled with sand or other material, submerged in the well until water equilibrium is attained, and then quickly pulling it out, and measuring the rate of rise. Slug tests are useful for partially penetrating wells in confined or unconfined conditions.

Potentiometric surveys of the aquifer enable the investigator to quantify the recharge area responsible for spring flow. This survey is normally conducted after the investigation of the structural geology and lithology of the project area has been determined. Steel tape and chalk are commonly used to measure water depth from a known surface elevation (Figure 24). Then, piezometric elevations can be determined at each point of interest in the project area and plotted on an overlay. Finally, a potentiometric map can be constructed from the plotted piezometric elevations, depicting distribution and occurrence of equipotential lines. General flow directions and water divides can be reasonably determined from the potentiometric map (Davis and DeWiest, 1966).

Water quality correlation can be used to identify aquifers responsible for spring flow (Walton, 1970). The Stiff (1951) graphical method using four parallel axes

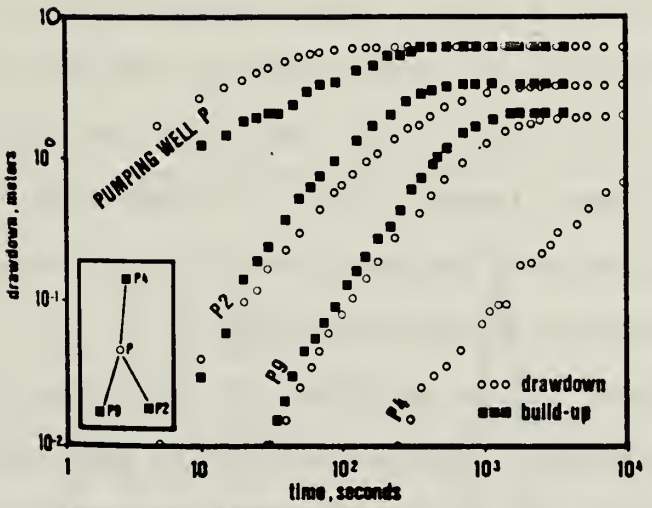

Figure 23. Drawdown and build-up curves for observation wells in a limestone karst aquifer (After Gringarten, 1982).

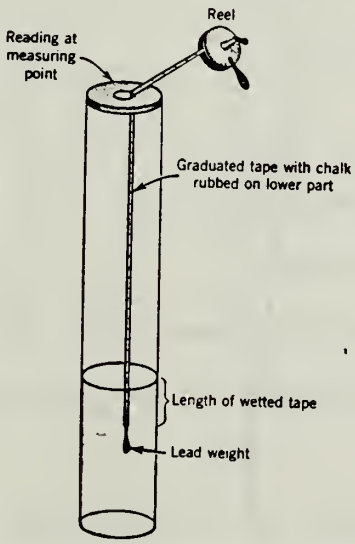

Figure 24. A sketch depicting water table depth measurement utilizing a steel surveyor's tape that can be read with an accuracy of .005 feet (After Davis and DeWiest, 1966).

and one vertical axis, may be useful in making comparisons of water types (Figure 25). Four cations (Na + K, Ca, Mg and Fe) are plotted along each axis to the left of zero, and four anions (Cl, HCO_3, SO_4, and CO_3) are plotted to the right of zero (Figure 25). Connecting the points of plotted anions and cations, depicts a characteristic shape for water of a given aquifer.

Storage coefficient of an aquifer can be obtained from well hydraulic methods. Another method to determine storage coefficient is based on water level fluctuations of a confined aquifer as a result of atmospheric pressure changes. The barometric efficiency, BE, is given by the following equation (Todd, 1959):

$$BE = \frac{\Delta h}{\Delta p_a / \gamma_w} = 1/(\alpha/n\beta+1) \qquad (2.34)$$

where

γ_w = specific weight of water,

Δh = change in water level,

Δp_a = change in barometric pressure,

α = compressibility factor of an aquifer,

n = porosity.

Also, the storage coefficient of a confined aquifer is defined by the following equation:

$$S_c = \gamma_w b\ (\alpha + n\beta\ ) \qquad (2.35)$$

where b is the aquifer thickness, and β is the compressibility factor of water. Once a barometric efficiency is

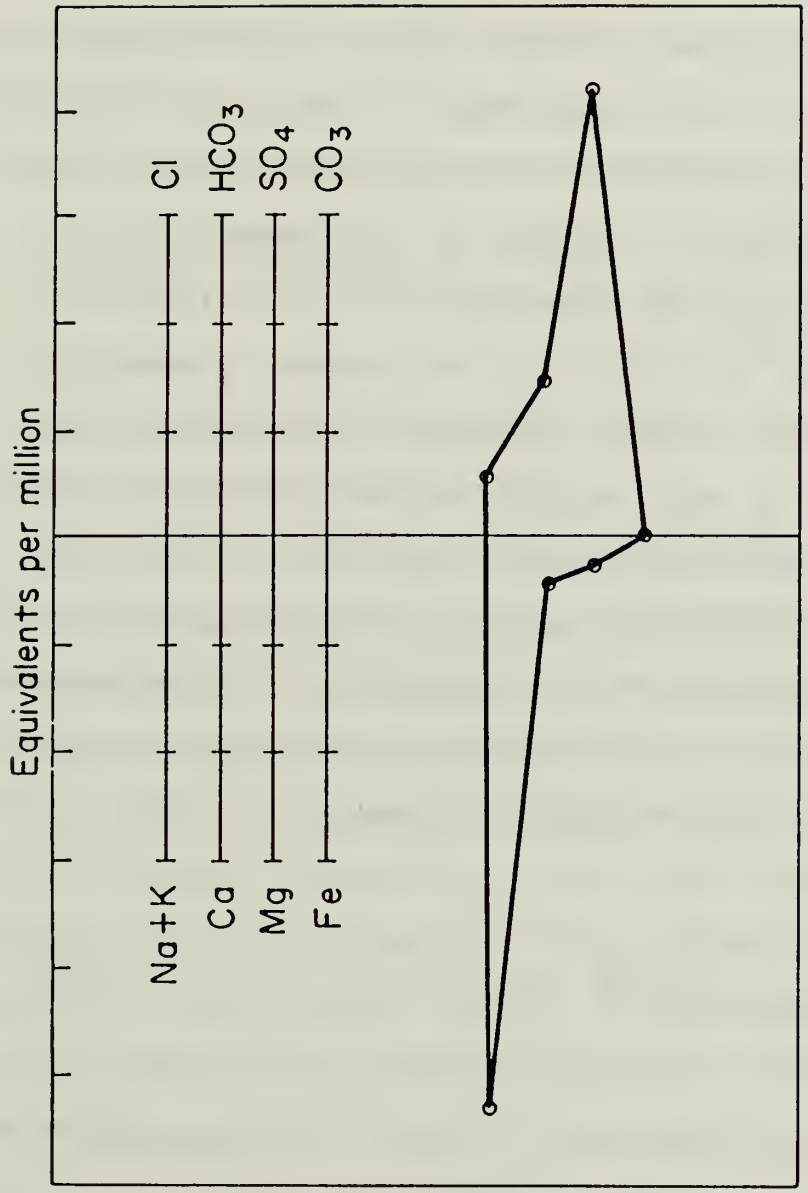

Figure 25. The Stiff graphical method (After Walton, 1970).

obtained (values range from .25 to .75), the aquifer compressibility, α, can be determined. Then, inserting the known value of α into Equation (2.35), yields the sought after storage coefficient. Davis and DeWiest (1966) assert that barometric efficiency is directly proportional to aquifer rigidity; where Δh (Equation 2.33) is small for rigid aquifers of low permeability, and large for unconsolidated sediments of high permeability.

Deprivation of spring discharge can be attributed to decreasing amounts of rainfall and nearby production wells. Harp et al. (1975), devised a methodology in which percentage of deprivation can be determined for each production well relative to one well in the same aquifer. The authors used a well hydraulics equation for a fully penetrating well in an unconfined, homogeneous aquifer of infinite aerial extent, to obtain total drawdown $s(x,y)$, due to adjacent production wells (x_i, y_i):

$$s^2(x,y) = \frac{1}{2\pi K} \sum_{i=1}^{n} Q_i \ln[(x - x_i)^2 + (y - y_i)^2] \qquad (2.36)$$

where

$s(x,y)$ = total drawdown, in feet, at some point x,y, due to n production wells,

$Q_i(x_i,y_i)$ = discharge in gallons per minute for the i^{th} production well at some point x_i,y_i.

The authors reasoned that s is a function of discharge Q,

and the natural logarithm of r^2

$$s^2 = f\ (Q,\ \ln\ r^2) \qquad (2.37a)$$

They deduced that discharge Q is inversely proportional to the natural logorithm of r^2. Based on the preceding logic, Harp et al. (1975), assert that the deprivation contribution for each production well in relation to a well in a common aquifer can be expressed as follows:

$$\text{Deprivation contribution of } i^{th} \text{ well} = \frac{Q_i/\ln\ (r_i^2)}{\sum_{i=1}^{n} (Q_i/\ln(r_i^2))} \qquad (2.37b)$$

The authors concluded that this concept should be applicable to confined aquifers also.

In summary, springs represent natural discharge points for a carbonate aquifer. Topographic relief provides the hydraulic gradient, and geologic structure influences the direction of groundwater to discharge points (White, 1977). The magnitude and variability of spring flow is closely related to: (1) the hydrogeological properties of the aquifer, (2) the piezometric level, (3) the area of the catchment basin, (3) the amount of annual recharge, and (4) deprivation effects of adjacent production wells.

2.5 Previous Hydrogeologic Findings of Artesian Spring Flow, Sulphur, Oklahoma, Area

Charles N. Gould (1906), a geologist, forwarded a report to the Secretary of the Interior. The contents of

the report focused primarily on location, amount of flow, status of development, and character of the springs in Platt National Park (Travertine District, Chickasaw National Recreation Area).

The report revealed that a total of 33 springs were located; of which 6 were freshwater springs, and the remainder were mineralized. Gould (1906) reported locations of the springs in relation to well known landmarks or springs. Unfortunately, a grid system was not utilized, and the exact location of some of these springs that have sinced ceased flowing, is unknown to date.

Gould (1906) estimated freshwater discharge to be approximately 2,000 gallons and 1,500 gallons per minute for Antelope and Buffalo, respectively. At the time of the report both springs were not developed or modified.

Gould (1906) postulated that the source of water for the springs in the park was from the upper part of the Simpson. He based this on one log from a well. He did not state the location of this well. Also, he reported that 4 artesian wells, north of the park, in the city of Sulphur, were flowing at an approximate rate of 200,000 gallons per day. He did not divulge locations of the artesian wells.

Gould and Schoff (1939) conducted a hydrogeologic investigation of the park during the summer of 1939 when Buffalo and Antelope ceased flowing. The authors con-

cluded that the dwindling spring flow in the park was due to diminished amounts of rainfall, and aquifer deprivation of the free flowing wells in the city of Sulphur.

Gould and Schoff (1939) reported that 14 springs could not be located since the initial investigation in 1906. Also noted, was that the Black Sulphur, Pavillion, and Hillside Springs combined flow for 1939 was one-fifth of the reported value in 1906.

Schoff (1939) determined the annual recharge to be approximately 1 foot. The source or area of recharge for the mineralized springs and the Sulphur artesian basin was ascertained to be approximately 12 square miles of the outcropping Simpson Group, in the Sulphur Syncline, southeast of Sulphur (Plate I). Schoff (1939) surmised that the surface elevation of the outcrop area was approximately 200 ft. higher than the surface elevations of the mineralized springs and flowing wells in the city of Sulphur, which would account for the artesian condition. In addition, the authors postulated that the permeable sandstone beds provided the main source of water for the mineralized artesian springs. The authors reasoned that the pressurized water of the Simpson Group flowed through the joints and fractures in the overlying Viola and Pontotoc.

Schoff (1939) claimed that the source of water for Antelope and Buffalo Springs, and the city of Sulphur

wells was from the outcrop of the Pontotoc, east and south of Sulphur. He also speculated that because the catchment basin for the freshwater springs is small, spring discharge is particularly dependent on sustained precipitation events. In addition, Schoff (1939) stated that freshwater for the springs and the city of Sulphur wells could originate from the Arbuckle Group. Also, the investigators assert that the Pontotoc and the Simpson are to a certain extent independent aquifers.

Prior to and during the investigation, an inventory of the artesian wells in the city of Sulphur were undertaken by the city officials. A list of 12 wells were submitted to the authors with a total combined discharge of 17,500 gallons per minute for the calendar year 1939. Finally, the authors concluded that the Vendome Well (an artesian well) was the primary reason for cessation of spring flow or reduced spring discharge. Gould and Schoff (1939) attributed this deprivation to a high, sustained flow rate of 2500 gallons per minute since 1922, and its close proximity to the park.

Hart (1972) deduced from his investigations of the area, that the west-northwest trending Sulphur Fault is the major controlling factor in the quality and quantity of water that flows from the springs in the park, and wells in the city of Sulphur. He postulated that the Sulphur Fault passes somewhere near Antelope and Buffalo,

exact location was unknown.

Contrary to previous investigators, Schoff and Gould (1939); Hart (1972) surmised that the outcrop of the Arbuckle Group, east of Sulphur, is the source of water for Antelope and Buffalo Springs. He substantiated this finding by the following correlations:

(1) water quality analysis (dissolved-solids content of 300 mg/l, calcium carbonate type),

(2) potentiometric head in the outcrop area of the Arbuckle Group versus surface elevations of Buffalo and Antelope, and

(3) well hydrographs of the outcrop area of the Arbuckle Group versus spring hydrographs. He also determined that the Pontotoc is relatively impremeable, and serves as a confining layer, lying unconformably over older formations.

Hart (1972) claimed that another recharge area was responsible for spring flow in the park. The author asserts that south and southeast of Sulphur, the outcrop area of the Simpson Group is the recharge area for the only "true" mineral springs in the park, Bromide and Medicine. Location of these two springs is in the far west end of the park (Plate III). Discharge from these two mineral springs was estimated to be 1 gallon per minute. Hart (1972) attributed the steady, low-flow rate and mineralization (dissolved-solids content of 4,000 mg/l,

sulphur type) to the slow, but steady recharge rate of the outcrop area of the Simpson Group, and the overlying confining layer of the Pontotoc.

Hart (1972) reported that mixed waters, consisting of water from the Simpson and the elevated Arbuckle were responsible for the character of the water of the springs (Hillside, Pavillion and Black Sulphur) in the middle of the park, and north of the park in the flowing wells of the city of Sulphur. The results of the water quality analysis in the form of Stiff diagrams, graphically depicted higher than normal amounts of sodium and chloride than are normally present in waters of the Arbuckle Group (Figure 26). The dissolved solids content of these springs was reported to be from 530 to 816 mg/l, with an estimated combined flow at 100 gallon per minute. The dissolved solids content of the Vendome Well was reported to be 1,200 mg/l, with an estimated discharge rate of 1,000 to 2,000 gallons per minute.

Hart (1972) concluded that the Sulphur Fault is the primary controlling feature isolating the freshwater springs, Antelope and Buffalo, from the remainder of the springs in the park. He attributes the occurrence of mixed waters in the center of the park and north of the park to waters from the small veneer of Simpson sediments overlying the elevated Arbuckle dolomite. He determined that the springs, Bromide and Medicine, originate from

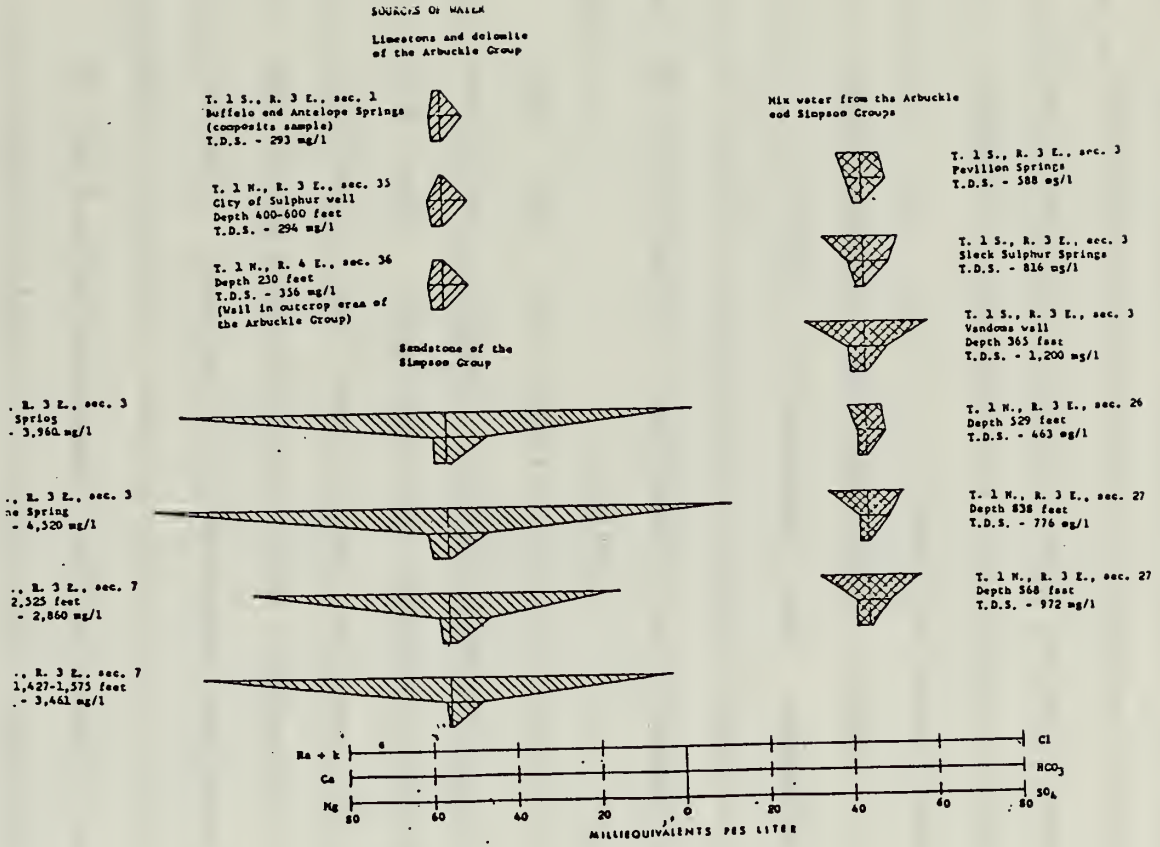

Figure 26. Water analysis of the Sulphur, Oklahoma, area by modified Stiff diagrams in milliequivalents per liter (After Hart, 1972).

the sandstone of the Simpson Group. He substantiated this particular finding by conducting a water quality analysis of the Simpson Group at depths of 2,525 feet and 1,575 feet in T.IN., R3E., Sec. 7 (Figure 26). Finally, Hart (1972) concurred with previous investigators, the occurrence of artesian springs in the park was the result of pressurized water flowing upward through fractures and joints in the younger, overlying formations; ultimately discharging from the Pontotoc Group.

Harp et al. (1976), conducted an investigation primarily to determine the deprivation effects of production wells on spring flow in the park. Also, the authors presented additional information to clarify and elucidate upon Hart's (1972) findings.

Harp et al. (1976), ascertained that two main aquifers, namely the Simpson and the Arbuckle, were responsible for spring discharge in the park. They estimated the recharge area for the mineralized springs to be approximately 20 square miles of the Simpson Group outcrop located south and southeast of the park. The recharge area for Buffalo and Antelope was estimated to be 40 square miles of the Arbuckle Group outcrop, east of the park. In addition, the authors correlated spring discharge, precipitation events, water quality analysis, and observation well hydrographs (two observation wells were completed in 1972) to substantiate the source and

occurrence of the freshwater springs. The two observation wells were completed in the Arbuckle Group, verified by a well-site geologist.

The authors provided information on location (Figure 27), water quality analysis (Table 6), and discharge rates of selected wells and springs in the project area. Bromide and Medicine springs were not flowing at the time the authors conducted the investigation. Harp et al., estimated the combined discharge of Pavillion, Hillside and Black Sulphur Springs to be between 100 and 200 gallons per minute. The authors concurred with Hart (1972), that these springs and the wells to the north, derive their water from both the Simpson and Arbuckle aquifers.

Harp et al. (1976), selected 3 well fields and 2 wells that discharge significant amounts of water annually, that could adversely affect spring discharge in the park (Figure 28). The authors presented pumpage data for the three well fields, and estimated average discharge rates for the two flowing wells, Vendome and Wyandotte.

To determine deprivation, the authors used the following steady-state, well hydraulics expression for total drawdown due to production wells in an isotropic, confined, homogeneous aquifer at some point of interest:

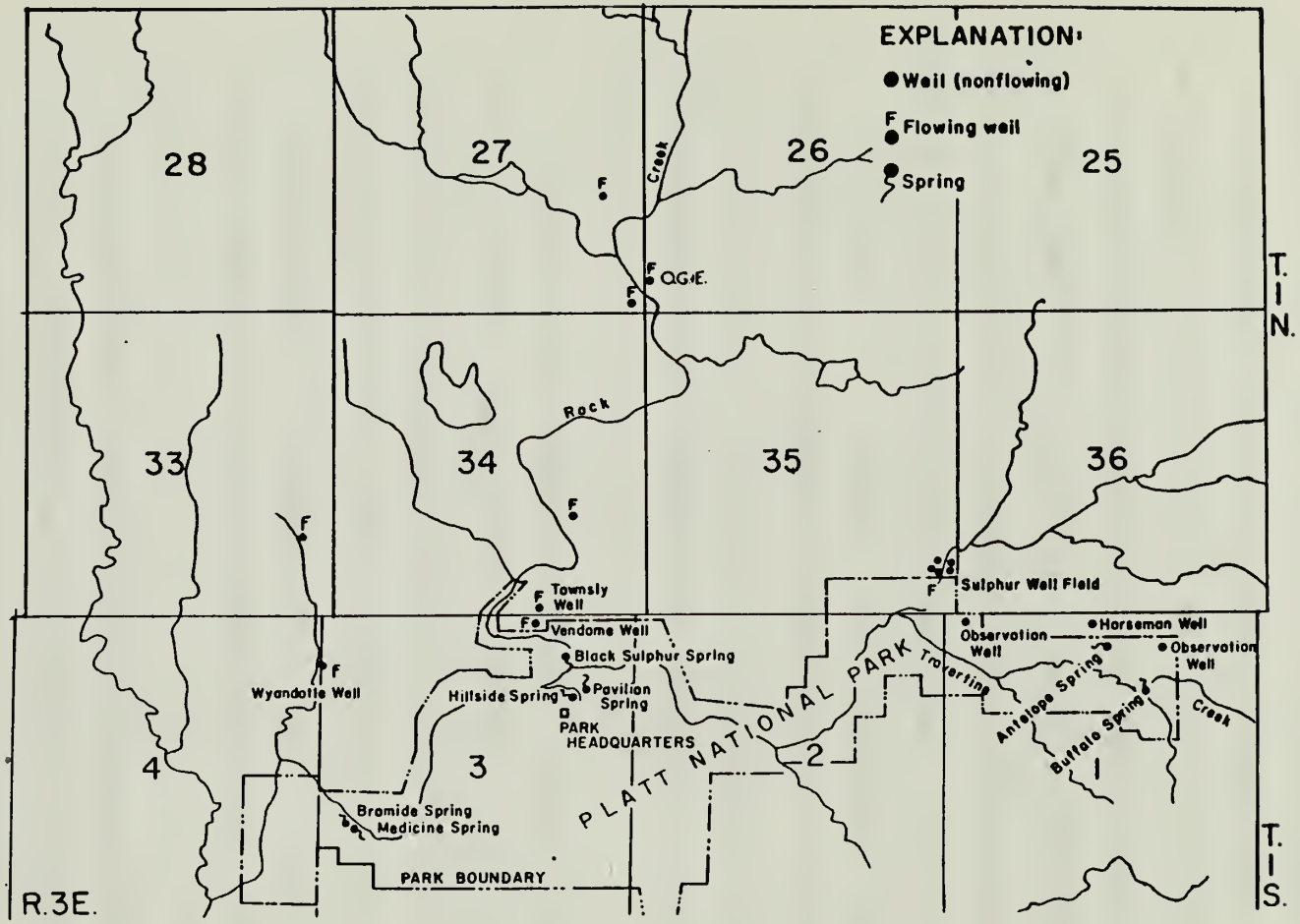

Figure 27. Location of selected wells and springs; Sulphur, Oklahoma, Area (After Harp, 1976).

Table 6. Water Quality Analysis of Selected Wells and Springs in Project Area (mg/l)

	Na	Ca	Mg	Cl	HCO_3	SO_4	$CaCO_3$	TDS
Observation Well No. 1	20	43	29	5.5	272	36	228	—
Observation Well No. 2	48	36	43	18	374	43	267	—
Buffalo and Antelope Springs	44	50	30	8	290	0	249	293
City of Sulphur Wells Depth 400-600 ft	9	52	32	7	305	0	262	294
T.IN.R4E Sec 36 Depth 230 ft	55	60	30	7	364	9.6	274	356
Bromide Spring	1,340	50	30	2,020	610	48	249	3,960
Medicine Spring	1,490	68	36	2,370	610	14	318	4,520
T.IN.R3E Sec 7 Depth 2,525 ft	990	40	16	1,480	609	96	67	2,860
T.IN.R3E Sec 7 Depth 1,427-1,575 ft	1,230	16	6	1,800	550	24	65	3,461
Pavilion Springs	110	60	38	140	305	0	307	588
Black Sulphur Springs	254	51	28	350	316	0	244	816
Vendome Well	252	51	37	350	318	0	281	1,200
T.IN.R3E Sec 27 Depth 838 ft	187	30	20	262	304	0	158	776
T.In.R3E sec 27 Depth 868 ft	254	50	30	404	310	0	208	972
Wyandotte Well	300	50	40	-	400	-	-	1,673

(after Harp, 1976)

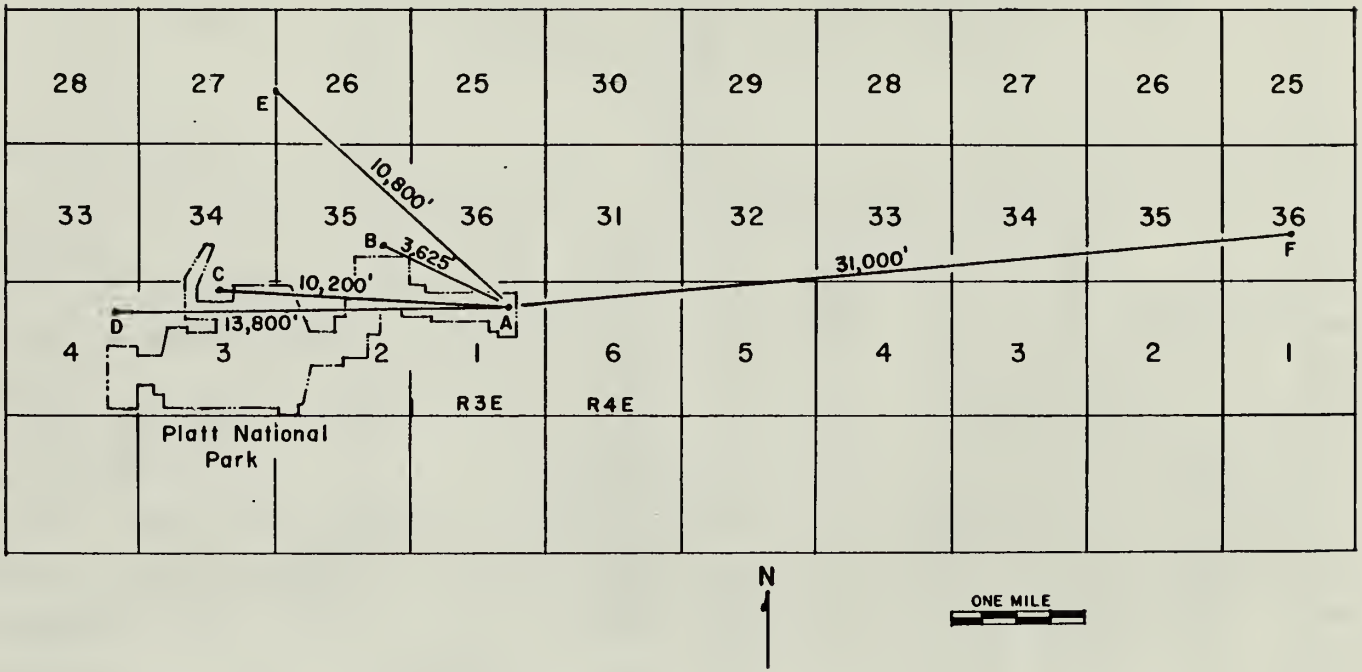

Figure 28. Well layout (After Harp, 1976).

$$s = \sum_{i=1}^{n} \frac{Q_i}{2\pi T} \ln \left(\frac{R_i}{r_i}\right) \tag{2.38}$$

where

n = 'n' number of wells,

s = total drawdown at some point due to 'n' number of wells,

Q_i = discharge rate at the i^{th} well,

T = transmissivity, constant for a homogeneous, isotropic, confined aquifer,

R_i = radius of influence,

r_i = radius from the point of interest to the i^{th} well.

They reasoned that $2\pi T$ is constant for a homogeneous, isotropic aquifer of constant thickness. Thus, equation (2.37) provides a simplified expression which relates the effect of i^{th} well to drawdown at the point of interest and assumes the form:

$$Q_i \ln \frac{R_i}{r_i} \tag{2.39}$$

Harp et al. (1976), assert that if $r_i > R_i$, then the production well will exert no influence on the point of interest. Hence, the proportional effect of each production well can be evaluated by using the pumpage data, Q, the distance from the i^{th} well to the production well, r, and the radius of influence, R, for each i^{th} well. The authors state that if R is unknown, then one can assume

that R is related to Q by some constant α', which is characteristic of the aquifer, such that

$$R = \alpha' Q \qquad (2.40)$$

Based on the preceding logic, the investigators determined the percentage of deprivation that each production well exerted on the area of Buffalo and Antelope Springs (Table 7). The computated data indicated that the highest deprivational effect in all instances, was the Vendome Well.

The major recommendation put forth by Harp et al. (1976), was that the flow of the Vendome Well and the Wyandotte Well be substantially decreased or plugged.

Fairchild et al. (1983), U.S.G.S. conducted an extensive hydrologic investigation of the Arbuckle Mountains. Even though their investigations did not focus specifically on the Sulphur area; their assessment of the aquifer characteristics of the Arbuckle-Simpson aquifer on a regional basis, is directly applicable to this study.

Fairchild et al. (1983), determined the average storage coefficient and transmissivity for the Arbuckle-Simpson aquifer in the outcrop area, to be .008 and 15,000 ft^2/day, respectively. The authors assumed that the aquifer behaves in a homogeneous manner on a regional basis. They determined the saturated thickness of the aquifer to be approximately 3,500 feet for the outcrop

Table 7. Relative Effects of Production Wells in the Vicinity of Antelope and Buffalo

Pumped Well	Pumpage Rate Q, gpm	Distance from well to Buffalo and Antelope, r, ft	α_1 = 8			α_2 = 10			α_3 = 20			α_4 = 30			α_5 = 40			α_6 = 50		
			R_1	$Q\ln\frac{R_1}{r}$	Depri-vation Contri-bution %	R_2	$Q\ln\frac{R_2}{r}$	Depri-vation Contri-bution %	R_3	$Q\ln\frac{R_3}{r}$	Depri-vation Contri-bution %	R_4	$Q\ln\frac{R_4}{r}$	Depri-vation Contri-bution %	R_5	$Q\ln\frac{R_5}{r}$	Depri-vation Contri-bution %	R_6	$Q\ln\frac{R_6}{r}$	Depri-vation Contri-bution %
Sulphur Wel Field B	488	3,625	3,902	36	13	4,887	146	20	9,754	483	22	14,631	681	20	19,510	821	20	24,387	930	19
Vendome Well C	1,498	10,200	11,983	241	87	14,978	576	80	29,957	1,614	73	44,936	2,221	67	59,915	2,652	63	74,894	2,988	61
Wyan-dotte Well	499	13,800	3,994	No Effect	0	4,992	No Effect	0	9,985	No Effect	0	14,977	41	1	19,970	185	4	24,962	296	6
O.G.& E. Well F	640	10,800	5,116	No Effect	0	6,395	No Effect	0	12,790	108	5	19,183	367	11	25,580	551	13	31,975	694	14
Winrock Well F	317	31,000	2,535	No Effect	0	3,168	No Effect	0	6,337	No Effect	0	9,506	No Effect	0	12,675	No Effect	0	15,844	No Effect	0

(after Harp et al., 1976)

area. In addition, the authors estimated the recharge to the aquifer at about 4.7 inches per year. Also, water-level fluctuations in the aquifer were reported to range from 8 to 53 feet each year in response to recharge from rainfall.

Fairchild et al. (1983), estimated that two-thirds of the Arbuckle-Simpson aquifer consists of limestones and dolomites. The authors claim that the occurrence and movement of groundwater in the Arbuckle-Simpson aquifer are strongly controlled by lithology and structure. They maintained that most springs are near faults or fractures that have been enlarged by solutioning of the more dense Arbuckle group. The authors assert that the resultant network of solution conduits occurs laterally along bedding planes; and along fractures, vertically and horizontally. Small sinks or swallow shafts in the valleys were encountered by the investigators in the outcrop area. Also, Fairchild et al. (1983), studied caliper logs of deep wells in the Arbuckle-Simpson aquifer. They concluded that solution cavities exist to a depth of at least 2,000 feet.

The authors conducted a potentiometric survey (Winter 1976, 1977) of the eastern part of the Arbuckle Mountains to determine the source and occurrence of groundwater. They concluded that generally the potentiometric surface follows the topography. They also stated

that the bulk of groundwater flow in the eastern portion of the Arbuckles is in an eastward direction with a typical hydraulic gradient of 20 feet per mile.

Fairchild et al. (1983), reasoned that the occurrence of artesian wells along Rock Creek in the vicinity of Sulphur, is due to the erosion of the land surface below the potentiometric surface of the confined Arbuckle-Simpson aquifer. The authors concurred with Hart (1972) that sufficiently higher surface elevations exist to the east in the recharge area, providing the necessary hydraulic head to warrant artesian conditions in the Sulphur area.

Fairchild et al. (1983), conducted an analysis of the ratio of recharge to average precipitation based on regional techniques proposed by Rorabaugh (1964, 1966). The authors reported that the ratio of recharge to average precipitation for the month of March to be.32, and for the months of May and June to be .15.

The authors conducted aquifer tests to determine storage coefficient, specific capacity, and transmissivity at point locations throughout the Arbuckle-Simpson aquifer. The specific capacity, amount of constant discharge in gallons per minute divided by the drawdown in feet for the period of pumpage, varied from .17 to 4.4 for the Simpson, and from .47 to 104 for the Arbuckle. The investigators reported that deep wells drilled in the

Arbuckle Group have the highest specific capacity. They attributed this phenomena to a greater probability of encountering interconnected solution cavities and fractures with increasing depth. The investigators obtained information from land owners and drillers that revealed the upper two hundred feet of the Arbuckle Group has a much lower permeability than the lower part.

Estimates of transmissivity were obtained from pump tests and regional techniques. Fairchild et al. (1983), used the modified nonequilibrium equation by Ferris (1962) to determine transmissivity T, from pump tests,

$$T = \frac{264Q}{\Delta s} \tag{2.41}$$

where discharge Q, is in gallons per minute, and Δs is change in residual drawdown, in feet, over one log cycle of time. The above equation assumes a fully penetrating well in a homogeneous, unconfined, isotropic aquifer of infinite areal extent. The investigators did realize that the Arbuckle-Simpson aquifer did not meet the above mentioned criteria, but decided that such tests would give only a rough estimate. Transmissivity determined from pump tests ranged from 40 to 2,500 ft^2/day. Fairchild et al. (1983), determined storage coefficient, S_c, from pump tests by the use of the modified nonequilibrium equation (Ferris, 1962)

$$S_c = \frac{.3T\ t_o}{r^2} \tag{2.42}$$

where

t_o = time intercept, in days, where the plotted straight line intersects the zero drawdown axis,

r = distance from the pumping well to the observation well.

The values of storage coefficient were reported to be in the range of 10^{-4} to 10^{-5}.

The authors determined the average storage coefficient and transmissivity by regional techniques developed by Rorabaugh (1966), to be .008 and 10,000 ft^2/day, respectively.

Another estimate of transmissivity, T, was determined by the use of Darcy's Law applied to spring discharge,

$$T = \frac{Q}{IW} \tag{2.43}$$

where

Q = spring discharge in cubic feet per day,

I = hydraulic gradient, in feet per feet,

W = width, in feet, of the cross section through which the discharge occurs.

The authors estimated the aquifer transmissivity to be 20,000 ft^2/day. The transmissivity of the aquifer was

based on only one spring in the area.

Fairchild et al. (1983), devised a hydrologic budget for the area,

$$P' = Q' + ET \qquad (2.44)$$

where

P' = average annual precipitation,

Q' = total average annual runoff,

ET = average annual evapotranspiration.

They estimated the annual average precipitation P, to be 38.4 in. This value was ascertained from 6 years of data and 3 rain gauge stations. The total average runoff Q', was determined to be 7.6 in. Average runoff was computed from discharge stations located on Mill Creek, Blue River and Pennington Creek at the periphery of the outcrop area. Then, the authors determined evapotranspiration to be 31 inches per year, or 80 percent of the average annual precipitation.

The authors reasoned that the surface runoff is divided between base flow and direct runoff. They arrived at an average value of 4.7 in. per year for base flow or groundwater flow. This value was based on low-flow periods when surface runoff is nil. Thus, groundwater flow accounts for 12 percent and direct runoff accounts for 8 percent of the average annual precipitation in the region.

Fairchild et al. (1983), conducted a water quality

analysis of 23 wells, 12 springs and 12 streams in the Arbuckle Mountain area. The authors reported an average dissolved solids content of 330 mg/l. Average water temperature of all groundwater surveyed was 62°F. This average temperature is almost identical to that of the mean annual air temperature of 62.5°. Also, samples taken at depths to 2,500 feet showed little or no change in dissolved solids content.

The investigators pointed out that beds of Arbuckle-Simpson aquifer become highly mineralized when they dip steeply beneath younger sediments along the periphery of the outcrop area. Fairchild et al. (1983), cited work done previously by Dott and Gunter (1930), and Case (1934) that dealt with the characteristics of waters of the Ordovician rocks that covered a broad area, including the Arbuckle Mountain area. The authors reported that these investigators had found that the concentration of dissolved solids increased at a rate of 10,000 mg/l per mile in the down-dip direction.

Finally, Fairchild et al. (1983), tabulated some well yields for the Simpson and Arbuckle groups. They reported that yields for the Simpson ranges from 100 to 400 gallons per minute. Also, yields for the Arbuckle range from 1 gallon per minute (shallow wells in dense dolomite with no interconnected fractures or solution cavities) to as high as 2,500 gallons per minute (deep

wells, in excess of 1,000 feet).

Hensch (1984) provided an update to the investigation conducted by Harp et al. (1976). He primarily addressed the stage versus flow relationship for the two freshwater springs, Buffalo and Antelope. In addition, Hensch (1984) was also tasked with updating pertinent hydrologic data for the study area and establishing a recession coefficient for the freshwater springs.

Hensch (1984) observed that Buffalo Spring wells up from a gravel bed into a circular retaining wall, 25 feet in diameter. Then, exits over a 4.5 ft. wide, rectangular-shaped spillway into a creek bed. He also observed additional water welling up into the creek bed, immediately downstream from the spillway. According to Hensch (1984) flow in the stream increased substantially. Estimating the discharge of springs in the creek to be three times that of the discharge from Buffalo Spring.

Hensch (1984) described Antelope Spring as a spring eminating from the base of the westward facing bluff into a shallow, irregular pool, approximately 100 square feet. Then, flow exits through an opening in the pool about 5 feet wide.

The author stated that stage measurements at both springs were done by park employees on an irregular basis. The stage readings, since 1969, were made on steel pins embedded at the base of each pool.

Hensch (1984) ascertained that both springs exit through a rectangular configuration, similar to that of a broad-crested weir. The author, together with previous investigators (Harp et al., 1976), determined that flow could be roughly approximated by the following expression

$$Q = (C)\ (b_w)\ H^{1.5} \tag{2.45}$$

where

Q = flow in c.f.s.,

C = constant dependent on weir shape,

b' = width of weir,

H = the depth of the pool at a specified point.

Since C and b_w are constants, the expressions can be simplified to the following equation:

$$Q = K'\ H^{1.5} \tag{2.46}$$

where K' is a constant. The investigator realized that both springs do not flow until a critical depth is reached. Hensch (1984) reasoned that the stage reading or pin reading P.R., for each spring must exceed the base of the weir-like opening before flow begins. Finally, after field reconnaissance, he formulated the following flow equation for Buffalo:

$$Q = 10.44\ (P.R. - 1.97)^{1.5} \tag{2.47}$$

and Antelope;

$$Q = 8.69\ (P.R. - .6)^{1.5} \tag{2.48}$$

The author attempted to determine the recession constant K_r, for the two springs. He used a method proposed

by Langbein (1940) and is referenced by Davis and DeWiest (1966). The method entails plotting discharge q_n (vertical scale), versus discharge q_{n+1}, where n = t (incremental time) - 1. Discharge values can be obtained from the recession limb of a stream hydrograph. Hensch determined the K_r, the total flow recession constant, to be approximately .7 for both springs.

He mentioned he could not determine which values represented groundwater flow, so he selected values, q_n and q_{n+1}, arbitrarily. It is unclear as to whether he understood, that all flow components the spring hydrograph represent groundwater flow. The difference in flow components (i.e., surface, interflow, etc.) between the stream hydrograph and the spring hydrograph is terminology. In all likelihood, he probably meant base flow, in lieu of ground water flow. In addition, he offered no explanation as to why it is necessary to determine a recession constant for the two springs, other than being tasked to do so.

It is apparent from previous investigations in the study area, that the regularity of spring flow in the park is declining at an alarming rate. Two separate aquifers, the Simpson and the Arbuckle, are responsible for the waters of the artesian springs in the park. The geology of the area, water quality, deprivation effects, and well and spring hydrographs in relation to precipita-

tion events have been addressed by various investigators in the past. It is also understood that each investigation provides additional input into the analysis of the artesian spring phenomena in the park. It is hoped that this author will provide additional insight to the parameters that govern artesian spring flow in the park.

CHAPTER III

METHODOLOGY

3.1 Geologic Control of Groundwater Flow

As stated previously, springs represent natural discharge points (sinks) of a carbonate aquifer. Determination of source occurrence and movement of groundwater to the springs requires an understanding of the geological parameters that govern groundwater flow (Table 8).

Geologic maps of the area were completed by Ham et al. (1945, 1954), and will be used extensively for this investigation. Aerial photographs (May and June, 1963) of the project area, scale of approximately 1:20,000, were acquired from the Oklahoma Geological Survey on a loan basis. Use of the aerial photographs and a stereoscope will enhance preliminary identification of structures, formation contacts, lineations (faults and fractures), and geomorphological features of the study area. Topographic maps (1978), scale 1:24,000, will be used in conjunction with aerial photographs to obtain locations of findings to within 1/16 of a mile, and provide information on surface elevations to within 5 feet of

Table 8. Effect of Hydrogeologic Setting on Carbonate Aquifers

Geologic Element	Control
Macro-Structure (folds, faults)	Placement of carbonate rock units relative to other rocks
Topographic Setting	Placement of recharge and discharge regions
Stratigraphic Sequence	Thickness and chemical character of aquifer
Mini-Structure (joints, fractures)	Orientation and transmissibility of primary flow paths
Relief	Defines hydraulic gradients

(after White, 1977)

accuracy.

Field reconnaissance will commence after the analysis of the aerial photographs and geologic map has been completed; to substantiate or refute previous findings. Structural features and lithology will be noted at selected sites. Also, the occurrence of surface features, such as sinks and shallow shafts, will be recorded.

In particular, field measurements of the fractures will be obtained in close proximity to the freshwater springs, Buffalo and Antelope. Fracture measurements will entail: the direction of traverse, the distance between fractures, fracture filling, fracture aperture and fracture orientation and dip. Fracture analysis and other field observations will be used to approximate the orientation and location of the Sulphur Fault in relation to the freshwater springs. In addition, the determination of the origin and occurrence of the freshwater springs will be discussed as a result of these findings and previous investigations (Hart, 1972).

A lineament map of the Arbuckle Group will be constructed from aerial photographs that depicts fracture orientation in relation to macro-structure, such as faults. This map will be used in conjunction with field measurements, structural geology of the area, and the potentiometric survey to assess general groundwater flow direction in the outcrop area (Davis and DeWiest, 1966).

A structural contour map of the surface elevation of the Arbuckle Group of the project will be constructed from: (1) well completion, reports and well logs submitted to the Oklahoma Corporation Commission; (2) domestic, municipal and industrial water well reports submitted to the Oklahoma Water Resources Board; and (3) thickness of stratigraphic units as determined by previous investigators (Ham et al., 1945, 1954, and 1978). The construction of this map should provide information for the inference of the Sulphur Fault and other faults in the area that lie at depth below the Pontotoc Group in the Sulphur area. In addition, a relationship could develop between potentiometric levels and the distribution of surface elevations of the Arbuckle Group.

3.2 Determination of the Physical Properties of the Simpson-Arbuckle Aquifer

Rock specimens will be obtained at selected sites from the project area during the field reconnaissance phase and returned to the petrophysics laboratory for determination of effective porosity and thin-section analysis.

Thin sections of representative lithologic units from the study area will be photographed, utilizing an Olympus Zoom Stereo Microscope, Model SZ-TR, and a Polaroid Land camera. Magnification of each thin section can be obtained by,

$$M = EP \times PEP \times Z \tag{3.1}$$

where

M = total magnification,

EP = Eyepiece magnification,

PEP = Photo eyepiece magnification,

Z = Zoom magnification.

Thin section analysis should reveal the general texture and fabric of the Pontotoc, Simpson and Arbuckle Groups.

Effective porosity measurements of selected core samples, representing the Pontotoc, Simpson, and Arbuckle Groups, will be ascertained by the use of the Helium Porosimeter. The porosity can be determined by the use of Boyles' Law (Collins, 1961):

$$P_1V_1 = P_2V_2 = \text{constant} \tag{3.2}$$

where

P_1 = Initial pressure,

V_1 = Initial volume,

P_2 = Final pressure,

V_2 = Final volume.

The following equations were derived by the author to obtain volume of the pores, V_p, for each core sample:

$$P_{vac} V_L + P_{vac} (\Delta V_{ch} - V_B + V_p) + P_1V_1 = P_2 (V_L - V_B + V_p + \Delta V_{ch}) \tag{3.3}$$

rearranging equation (3.3) and solving for V_p;

$$V_p = \frac{P_{vac} (V_L + \Delta V_{ch} - V_B) + (P_1V_1) - P_2(V_L - V_B + \Delta V_{ch} + V_1)}{(P_2 - P_{vac})} \tag{3.4}$$

where

V_p = pore volume of the core sample (c.c.),

V_B = bulk volume of the core sample (c.c.),

V_L = volume of the lines (c.c.),

V_{ch} = volume of the sample chamber (c.c.),

V_D = volume of disks in the sample chamber (c.c.),

$\Delta V_{ch} = V_{ch} - V_D$ (c.c.),

V_1 = volume of reference chamber number 1 (c.c.),

P_{vac} = initial vacuum pressure of V_L and $[V_P+\Delta V_{ch}-V_B]$ (negative gage pressure, p.s.i),

P_1 = initial pressure of V_1 (positive gage pressure, p.s.i.),

P_2 = final pressure of V_1, V_L and $[V_P+\Delta V_{ch}-V_B]$ (positive or negative gage pressure, p.s.i.).

Finally, effective porosity, n, can be determined by (Collins, 1961):

$$n = V_p/V_B \tag{3.5}$$

where V_p is the volume of the pores, and V_B is the bulk volume of the core sample.

Determination of the storage coefficient and the transmissivity of the Arbuckle Group, in close proximity to the freshwater springs, will be determined by several field methods and by the use of the groundwater model devised by Prickett and Lonnquist (1975). In addition, a regional technique utilized by Fairchild et al. (1983), will be employed to determine aquifer transmissivity in

relation to spring discharge.

An attempt will be made to determine the storage coefficient of the Arbuckle aquifer by a method derived originally by Jacob (1940) and reported by Todd (1959). This method is based on water level fluctuations in an elastic, confined aquifer in response to atmospheric pressure changes.

As discussed previously, the barometric efficiency BE is,

$$BE = \gamma_w \frac{\Delta h}{\Delta P_a} = \frac{1}{\frac{\alpha}{n\beta} + 1} \qquad (3.6)$$

where

γ_w = specific weight of water,

Δh = change in water level,

ΔP_a = change in barometric pressure,

α = aquifer compressibility factor,

n = porosity of the aquifer,

β = water compressibility factor.

Also, the storage coefficient S_c for a confined aquifer can be expressed as

$$S_c = b'\gamma_w (\alpha + n\beta) \qquad (3.7)$$

were b' is the thickness of the confined aquifer.

The procedure to obtain barometric efficiency for this investigation is as follows:

A microbarograph will be acquired from the Meteorology Department, University of Oklahoma. Then, the microbarograph will be positioned inside the Travertine District Nature Center, located in close proximity to the observation wells. Continuous readings of barometric pressure for an entire month will be recorded on the strip charts of the microbarograph. The strip charts will then be analyzed for pressure changes (inches of Hg) during incremental periods of time (hours). This then will be correlated with the strip chart data of the Steven's Water-Level Recorders, positioned at the East and West Observation Wells, for the same incremental periods of time. Data will then be plotted, ΔP_a (horizontal axis) versus Δh (vertical axis). The slope of the line will yield the barometric efficiency. From the known value of barometric efficiency, the storage coefficient S_c, can be obtained.

Slug tests will be accomplished at selected sites in the project area. This rate of rise technique to determine hydraulic conductivity K, for confined and unconfined aquifers, fully or partially penetrated wells can be expressed as (Bouwer, 1978):

$$K = \frac{r_c^2 \ln (Re/r_w)}{2L_e} \frac{1}{t} \ln \frac{y_o}{Y_t} \qquad (3.8)$$

where

Re = effective radial distance (connotes the same meaning as effective radius in well hydraulics),

r_w = distance from the well center to aquifer, uncased section,

r_c = distance from the well center to the casing,

L_e = length of the open section of the well where water enters,

y_o = y at time zero,

y_t = y at time t,

t = time since Y_o.

For flow in partially penetrating wells it was determined experimentally that ln (Re/r_w) can be determined from an empirical equation (Bouwer, 1978):

$$\ln \frac{Re}{r_w} = \frac{1}{\frac{1.1}{\ln (L_w/r_w)} + \frac{A + B \ln [(H-L_w)/r_w]}{(L_e/r_w)}} \qquad (3.9)$$

where A and B are constants that can be obtained from a nomograph devised by Bouwer (1978), if (L_e/r_w) is known; and H is the saturated thickness of the aquifer. If the ln $[(H-L_w)/r_w]$ exceeds the value of 6, a value of 6 should still be used.

The procedure for the slug tests is as follows:

A cylinder filled with sand, capped at both ends, will be lowered into a well. A pressure

transducer will be lowered into the well to monitor water level fluctuations. The probe (capped cylinder) will remain submerged until the water level is stabilized, as indicated by the pressure transducer. The pressure head above the transducer is recorded at this time. The probe will be withdrawn, the water level Y, will drop momentarily, and begin to rise. The pressure transducer will monitor the rise of head, and the investigator records time versus head readings. This data can then be plotted on semilog paper, Y (pressure head of water) vs. time t. The hydraulic conductivity can then be calculated by inserting known values from the nomograph devised by Bouwer (1978) and from the semilog plot, into Equations (3.9) and (3.8). Disadvantages of this technique are that K is measured over a relatively small portion of the aquifer; and is not adequate for determination of storage coefficient, S_c.

The Prickett-Lonnquist (1975) model will be used to simulate drawdown of a recently implaced municipal well of the city of Sulphur wellfield. The data furnished by the firm that conducted the pump test was constant discharge, water temperature, duration of test, and total drawdown at the end of the test. The approximate range of unknown values, S_c and T, should be obtained with the

use of Prickett-Lonnquist Model by trial and error for a time t. The two observation wells, East and West, are located approximately 3,000 and 2,500 feet, respectively, from the municipal well. Strip charts from the Steven's Water-Level Recorders positioned at each observation well will be analyzed for drawdown, if any, during the period the pump test was conducted.

The Prickett-Lonnquist model is capable of handling the transient flow equation of a confined aquifer that is either isotropic or anisotropic, homogeneous or heterogeneous. Production wells at specified nodes in the program are considered to be fully penetrating the saturated thickness of the confined aquifer. It is recognized by this author that the municipal well only partially penetrates the Upper Arbuckle Group, resulting in a possible vertical flow component at the base of a well. It is obvious that the values obtained from this simulation are rough estimates at best. Also, Gringarten (1982), asserts that if a well intersects a vertical fracture. lateral hydraulic conductivity estimates could be in error by as much as 40 percent.

The following assumptions will be made in the set-up of the model.

(1) The aquifer is relatively infinite, homogeneous and isotropic in aerial extent. Boundary conditions will not be considered.

(2) The likelihood of intercepting an interconnected vertical fracture is small. Majority of solution activity occurs along bedding planes. Hence, lateral flow predominates (Boulton and Streltsova, 1977).

(3) The homogeneous model is adequate for drawdown analysis at the sink node.

(4) Transmissivity values will be correlated to drawdown, if any, at the observation wells.

(5) Values obtained from this analysis is representative of only the saturated thickness penetrated by the production well.

(6) The base of the partially penetrating well will be considered relatively impermeable in the vertical direction; hence a fully penetrating well.

The regional technique employed by Fairchild et al. (1983), will be used to determine transmissivity T, expressed in the form of Darcy's Law:

$$T = \frac{Q}{IW} \tag{3.10}$$

where

Q = spring discharge (ft^3/day),

I = average gradient of the aquifer to the spring discharge point (ft/ft),

W = average width of the aquifer contributing to the spring discharge.

Average values of stage readings of Antelope and Buffalo will be obtained during the potentiometric survey of the project area. The average gradient of the aquifer(s) contributing to the spring discharge will be determined from the survey. Likewise, the average width of the contributing aquifer(s) to spring discharge will be ascertained from the survey.

3.3 Wells and Springs

Spring response to long-term precipitation events will be analyzed with the use of a 66-year precipitation histogram that also depicts periods of no flow for Buffalo and Antelope. From this histogram, an inch-years, time bar chart will be constructed. This chart will depict the summation of annual precipitation events as positive or negative for a specified period of time. Annual rainfall that exceeds the mean-annual rainfall is considered positive. Conversely, annual rainfall that is below the mean annual is negative. The area (inch-years) will be summed for a specified time period with the mean annual rainfall as the reference datum. The results will be graphically shown on the inch-years bar chart. Included in each bar will be the periods of no flow. It is hoped, that this graphical illustration will demonstrate

the deprivation effects of nearby production wells for the 66-year period.

Well and spring hydrograph versus precipitation events will be scrutinized. Information that can be obtained from this analysis is: (1) minimum piezometric elevation of observation wells before discharge of springs commence; (2) long-term trend hydrograph of observation wells to forecast possible, spring-flow cessation; (3) correlates the magnitude of discharge of the springs and water-level fluctuations of the observation wells to precipitation events on a seasonal and yearly basis; and (4) hopefully provide a confirmation of the approximate size of the recharge area as determined from the potentiometric survey and the analysis of geologic control.

A diffusivity coefficient, K_d (months^{-1}), of the aquifer(s) responsible for the freshwater springs will be determined by methods reported by E. White (1974) and W. White (1977). Also, an approximate response time, t_r (days), will be ascertained to aid in a concise classification of the freshwater springs (E. White, 1974).

The recession limb of the spring hydrograph can be expressed as a decaying exponential function (W.White, 1977),

$$Q = Q_o e^{-K_d t} \tag{3.11}$$

where

Q = spring discharge (cfs) at some time t (mos.),

Q_o = initial spring discharge located at the inflection point just below the peak discharge of the spring hydrograph (cfs),

K_d = diffusivity coefficient (mos.$^{-1}$),

t = time in months.

In addition, response time t_r, can be obtained by the following expression (E. White, 1974),

$$t_r = \frac{30}{K_d} \tag{3.12}$$

where

t_r = time of response (days),

K_d = diffusivity constant (months^{-1}).

Another parameter, spring variance or variability of springs, can be used to generalize storage capacity of an aquifer responsible for spring discharge (Davis and DeWiest, 1966). The spring variance V'_a, for a specified period of time can be expressed as:

$$V'_a = \frac{Q_{max} - Q_{min}}{Q_{med}} \tag{3.13}$$

where

Q_{max} = maximum recorded spring discharge for the specified time period,

Q_{min} = minimum recorded spring discharge for the specified time period,

Q_{med} = median discharge for the prescribed time period.

Spring variance analysis will be conducted on Antelope and Buffalo.

Tables and maps will depict location and flow of artesian and production wells in close proximity to the park. A hydrologic budget will be developed to demonstrate deprivation effects of artesian and production wells in the city of Sulphur versus the total annual recharge rate in the recharge area.

A statistical analysis will be utilized to determine average flow rate of Buffalo and Antelope on a monthly and yearly basis. This then will be correlated with precipitation on a monthly and yearly basis. Definite trends in fluctuations of spring discharge should be established.

Downhole TV logs of two separate artesian wells in the project area will be viewed. Both surveys were completed by the National Park Service in August 1980. Information that might be divulged from these tapes include: (1) flow direction, (2) occurrence of solution cavities and fractures with depth, (3) depth of well and casing, and (4) formation contacts.

3.4 Determination of Recharge Areas

Pervious investigators Hart (1972), and Harp et al.

(1976), identified two separate recharge areas responsible for spring flow in the park. Location of these recharge areas were given in general terms, no specific locations were cited.

The aerial extent of this potentiometric survey will be considerably refined, because of a previous potentiometric survey (Winter 1976, 1977) conducted by Fairchild et al. (1983), of the Arbuckle Mountain region (Plate II). The purpose of this potentiometric survey is to define the recharge areas for the springs and establish a groundwater divide for the Sulphur area. This is necessary in estimating the hydrologic budget for the Sulphur area.

The procedure to obtain piezometric elevations of selected well sites throughout the project are as follows:

The survey will occur during the winter months of 1985, when precipitation rates are low and the aquifer system is fairly stable. The survey will be taken in the span of two weeks, to minimize error of water level fluctuations. Surface elevations (feet above sea level) will be obtained from topographic maps at each well site, accuracy should be within 5 feet. Depth to water table at each well site will be read with chalk and steel tape. The piezometric level (feet above sea level) at each well site, will

be the difference between the surface elevation and the depth to water table reading. Total depth of well readings will not be taken due to lack of proper equipment. However, inquiry with landowners will be made to determine approximate depth of well and the general stratigraphy the drillers encountered.

Once the survey is completed, a potentiometric map will be constructed from the piezometric elevations. General flow direction, recharge areas and water table divides should be reasonably ascertained. This information will then be depicted on the geologic and hydrogeologic map of the study area.

CHAPTER IV

FINDINGS

4.1 Geology

A small outcrop or fenster of dolomitic carbonates in the midst of the Pontotoc Group was discovered just east of the Travertine District, Chickasaw National Recreational Area (Plate III). The outcrop was mapped, attitudes (dip and strike) of beds were taken, and a general lithologic description was accomplished (Appendix III). Rock specimens collected from this area were shown to Dr. Robert O. Fay, Oklahoma Geological Survey, who has extensive field experience in this region. He identified the rocks with reasonable certainty as being from the Bromide Massive and the Bromide Basal, the upper-most formation of the Simpson Group.

Photogeologic analysis of the study area revealed the following information. The heavily fractured Arbuckle Group with numerous surface outcrops can be readily distinguished from the Pontotoc and the Simpson Groups in the study area. The Simpson is usually detected where beds dip steeply, otherwise soil cover is

present, especially where the basal sands outcrop close to the surface (Ham, 1945). Lineaments in the Simpson are few and well spaced. Some lineaments were detected in the Simpson Group, vicinity of Hickory. Small, dark, circular-shaped areas were observed in the stream valleys of the Arbuckle Group, especially concentrated in Section 4, Southwest 1/4 Section, T1S, R4E. The Pontotoc Group is heavily dissected with intermittent streams, and appears white in color where it outcrops along the periphery of the Arbuckle Group, east of Sulphur. A strong occurrence of lineation was noted, east-southeast of the park, in the Pontotoc Group in NE¼ SE¼ of Sec. 1, T1S, R3E; and NW¼ SW¼ of Sec. 6, T1S R4E.

A lineament map was constructed from lineations in rock outcrops, observed from the black and white aerial photographs of the project area (Plate IV). The map was completed to facilitate correlation between field reconnaissance of fractures and those observed from aerial photos, and to demonstrate linear trends with respect to macrostructures, such as faults. Favorable correlation exists between orientation of lineaments and trends of faults (Plate IV).

Interestingly enough, there are few recognizable lineaments other than stream alignment along the Sulphur Fault. In fact, one cannot discern the exact location of Sulphur Fault from the aerial photos, unless rock

outcrops of the Simpson and Arbuckle are present. Lack of lineation can be attributed to accelerated weathering of the regolith because of intense fracturing in the fault zone (Fetter, 1980). In addition, inspection of the aerial photographs revealed that intermittent stream direction and preferred orientation of lineaments at various locations are nearly identical.

Fracture measurements were taken at Antelope Spring when it ceased flowing (Table 9). Fractures are exposed along a west-facing escarpment of broken conglomerate, approximately 20 feet high and 20 feet wide. Later in the investigation, spring flow was observed to originate from the base of the west-facing escarpment at the north end.

Attitude of the Pontotoc beds are nearly horizontal at or near Antelope Spring. Orthogonal fracture sets were noted. Major trends of fractures are S70°W and N25°W. Dips of fracture planes range from 66° to vertical. Fracture width ranges from .25 inches to 3 inches at the surface outcrop.

There were no fracture measurements taken at Buffalo Spring. Soil cover is well established in and around the spring area. A man-made, circular retaining wall consisting of native rock, encompasses a gravel bed that contains mainly lime cobbles, and some chert and quartz sand; from which Buffalo Spring eminates and flows over a

Table 9. Fracture Measurements of the Pontotoc Group, Antelope Spring*

STATION	ORIENTATION	DIP (degrees)	FRACTURE WIDTH (inches)	DISTANCE BETWEEN STATIONS (feet)	TOTAL DISTANCE (feet)
		TRAVERSE DIRECTION IS SOUTH			
1	S70E	72S	.5	0.	0.
2	S27E	66S	.5-2.0	10.0	10.0
3	N70E	82N	2.0	13.0	23.0
		TRAVERSE DIRECTION IS S35E			
1	N40E	81S	.5	0.	0.
2	N70E	90S	.25	2.0	2.0
3	S25E	85S	.25-.5	17.0	19.0
4	S52E	78S	.5-1.0	2.0	21.0
		ONE READING			
1	N55E	84N	.5-2.0	0.	0.

* Location - SE¼ NW¼ NW¼ NE¼ of Sec. 1, T1S, R3E

weir-like opening (4.5 feet wide) into a small unnamed creek.

After preliminary photogeologic analysis, fracture measurements were taken in the Pontotoc Group, east of the park boundary. The fractures that were measured did not coincide with the exact location of those observed on the aerial photos. Upon completion of the fracture measurement, closer inspection of the site on aerial photos depicted subtle lineament trends that corresponded exactly with those measured (Table 10). Distance between fractures in the Pontotoc Group at this site, range from .5 to 36 feet. Preferred orientation of fractures are west-northwest (N60W to W).

Fracture measurements were taken of a durable calcite cemented sandstone, approximately 1 to 2 feet thick, exposed in the glass-sand quarry (Table 11). The bed is located in the friable, basal sand of the Oil Creek Formation, Simpson Group. The bulk of the fractures trend west-northwest (N60W to W) and southwest (S30W to S60W). The macrostructure of the area, two major faults just north of the quarry, Section 11 and 12 of T1S, R4E, trend in the same direction as the preferred orientation of the fractures. The distance between fractures range from 0 to 6 feet. Fracture width ranged from .0625 to 1.0 inches. Attitude of the beds at this locale, strike at N55W, with a dip of 7 degrees to the

Table 10. Fracture Measurements of the Pontotoc Group*

STATION	ORIENTATION	DIP (degrees)	FRACTURE WIDTH (inches)	DISTANCE BETWEEN STATIONS (feet)	TOTAL DISTANCE (feet)
		TRAVERSE DIRECTION IS N5E			
1	N70W	UNK	+1.0-2.0	0.	0.
2	N75W	"	"	2.0	2.0
3	N75W	"	"	2.0	4.0
4	S87W	"	"	1.5	5.5
5	N72W	"	"	1.5	7.0
6	N60W	"	"	.5	7.5
7	N60W	"	"	2.0	9.5
8	W	"	"	3.0	12.5
9	N88W	"	"	1.5	14.0
10	N64W	"	2.0	3.0	17.0
11	N75W	"	.5-1.5	6.0	23.0
12	N65W	"	+1.0-2.0	8.0	31.0
13	N50W	"	"	36.0	67.0
14	N75W	"	"	12.0	79.0
15	N80W	"	"	4.0	83.0
16	S89W	"	"	26.0	109.0
17	N88W	"	"	10.0	119.0
18	N87W	"	"	6.0	125.0
19	N72W	"	"	10.0	135.0

* Location - SE¼ NE¼ NE¼ of Sec. 1, T1S, R3E

+ Fracture is filled with soil and vegetation.

Table 11. Fracture Measurements of an Indurated Sandstone of the Simpson Group Glass Sand Quarry*

STATION	ORIENTATION	DIP (degrees)	FRACTURE WIDTH (inches)	DISTANCE BETWEEN STATIONS (feet)	TOTAL DISTANCE (feet)
		TRAVERSE DIRECTION IS N25W			
1	S55W	UNK	.5-1.0	0.	0.
2	S70W	"	.25	3.5	3.5
3	S60W	"	.25	3.5	7.0
4	S62W	"	.125	3.5	10.5
5	S25W	"	.25	3.0	13.5
5a	S67W	"	.25	0.	13.5
6	S75W	"	.125	4.0	17.5
6a	N70W	"	.125	0.	17.5
7	S70W	"	.125	4.0	21.5
7a	N30W	"	.25	0.	21.5
8	N80W	"	.25	6.0	27.5
8a	S55W	"	.25	0.	27.5
9	N80W	"	.25	3.0	30.5
10	S45W	"	.25	2.0	32.5
11	N75W	"	.125	4.5	37.0
12	S70W	"	.125	4.0	41.0
12a	N40W	"	.125	0.	41.0
13	S50W	"	.25-.5	3.0	44.0
13a	N80W	"	.5	0.	44.0
14	S50W	"	.5	1.5	45.5
15	S35W	"	.125	6.0	51.5
15a	N82W	"	.125	0.	51.5
16	N80W	"	.125	6.0	57.5
17	S55W	"	.25-.5	1.5	59.0
18	N80W	"	.25	1.5	60.5
19	N80W	"	.75	6.0	66.5
19a	N45W	"	.75	0.	66.5
20	S35W	"	.25-.5	15.0	81.5
20a	N82W	"	.125	0.	81.5
21	S50W	"	.25-.5	3.0	84.5
21a	N30W	"	.125	0.	84.5
22	N75W	"	.125	10.0	94.5
22a	S15W	"	.0625	0.	94.5
23	N10W	"	.125	6.0	100.5
24	S40W	"	.25	3.0	103.5

* Location - SW¼ SW¼ NW¼ NE¼ of Sec. 14, T1S, R4E

northeast.

The field reconnoiter of the Arbuckle Group revealed intensely fractured dolomites. A distance of one inch or less between fractures is not uncommon. Most of the small fractures (less than .125 inches thick) at the surface are filled with limonite and silica. Fracture width ranges from .0625 to 3 inches. A fair amount of swallow shafts and small sinks are located in and along intermittent streams.

The primary directions of fracture orientation in the Arbuckle Group measured at 3 sites, (Tables 12, 13 and 14) correlates extremely well with the lineament map (Plate IV). The majority of the fracture measurements were oriented in the north-northwest (N30W to N) and the south-southwest (S60W to W) directions. The bulk of the stream directions in the project area, east of Sulphur, are aligned with the preferred orientation of the fractures. The beds of the Arbuckle Group, east of Sulphur, gently dip to the northwest (Plate I).

Generally, other than the small outcrop that was discovered east of the park and nomenclature of the confining bed, the Pontotoc group; the geologic structure and the stratigraphy of the area defined by previous investigations versus this investigation, are in good agreement.

A structural contour map of the surface of the

Table 12. Fracture Measurements of the Arbuckle Group, Mill Creek and State Highway 7*

STATION	ORIENTATION	DIP (degrees)	FRACTURE WIDTH (inches)	DISTANCE BETWEEN STATIONS (feet)	TOTAL DISTANCE (feet)
		TRAVERSE DIRECTION IS N70W			
1	S60W	near vertical	1.0	0.	0.
2	S70W	"	1.5	.5	.5
3	S70W	"	1.5	.5	1.0
4	S40W	"	.5	1.0	2.0
5	N5W	"	.5	2.0	4.0
6	N35W	"	1.5	2.0	6.0
7	S60W	"	.5	.5	6.5
8	N50W	"	.5	1.0	7.5
8a	N30W	"	.25	0.	7.5
8b	S70W	"	.25	0.	7.5
9	S5W	"	.75	0.	8.5
9a	S85W	"	.75	0.	8.5
10	S60W	"	.125	.5	9.0
10a	S10W	"	.125	0.	9.0
11	S	"	1.0	.5	9.5
11a	S80W	"	.5	0.	9.5
11b	S10W	"	.25	0.	9.5
12	S45W	"	2.0	2.0	11.5
13	S75W	"	1.0	1.0	12.5
14	N40W	"	1.0	1.0	13.5
14a	W	"	2.0	0.	13.5
15	S45W	"	1.5	.5	14.0
15a	N15W	"	2.0	0.	14.0
16	S80W	"	2.0	1.0	15.0
17	N70W	"	2.0	2.0	17.0
18	N50W	"	1.0	1.0	15.0
19	N70W	"	2.0	2.0	20.0
20	S70W	"	3.0	5.0	25.0
20a	N15W	"	1.0	0.	25.0
21	N15W	"	1.0	1.0	26.0
21a	S60W	"	1.0	0.	26.0
22	S40W	"	2.0	4.0	30.0
22a	N20W	"	2.0	0.	30.0

* Location - SE¼ NE¼ SE¼ SE¼ of Sec. 32, T1N, R4E

Table 13. Fracture Measurements of the Arbuckle Group, Intersection of State Highways 7 and 12*

STATION	ORIENTATION	DIP (degrees)	FRACTURE WIDTH (inches)	DISTANCE BETWEEN STATIONS (feet)	TOTAL DISTANCE (feet)
		TRAVERSE DIRECTION IS S30W			
1	S65W	near vertical	.125	0.	0.
2	N20W	"	.25	.1	.1
3	S65W	"	.125	.1	.2
4	S70W	"	.125	1.0	1.2
5	S75W	"	.125	.1	1.3
6	S60W	"	.25	.1	1.4
7	S65W	"	.0625	.6	2.0
8	S60W	"	.0625	.1	2.1
9	W	"	.0625	.2	2.3
10	S60W	"	.125	.1	2.4
11	S65W	"	.125	.2	2.6
12	S55W	"	.125	.2	2.8
13	S	"	.25	.5	3.3
13a	S65W	"	.125	0.	3.3
14	N25W	"	.5	.2	3.5
		TRAVERSE DIRECTION IS W			
1	N20W	near vertical	.125	0.	0.
2	N40W	"	.25	.3	.3
3	N30W	"	.25	.3	.6
4	N30W	"	.25	.6	1.2
4a	N10W	"	.5	0.	1.2
4b	S40W	"	1.0	0.	1.2

* Location - NE¼ NE¼ NW¼ NW¼ of Sec. 2, T1S, R4E

Table 14. Fracture Measurements of the Arbuckle Group, Collins' Ranch*

STATION	ORIENTATION	DIP (degrees)	FRACTURE WIDTH (inches)	DISTANCE BETWEEN STATIONS (feet)	TOTAL DISTANCE (feet)
		TRAVERSE DIRECTION IS WEST			
1	S35	near vertical	.125	0.	0.
1a	N40W	"	.125	0.	0.
2	S40W	"	.25	.25	.25
2a	N	"	.125	0.	.25
3	S30W	"	.125	.25	.50
4	S20W	"	.0625	.1	.60
5	S55W	"	.125	.2	.80
6	N70W	"	.0625	.2	1.0
6a	S45W	"	.125	0.	1.0
		TRAVERSE DIRECTION IS N10W			
1	S80W	near vertical	1.5	0.	0.
1a	S55W	"	1.5	0.	0.
2	S70W	"	1.0	.8	.8
2a	S5W	"	.25	0.	.8
3	S45W	"	.25	.7	1.5

* Location - NW¼ NE¼ NE¼ of Sec. 6, T1S, R4E

Arbuckle Group of the Sulphur area was constructed to infer subsurface structure under the confining layers of the Pontotoc (Figure 29). Inferrence of the Sulphur Fault is based on: spring occurrence, observation well lithology, comparatively large discharge of the Vendome Well, general structural trends of the area, and elevation tops of the Arbuckle Group from well completion reports and well logs. South Hickory Fault was inferred with reasonable assurance to Sec. 20 of T1N, R3E (Figure 29). This was based on a reported fault in the SW½ of Sec. 20 of the basal Simpson and Upper Arbuckle from a well completion report. An unnamed fault, now called South Sulphur Fault for this investigation, is inferred to the Bromide Spring area (Figures 29 and 30).

Only a small veneer of Simpson overlain by the Pontotoc is present on the upthrown side of the Sulphur Fault; except for a thicker sequence of Simpson in the drag fold of the down-thrown side of the inferred South Hickory Fault, north of Sulphur (Figure 29).

The thickness of the Pontotoc increases in a westerly and northerly direction; ranging from less than one foot at the contact with the Arbuckle Group in Sec. 6 of T1S, R4E, to 900 feet thick in Sec. 31 of T1N, R3E. Information on stratigraphic thickness was obtained from well completion reports.

Finally, a geologic and hydrogeologic map was con-

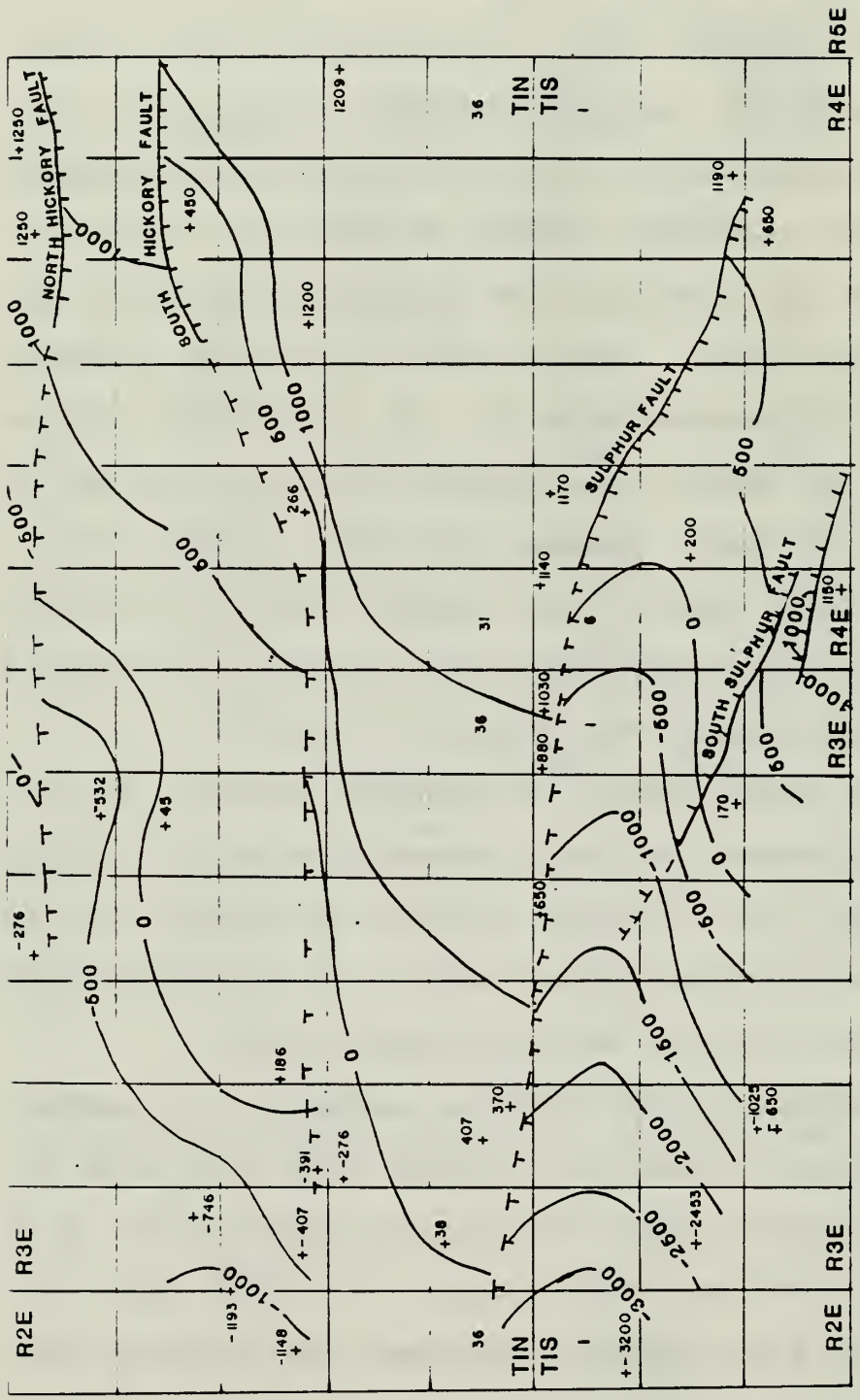

Figure 29. Structural contour map of the surface of the Arbuckle Group.

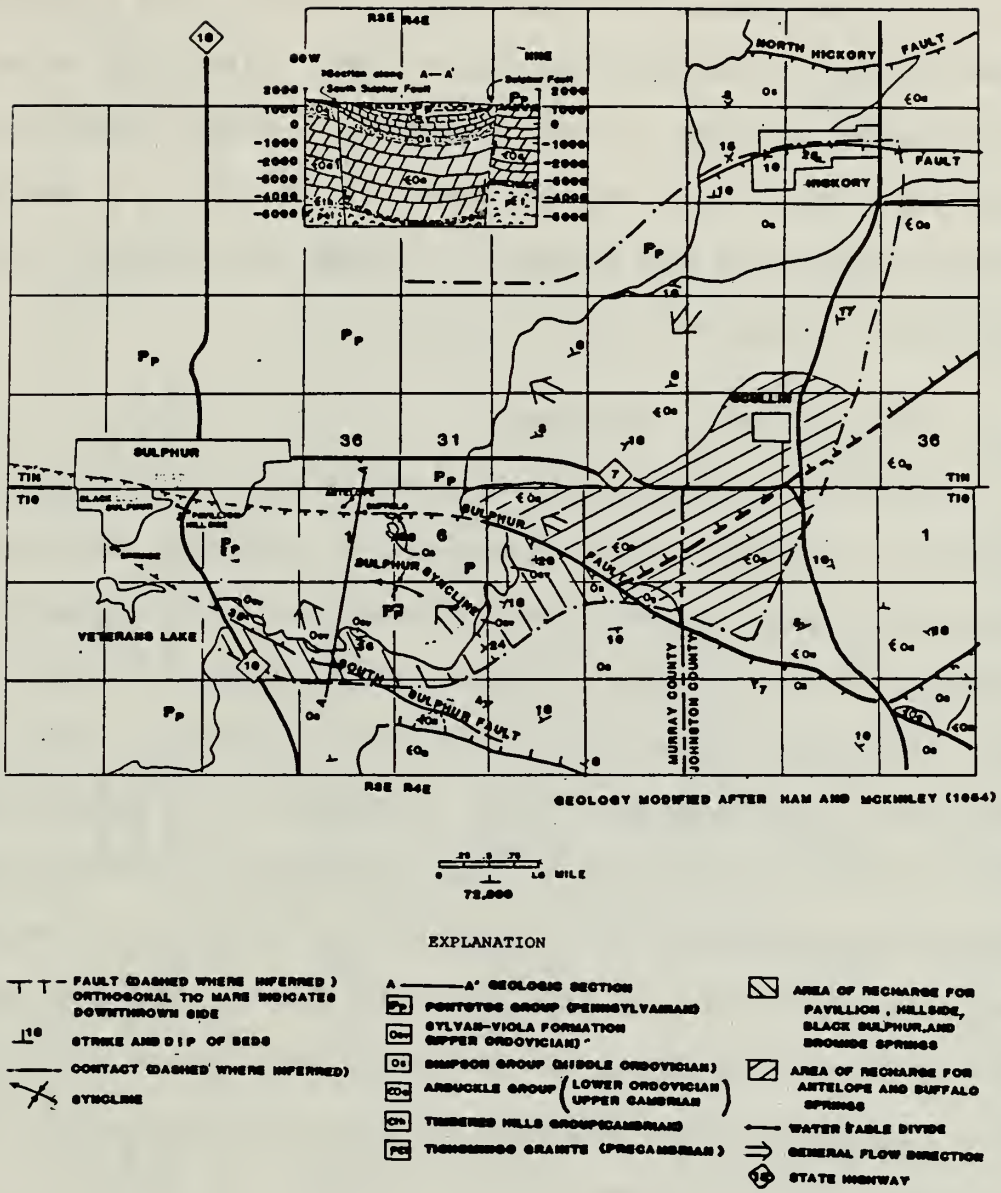

Figure 30. Geologic and hydrogeologic map of the Sulphur, Oklahoma, Area.

structed (Figure 30). The geology is modified after Ham (1954). Inferrence of the Sulphur Fault, with reasonable certainty, is depicted in Figure 30. Also, the recently discovered outcrop of the Simpson, located southeast of the freshwater springs, is shown on the map. A geologic cross section of the Sulphur Syncline and the area of the springs is depicted also in Figure 30.

4.2 Petrophysical Results

Effective porosity measurements with the use of the Helium Porosimeter were conducted on selected rock specimens from the project area (Table 15). The primary porosity of the Arbuckle Group ranged from 7.4 to 10.4%. The confining layer for the Sulphur artesian basin, the Pontotoc conglomerate, had extremely low porosities, ranging from .13 to 2.5%. The porosities for the Simpson Group ranged from 2.3 to 11.4%. Thin sections of selected rock specimens of the Arbuckle Group, Simpson Group, and the Pontotoc Group are depicted in Figures 31 through 34. Classification schemes of thin sections are in accordance with Williams et al. (1954).

Analysis of the specimens of the Arbuckle Group revealed a mosaic of aphanitic dolomite anhedra. Selected specimens from the Simpson Group included poorly-sorted, calcite-cemented calcarenites; and calcite-cemented, fairly well sorted, medium-grained, subangular to sub-

Table 15. Laboratory Data and Effective Porosity Measurements of Selected Rock Specimens

Core Sample	L Core Length (cm)	d Core Diameter (cm)	*V_B Bulk Volume (cc)	P_1 Initial Pressure (gage psi)	P_2 Final Pressure (gage psi)	P_{vac} Vacuum Pressure (gage psi)	**V_P Volume of the pores (cc)	*** n Effective Porosity (%)
Arbuckle Dolomite								
#1	5.42	1.91	15.529	100.4	-1.2	-13.5	1.146	7.4
#2	5.05	1.91	14.469	100.7	-1.3	-13.5	1.500	10.4
Pontotoc Conglomerate								
#1	4.85	1.86	13.178	100.6	-1.3	-13.5	.093	.7
#2	4.63	1.86	12.580	100.1	-1.4	-13.5	.016	.1
#3	4.81	1.86	13.070	100.9	-1.3	-13.5	.331	2.5
Oil Creek Limestone Simpson Group								
#1	4.47	1.85	12.015	100.3	-1.5	-13.5	.771	6.4
Bromide Limestone Simpson Group								
#1	4.05	1.87	11.123	100.4	-1.6	-13.5	1.118	10.1
#2	3.64	1.86	9.890	100.4	-1.7	-13.5	1.028	10.4
Upper Oil Creek Limestone Simpson Group								
#1	3.89	2.52	19.402	100.2	-1.6	-13.5	1.150	4.2

(continued)

Table 15. Laboratory Data and Effective Porosity Measurements of Selected Rock Specimens (continued)

Core Sample	L Core Length (cm)	d Core Diameter (cm)	*V_B Bulk Volume (cc)	P_1 Initial Pressure (gage psi)	P_2 Final Pressure (gage psi)	P_{vac} Vacuum Pressure (gage psi)	**V_P Volume of the pores (cc)	*** n Effective Porosity (%)
Basal Oil Creek Cemented Sandstone Simpson Group								
#1	3.73	1.86	10.135	100.3	-1.7	-13.5	1.150	11.4
#2	3.80	1.87	10.437	100.2	-1.6	-13.5	.236	2.3

$$*V_B = \frac{\pi d^2 L}{4}$$

$$** V_p = \{P_{vac} (V_L + \Delta V_{CH} - V_B) + (P_1 V_1) - P_2 (V_L - V_B + \Delta V_{CH} + V_1\}/(P_2 - P_{vac})$$

where V_L = volume of the lines = 9.492 cc

V_{CH} = volume of sample chamber = 214.55 cc

V_D = volume of the disks # 1 and #5 = 80.047 + 12.433 = 93.48 cc

$\Delta V_{CH} = V_{CH} - V_D = 214.55 - 93.48 = 121.07$ cc

V_1 = volume of reference chamber # 1 = 14.065 cc

*** $n = V_P/V_B$

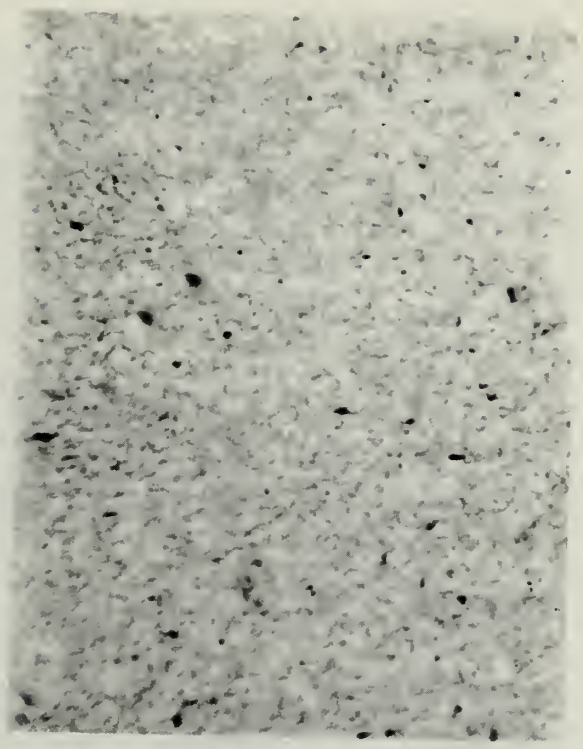

Figure 31. Magnification is 39X; mosaic of aphanitic dolomite anhedra of the West Spring Formation, Arbuckle Group. Specimen obtained from surface outcrop at C NE¼ NW¼ NW¼ of Sec. 2, T1S, R4E.

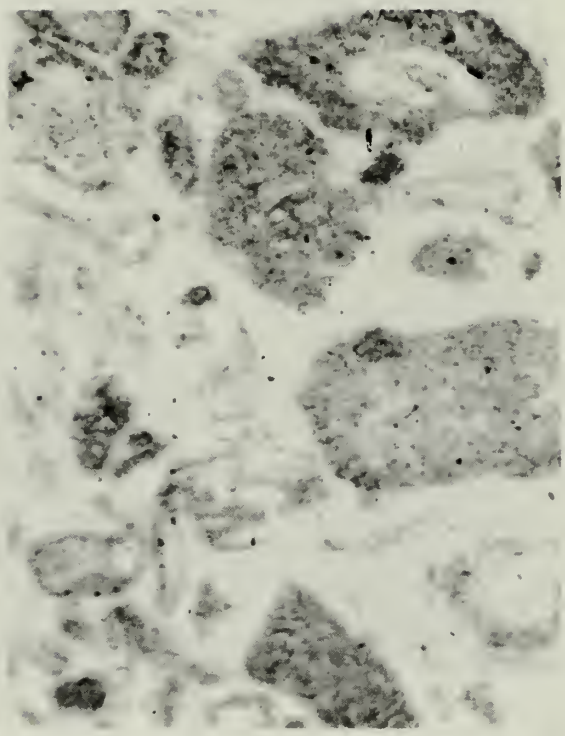

Figure 32. Magnification is 39X; poorly-sorted, calcite-cemented calcarenite of the Oil Creek Formation, Simpson Group. Specimen obtained from quarry at C NE¼ SW¼ NE¼ of Sec. 14, T1S, R4E.

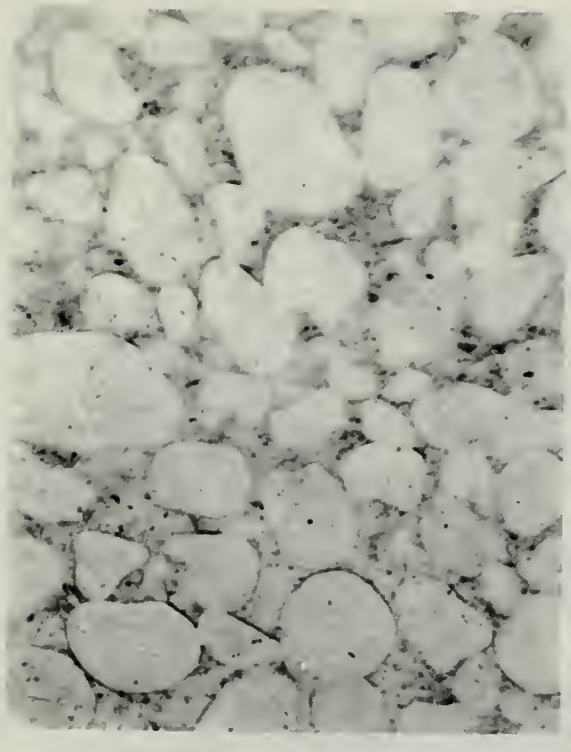

Figure 33. Magnification is 39X; calcite-cemented, fairly well sorted, subangular to sub-rounded arenite of the Basal Oil Creek Formation, Simpson Group. Specimen obtained from quarry at C NE¼ SW¼ NE¼ of Section 14, T1S, R4E.

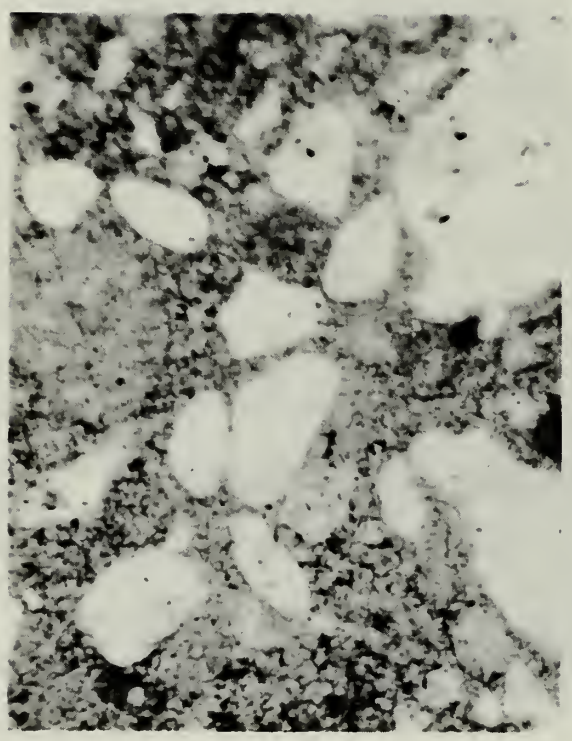

Figure 34 . Magnification is 39X; conglomerate of the Pontotoc Group consisting of some fine to medium grained quartz particles, and fine grained to *pebble-size lime clasts, embedded in a calcite and argillaceous cement. Specimen obtained from NW¼ NW¼ NW¼ NW¼ of Sec. 2, T1S, R3E.

* It is not shown on thin section, but quite apparent in the core sample.

rounded, arenites. Analysis of the specimen of the Pontotoc Group revealed a conglomerate consisting of some subangular to subrounded, fine to medium grained quartz particles and fine grained to pebble-size lime clasts embedded in a calcite and argillaceous cement. Pebble-size lime clasts were not observed in the thin section, but were quite evident from the core sample.

4.3 Assessment of Aquifer Properties

A slug test was performed on an abandoned wildcat well in the Arbuckle Group, located in C NE¼ SE¼ SE¼ of Sec. 31, T1N, R4E. Dimensions of the well were obtained from a well completion report dated 21 April 1964. The depth to water table reading was 105 feet. Total well depth is 237 feet. The method employed was the sudden withdrawal of a probe and then measuring the rate of rise with a pressure transducer. The recorded data is listed in Table 16. The data was then plotted on semilog paper and a hydraulic conductivity for a partially penetrating well in an unconfined aquifer was calculated (Figure 35). The average value of hydraulic conductivity was determined to be 1.6 ft/day for an uncased, unmodified, open-well length of 79 feet (Figure 35).

In addition, slug tests were performed on the two observation wells, East and West, that were completed in the Arbuckle Group (Plate III). The results proved nega-

Table 16. Slug Test Data of Crawford's Well*

Time t (sec)	Pressure Head P P (psi)	+Head of Water H (ft)	Rise Y(ft)
6.78	23.69	54.68	2.56
15.26	23.79	54.91	2.33
21.76	23.85	55.05	2.19
31.65	23.93	55.23	2.01
40.83	24.00	55.39	1.85
50.64	24.07	55.55	1.69
58.61	24.12	55.67	1.57
65.57	24.16	55.76	1.48
74.80	24.21	55.88	1.36
83.60	24.25	55.97	1.27
92.78	24.29	56.06	1.18
111.03	24.36	56.22	1.02
124.48	24.41	56.34	.90
125.60	24.45	56.43	.81
149.15	24.49	56.52	.72
160.52	24.52	56.39	.65
175.35	24.56	56.68	.56
190.38	24.59	56.75	.49
201.70	24.61	56.80	.44
220.73	24.64	56.87	.37
234.39	24.66	56.92	.32
245.56	24.67	56.94	.30
272.99	24.69	56.98	.26
308.71	24.71	57.03	.21
337.74	24.73	57.08	.16
469.83	24.74	57.10	.14
630.00	24.75	57.12	.12
819.75	24.75	57.12	.12

Note: Initial or stabilized pressure is 24.80 psi or 57.24 feet of water above the transducer prior to withdrawal of the probe.

* Location - C NE¼ SE¼ SE¼ of Sec. 31, T1N, R4E

+ Where $H = \frac{P}{\gamma_w} = P \frac{1b}{in^2} \times \frac{144 in^2}{ft^2} \times \frac{1}{62.4 lb/ft^3} = (2.308)P$

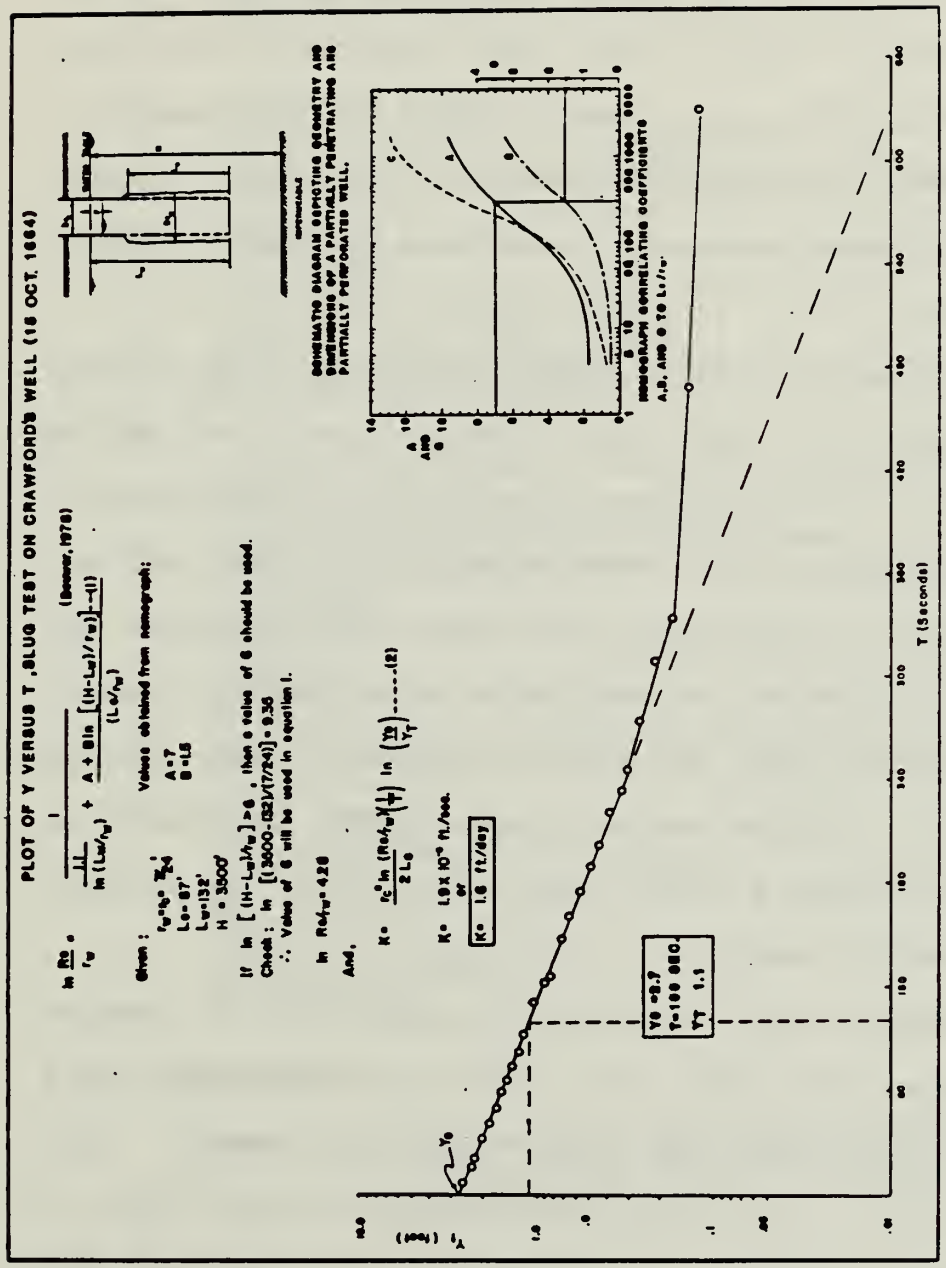

Figure 35. Results of a slug test performed on a selected well in the Arbuckle Group outcrop.

tive for both wells. The rate of rise of the West Observation Well was extremely slow and actually stabilizes at a depth of one foot below the original piezometric level.

The rate of rise of the East Observation Well was also extremely slow. As a result, data was determined to be unreliable. In addition, naturally occurring asphalt in this well could conceivably obstruct hydraulic conductivity tests.

The Prickett-Lonnquist model (1975) was used to simulate drawdown at a sink node within a specified period of time (Figure 36). Unknown parameters, storage coefficient and transmissivity, were entered on a trial and error basis until reasonable values were attained that coincided with drawdown at designated nodes within a specified period of time. A 10 x 10 array with node spacing of 2,640 ft. (.5 mile) was utilized. NSTEP was chosen to be 10, which gives a total time of 25.92 hours; closely approximating 24 hours.

The artesian well selected for simulation is located approximately 3,000 feet from the West Observation Well and 2,500 feet from the East Observation Well. This flowing well is a municipal water well for the city of Sulphur, and flows at approximately 150 gallons per minute at a surface elevation of 1,060 feet above sea level. Upon completion of the well, the drilling company conducted a pump test (probably a specific capacity test)

```
c       modified illinois state water survey
c       basic aquifer simulation program
c      groundwater model study of the sulphur, oklahoma, area
c      cpt. charles j. oarthel jr., investigator
c
c
c
c      definition of variables
c
c      ho(i,j)-----heads at start of time increment (i.j)
c      h(i,j)------heads at end of increment (ft)
c      sf1(i,j)----storage factor for artesian conditions (sq. ft.)
c      q(i,j)------constant withdrawal rates (+) or injection rates (-)
c      (cubic ft./day)
c      t(i,j,1)----aquifer transmissivity between i,j and i,j+1
c      (sq. ft./day)
c      t(i,j,2)----aquifer transmissivity between i,j and i+1,j
c      (sq. ft./day)
c      aa,bb,cc,dd-coefficients in water balance equations
c      nr----------no. of rows in model
c      nc----------no of columns in model
c      nsteps------no. of time increments
c      delta-------time increments (days)
c      hh,s1,qq,tt-default values
c      j-----------model column number
c      j-----------model row number
c
c
c
       dimension h(50,50),ho(50,50),sf1(50,50),q(50,50),t(50,50,2),
      1b(50),g(50),dl(50,50)
c
c      read parameter card and default value card
       read(5,10)nsteps,delta,error,nc,nr,tt,s1,hh,qq
10     format(i3,2f6.0/2i3,4f6.0)
c      fill arrays with default values
       do 20 i=1,nc
       do 20 j=1,nr
       t(i,j,1)=tt
       t(i,j,2)=tt
       sf1(i,j)=s1
       h(i,j)=hh
       ho(i,j)=hh
20     q(i,j)=qq
c      read node cards
30     read(5,40,end=50)i,j,t(i,j,1),t(i,j,2),sf1(i,j),h(i,j),q(i,j)
40     format(2i3,2f6.0,2f4.0,1f5.0)
       go to 30
c      start of simulation
50     time=0
       do 320 istep=1,nsteps
       time=time+delta
c      predict heads for next time increment
       do 70 i=1,nc
       do 70 j=1,nr
       d=h(i,j)-ho(i,j)
       ho(i,j)=h(i,j)
       f=1.0
       if(dl(i,j).eq.0.0)go to 60
       if(istep.gt.2)f=d/dl(i,j)
       if(f.gt.5)f=5.0
       if(f.lt.0.0)f=0.0
```

(continued)

Figure 36. Prickett-Lonnquist Model (1971) that was used to simulate drawdown at a sink node.

```
60    sl(i,j)=1
70    h(i,j)=h(i,j)+1*f
c     refine estimates of heads by iadi method
      iter=0
80    e=0.0
      iter=iter+1
c     column calculations
      do 190 ii=1,nc
      i=ii
      if(mod(istep+iter,2).eq.1) i=nc-i+1
      do 170 j=1,nr
c     calculate b and g arrays
      bb=sf1(i,j)/delta
      dd=ho(i,j)*sf1(i,j)/delta-q(i,j)
      aa=0.0
      cc=0.0
      if(j-1)90,100,90
90    aa=-t(i,j-1,1)
      bb=bb+t(i,j-1,1)
100   if(j-nr)110,120,110
110   cc=-t(i,j,1)
      bb=bb+t(i,j,1)
120   if(i-1)130,140,130
130   bb=bb+t(i-1,j,2)
      dd=dd+h(i-1,j)*t(i-1,j,2)
140   if(i-nc)150,150,150
150   bb=bb+t(i,j,2)
      dd=dd+h(i+1,j)*t(i,j,2)
160   w=bb-aa*b(j-1)
      b(j)=cc/w
170   g(j)=(dd-aa*g(j-1))/w
c     re-estimate heads
      e=e+abs(h(i,nr)-g(nr))
      h(i,nr)=g(nr)
      n=nr-1
180   ha=g(n)-b(n)*h(i,n+1)
      e=e+abs(ha-h(i,n))
      h(i,n)=ha
      n=n-1
      if(n)190,190,180
190   continue
c     row calculations
      do 300 jj=1,nr
      j=jj
      if(mod(istep+iter,2).eq.1) j=nr-j+1
      do 290 i=1,nc
      bb=sf1(i,j)/delta
      dd=ho(i,j)*sf1(i,j)/delta-q(i,j)
      aa=0.0
      cc=0.0
      if (j-1)200,210,200
200   bb=bb+t(i,j-1,1)
      dd=dd+h(i,j-1)*t(i,j-1,1)
210   if(j-nr)220,230,220
220   dd=dd+h(i,j+1)*t(i,j,1)
      bb=bb+t(i,j,1)
230   if(i-1)240,250,240
240   bb=bb+t(i-1,j,2)
      aa=-t(i-1,j,2)
250   if(i-nc)260,270,260
260   bb=bb+t(i,j,2)
      cc=-t(i,j,2)
270   w=bb-aa*b(i-1)
      b(i)=cc/w
280   g(i)=(dd-aa*g(i-1))/w
c     re-estimate heads
      e=e+abs(h(nc,j)-g(nc))
      h(nc,j)=g(nc)
      n=nc-1
290   ha=g(n)-b(n)*h(n+1,j)
      e=e+abs(h(n,j)-ha)
      h(n,j)=ha
      n=n-1
      if(n)300,300,290
300   continue
      if(e.gt.error) go to 80
c     print results
      delta=delta*1.2
      do 320 j=1,nr
320   write(6,330)j,(h(i,j),i=1,nc)
330   format(i5,5x,10f10.4/(12x10f10.4))
      write(6,340)time,e,iter
340   format(5h2time=,f6.2///,e20.7,i5)
      stop
      end
```

Figure 36. Prickett-Lonnquist Model (1971) that was used to simulate drawdown at a sink node (continued).

and submitted the appropriate data on a Multi-Purpose Water Well Report to the Oklahoma Water Resources Board (Figure 37). This data was presumed to be correct and was used as the basis for the simulation.

Strip charts from the Stevens Water-Level Recorders positioned at each observation well, for the months of March and April, calendar year 1983, were acquired from the National Park Service. These charts will be used in quantifying values of transmissivity and storage coefficient in relation to drawdown around the sink node.

Results of the simulation of drawdown of 85 feet in 24 hours and analysis of the strip charts are as follows (Table 17 and 18):

(1) Drawdown in and around the well bore is primarily a function of the storage coefficient of an aquifer.

(2) Storage coefficient, S_c, was determined to be approximately 1,200 ft^2 per .25 mi^2 or 1.7 x 10^{-4}.

(3) The drawdown at the West Observation Well as a result of the pump test was nil. The drawdown at the East Observation Well could not be discerned because the recorder was inoperative part of the time.

(4) Transmissivity, T, was determined to be between .1 ft^2/hour (Table 17) to 1 ft^2/hour (Table 18).

Distillers Coop
Ink Distillers Coop

STATE OF OKLAHOMA
WATER RESOURCES BOARD
1000 N E 10TH STREET, P O BOX 53585
OKLAHOMA CITY, OKLAHOMA 73152

MULTI PURPOSE WATER WELL REPORT

Aquifer
Stream System Code
Use Code
County
(Official Use Only)
18

OWNER Sulphur Municipal Authority ADDRESS City Hall, 400 West Muskogee, Sulphur, Oklahoma PHONE

LEGAL DESCRIPTION OF WELL EIM WIM

SE ¼ of NE ¼ of SW ¼ of sec. 36 ; TWP. 1 N Rge. 3E ECM; COUNTY Murray

TYPE OF WORK
☒ New Well ☐ Plugging
☐ Reconditioning Work ☐ Test

4. PROPOSED / PAST USE
☐ Domestic ☐ Irrigation ☐ Stock
☒ Municipal ☐ Industrial ☐ Test

5 DRILLING METHOD
☒ Rotary ☐ Rev Rotary
☐ Cable ☐ Other

LOG

Material	From	To	Water rated ✓
Conglomerate w/tar sand	0	55	
Sandy shale & limestone	55	80	
Limestone & chert	80	115	
Limestone & shale	115	135	
Limestone	135	177	
Shale	177	188	
Limestone	188	260	
Limestone & shale	260	285	
Limestone & white sand	285	340	
Limestone & chert	340	500	
Limestone	500	565	
Limestone & chert	565	750	

RECEIVED
MAY 2 1983
Oklahoma Water Resources Board

7. NEW WELL CONSTRUCTION DATA

Dates: Started 3/7/83 Completed 4/1/83
Contractor Layne-Western Company, Inc.
Driller Philip L. Harris
Diameter Hole 12 in. Total Depth 750 ft.

CASING RECORD

Diameter		From		To	
12	in.	0	ft.	240	ft.
	in.		ft.		ft.

Surface Seal: ☒ Yes ☐ No Type: Cement grout
Depth of Seal: 240 ft.
Gravel Packed: No
Gravel Packed From ft. to ft.
Amount Used:

PERFORATION RECORD

Type From ft. To ft.
Size From ft. To ft.
" From ft. To ft.

8. WELL TEST DATA

Static Water Level Below Land Surface 0 ft.
If Artesian: Flows 150 gpm.
Water Temp. 62 °F Quality Good

BAILER TEST

Drawdown ft. After Pumping hrs. At gpm.
Size of Bailer: gal.

PUMPING TEST

Drawdown 85 ft. After Pumping 24 hrs. At 537 gpm.

1. PLAT

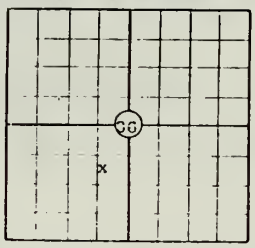

SE ¼ of NE ¼ of SW ¼ of SEC 36 ;
N
P 1 R RGE 3E EIM,WIM,ECM

9. PLUGGING DATA

Date Plugged
Backfilled With Material To ft.
Grouted or Cemented From ft. To ft.
Plot Location in Item 11. Show Distances From 2 Section Lines.

10. RECONDITIONING WORK

Date Completed
☐ Replaced Casing From ft. To ft.
☐ Replaced Screen From ft. To ft.
Deepened Well From ft. To ft.
Redeveloped Well By

PUMP INFORMATION

Pump Type Vertical turbine
Power Source Electric
Rated Capacity 800 gpm.
Depth of Bowls or Cylinder 200 ft.

11. CERTIFICATION

The work described above was done under my supervision, and this report is true and correct to the best of my knowledge.

Name Layne-Western Co., Inc. License # WD-38
Address 620 S. 38th St. K. C. Ks Phone # 913/321-5000
Signed Date 4-

USE ADDITIONAL SHEETS IF NECESSARY

Figure 37. Multi-purpose water well report on Municipal Well No. 9, city of Sulphur.

Table 17. Input Parameters (T = .1 Ft^2/Hour) and Resultant Output

INPUT 10 1.0 2.0
5 10 .10 10 .10 12e2 12e2 0.0 0.0 4307. 0.0

1	-0.0000	-0.0000	-0.0000	-0.0000	-0.0000	-0.0000	-0.0000	-0.0000	-0.0000	-0.0000
2	-0.0000	-0.0000	-0.0000	-0.0000	-0.0000	-0.0000	-0.0000	-0.0000	-0.0000	-0.0000
3	-0.0000	-0.0000	-0.0000	-0.0000	-0.0000	-0.0000	-0.0000	-0.0000	-0.0000	-0.0000
4	-0.0000	-0.0000	-0.0000	-0.0000	-0.0003	-0.0000	-0.0000	-0.0000	-0.0000	-0.0000
5	-0.0000	-0.0000	-0.0000	-0.0003	-3.5380	-0.0003	-0.0000	-0.0000	-0.0000	-0.0000
6	-0.0000	-0.0000	-0.0000	-0.0000	-0.0003	-0.0000	-0.0000	-0.0000	-0.0000	-0.0000
7	-0.0000	-0.0000	-0.0000	-0.0000	-0.0000	-0.0000	-0.0000	-0.0000	-0.0000	-0.0000
8	-0.0000	-0.0000	-0.0000	-0.0000	-0.0000	-0.0000	-0.0000	-0.0000	-0.0000	-0.0000
9	-0.0000	-0.0000	-0.0000	-0.0000	-0.0000	-0.0000	-0.0000	-0.0000	-0.0000	-0.0000
10	-0.0000	-0.0000	-0.0000	-0.0000	-0.0000	-0.0000	-0.0000	-0.0000	-0.0000	-0.0000
1	-0.0000	-0.0000	-0.0000	-0.0000	-0.0000	-0.0000	-0.0000	-0.0000	-0.0000	-0.0000
2	-0.0000	-0.0000	-0.0000	-0.0000	-0.0000	-0.0000	-0.0000	-0.0000	-0.0000	-0.0000
3	-0.0000	-0.0000	-0.0000	-0.0000	-0.0000	-0.0000	-0.0000	-0.0000	-0.0000	-0.0000
4	-0.0000	-0.0000	-0.0000	-0.0000	-0.0011	-0.0000	-0.0000	-0.0000	-0.0000	-0.0000
5	-0.0000	-0.0000	-0.0000	-0.0011	-7.8918	-0.0011	-0.0000	-0.0000	-0.0000	-0.0000
6	-0.0000	-0.0000	-0.0000	-0.0000	-0.0011	-0.0000	-0.0000	-0.0000	-0.0000	-0.0000
7	-0.0000	-0.0000	-0.0000	-0.0000	-0.0000	-0.0000	-0.0000	-0.0000	-0.0000	-0.0000
8	-0.0000	-0.0000	-0.0000	-0.0000	-0.0000	-0.0000	-0.0000	-0.0000	-0.0000	-0.0000
9	-0.0000	-0.0000	-0.0000	-0.0000	-0.0000	-0.0000	-0.0000	-0.0000	-0.0000	-0.0000
10	-0.0000	-0.0000	-0.0000	-0.0000	-0.0000	-0.0000	-0.0000	-0.0000	-0.0000	-0.0000
1	-0.0000	-0.0000	-0.0000	-0.0000	-0.0000	-0.0000	-0.0000	-0.0000	-0.0000	-0.0000
2	-0.0000	-0.0000	-0.0000	-0.0000	-0.0000	-0.0000	-0.0000	-0.0000	-0.0000	-0.0000
3	-0.0000	-0.0000	-0.0000	-0.0000	-0.0000	-0.0000	-0.0000	-0.0000	-0.0000	-0.0000
4	-0.0000	-0.0000	-0.0000	-0.0000	-0.0027	-0.0000	-0.0000	-0.0000	-0.0000	-0.0000
5	-0.0000	-0.0000	-0.0000	-0.0027	-13.0540	-0.0027	-0.0000	-0.0000	-0.0000	-0.0000
6	-0.0000	-0.0000	-0.0000	-0.0000	-0.0027	-0.0000	-0.0000	-0.0000	-0.0000	-0.0000
7	-0.0000	-0.0000	-0.0000	-0.0000	-0.0000	-0.0000	-0.0000	-0.0000	-0.0000	-0.0000
8	-0.0000	-0.0000	-0.0000	-0.0000	-0.0000	-0.0000	-0.0000	-0.0000	-0.0000	-0.0000
9	-0.0000	-0.0000	-0.0000	-0.0000	-0.0000	-0.0000	-0.0000	-0.0000	-0.0000	-0.0000
10	-0.0000	-0.0000	-0.0000	-0.0000	-0.0000	-0.0000	-0.0000	-0.0000	-0.0000	-0.0000
1	-0.0000	-0.0000	-0.0000	-0.0000	-0.0000	-0.0000	-0.0000	-0.0000	-0.0000	-0.0000

(continued)

Table 17. Input Parameters($T = .1\ Ft^2/Hour$) and Resultant Output (continued)

2	-0.0000	-0.0000	-0.0000	-0.0000	-0.0000	-0.0000	-0.0000	-0.0000	-0.0000	-0.0000
3	-0.0000	-0.0000	-0.0000	-0.0000	-0.0000	-0.0000	-0.0000	-0.0000	-0.0000	-0.0000
4	-0.0000	-0.0000	-0.0000	-0.0000	-0.0054	-0.0000	-0.0000	-0.0000	-0.0000	-0.0000
5	-0.0000	-0.0000	-0.0000	-0.0054	-19.2450	-0.0054	-0.0000	-0.0000	-0.0000	-0.0000
6	-0.0000	-0.0000	-0.0000	-0.0000	-0.0054	-0.0000	-0.0000	-0.0000	-0.0000	-0.0000
7	-0.0000	-0.0000	-0.0000	-0.0000	-0.0000	-0.0000	-0.0000	-0.0000	-0.0000	-0.0000
8	-0.0000	-0.0000	-0.0000	-0.0000	-0.0000	-0.0000	-0.0000	-0.0000	-0.0000	-0.0000
9	-0.0000	-0.0000	-0.0000	-0.0000	-0.0000	-0.0000	-0.0000	-0.0000	-0.0000	-0.0000
10	-0.0000	-0.0000	-0.0000	-0.0000	-0.0000	-0.0000	-0.0000	-0.0000	-0.0000	-0.0000
1	-0.0000	-0.0000	-0.0000	-0.0000	-0.0000	-0.0000	-0.0000	-0.0000	-0.0000	-0.0000
2	-0.0000	-0.0000	-0.0000	-0.0000	-0.0000	-0.0000	-0.0000	-0.0000	-0.0000	-0.0000
3	-0.0000	-0.0000	-0.0000	-0.0000	-0.0000	-0.0000	-0.0000	-0.0000	-0.0000	-0.0000
4	-0.0000	-0.0000	-0.0000	-0.0000	-0.0100	-0.0000	-0.0000	-0.0000	-0.0000	-0.0000
5	-0.0000	-0.0000	-0.0000	-0.0100	-26.6690	-0.0100	-0.0000	-0.0000	-0.0000	-0.0000
6	-0.0000	-0.0000	-0.0000	-0.0000	-0.0100	-0.0000	-0.0000	-0.0000	-0.0000	-0.0000
7	-0.0000	-0.0000	-0.0000	-0.0000	-0.0000	-0.0000	-0.0000	-0.0000	-0.0000	-0.0000
8	-0.0000	-0.0000	-0.0000	-0.0000	-0.0000	-0.0000	-0.0000	-0.0000	-0.0000	-0.0000
9	-0.0000	-0.0000	-0.0000	-0.0000	-0.0000	-0.0000	-0.0000	-0.0000	-0.0000	-0.0000
10	-0.0000	-0.0000	-0.0000	-0.0000	-0.0000	-0.0000	-0.0000	-0.0000	-0.0000	-0.0000
1	-0.0000	-0.0000	-0.0000	-0.0000	-0.0000	-0.0000	-0.0000	-0.0000	-0.0000	-0.0000
2	-0.0000	-0.0000	-0.0000	-0.0000	-0.0000	-0.0000	-0.0000	-0.0000	-0.0000	-0.0000
3	-0.0000	-0.0000	-0.0000	-0.0000	-0.0000	-0.0000	-0.0000	-0.0000	-0.0000	-0.0000
4	-0.0000	-0.0000	-0.0000	-0.0000	-0.0174	-0.0000	-0.0000	-0.0000	-0.0000	-0.0000
5	-0.0000	-0.0000	-0.0000	-0.0174	-35.5705	-0.0174	-0.0000	-0.0000	-0.0000	-0.0000
6	-0.0000	-0.0000	-0.0000	-0.0000	-0.0174	-0.0000	-0.0000	-0.0000	-0.0000	-0.0000
7	-0.0000	-0.0000	-0.0000	-0.0000	-0.0000	-0.0000	-0.0000	-0.0000	-0.0000	-0.0000
8	-0.0000	-0.0000	-0.0000	-0.0000	-0.0000	-0.0000	-0.0000	-0.0000	-0.0000	-0.0000
9	-0.0000	-0.0000	-0.0000	-0.0000	-0.0000	-0.0000	-0.0000	-0.0000	-0.0000	-0.0000
10	-0.0000	-0.0000	-0.0000	-0.0000	-0.0000	-0.0000	-0.0000	-0.0000	-0.0000	-0.0000
1	-0.0000	-0.0000	-0.0000	-0.0000	-0.0000	-0.0000	-0.0000	-0.0000	-0.0000	-0.0000
2	-0.0000	-0.0000	-0.0000	-0.0000	-0.0000	-0.0000	-0.0000	-0.0000	-0.0000	-0.0000

(continued)

Table 17. Input Parameters (T = .1 Ft^2/Hour) and Resultant Output (continued)

3	-0.0000	-0.0000	-0.0000	-0.0000	-0.0000	-0.0000	-0.0000	-0.0000	-0.0000	-0.0000
4	-0.0000	-0.0000	-0.0000	-0.0000	-0.0239	-0.0000	-0.0000	-0.0000	-0.0000	-0.0000
5	-0.0000	-0.0000	-0.0000	-0.0239	-46.2417	-0.0239	-0.0000	-0.0000	-0.0000	-0.0000
6	-0.0000	-0.0000	-0.0000	-0.0000	-0.0239	-0.0000	-0.0000	-0.0000	-0.0000	-0.0000
7	-0.0000	-0.0000	-0.0000	-0.0000	-0.0000	-0.0000	-0.0000	-0.0000	-0.0000	-0.0000
8	-0.0000	-0.0000	-0.0000	-0.0000	-0.0000	-0.0000	-0.0000	-0.0000	-0.0000	-0.0000
9	-0.0000	-0.0000	-0.0000	-0.0000	-0.0000	-0.0000	-0.0000	-0.0000	-0.0000	-0.0000
10	-0.0000	-0.0000	-0.0000	-0.0000	-0.0000	-0.0000	-0.0000	-0.0000	-0.0000	-0.0000
1	-0.0000	-0.0000	-0.0000	-0.0000	-0.0000	-0.0000	-0.0000	-0.0000	-0.0000	-0.0000
2	-0.0000	-0.0000	-0.0000	-0.0000	-0.0000	-0.0000	-0.0000	-0.0000	-0.0000	-0.0000
3	-0.0000	-0.0000	-0.0000	-0.0000	-0.0000	-0.0000	-0.0000	-0.0000	-0.0000	-0.0000
4	-0.0000	-0.0000	-0.0000	-0.0001	-0.0464	-0.0001	-0.0000	-0.0000	-0.0000	-0.0000
5	-0.0000	-0.0000	-0.0000	-0.0464	-59.0319	-0.0464	-0.0000	-0.0000	-0.0000	-0.0000
6	-0.0000	-0.0000	-0.0000	-0.0001	-0.0464	-0.0001	-0.0000	-0.0000	-0.0000	-0.0000
7	-0.0000	-0.0000	-0.0000	-0.0000	-0.0000	-0.0000	-0.0000	-0.0000	-0.0000	-0.0000
8	-0.0000	-0.0000	-0.0000	-0.0000	-0.0000	-0.0000	-0.0000	-0.0000	-0.0000	-0.0000
9	-0.0000	-0.0000	-0.0000	-0.0000	-0.0000	-0.0000	-0.0000	-0.0000	-0.0000	-0.0000
10	-0.0000	-0.0000	-0.0000	-0.0000	-0.0000	-0.0000	-0.0000	-0.0000	-0.0000	-0.0000
1	-0.0000	-0.0000	-0.0000	-0.0000	-0.0000	-0.0000	-0.0000	-0.0000	-0.0000	-0.0000
2	-0.0000	-0.0000	-0.0000	-0.0000	-0.0000	-0.0000	-0.0000	-0.0000	-0.0000	-0.0000
3	-0.0000	-0.0000	-0.0000	-0.0000	-0.0001	-0.0000	-0.0000	-0.0000	-0.0000	-0.0000
4	-0.0000	-0.0000	-0.0000	-0.0001	-0.0730	-0.0001	-0.0000	-0.0000	-0.0000	-0.0000
5	-0.0000	-0.0000	-0.0001	-0.0730	-74.3582	-0.0730	-0.0001	-0.0000	-0.0000	-0.0000
6	-0.0000	-0.0000	-0.0000	-0.0001	-0.0730	-0.0001	-0.0000	-0.0000	-0.0000	-0.0000
7	-0.0000	-0.0000	-0.0000	-0.0000	-0.0001	-0.0000	-0.0000	-0.0000	-0.0000	-0.0000
8	-0.0000	-0.0000	-0.0000	-0.0000	-0.0000	-0.0000	-0.0000	-0.0000	-0.0000	-0.0000
9	-0.0000	-0.0000	-0.0000	-0.0000	-0.0000	-0.0000	-0.0000	-0.0000	-0.0000	-0.0000
10	-0.0000	-0.0000	-0.0000	-0.0000	-0.0000	-0.0000	-0.0000	-0.0000	-0.0000	-0.0000
1	-0.0000	-0.0000	-0.0000	-0.0000	-0.0000	-0.0000	-0.0000	-0.0000	-0.0000	-0.0000
2	-0.0000	-0.0000	-0.0000	-0.0000	-0.0000	-0.0000	-0.0000	-0.0000	-0.0000	-0.0000
3	-0.0000	-0.0000	-0.0000	-0.0000	-0.0001	-0.0000	-0.0000	-0.0000	-0.0000	-0.0000

(continued)

Table 17. Input Parameters (T = .1 Ft^2/Hour) and Resultant Output (continued)

4	-0.0000	-0.0000	-0.0000	-0.0002	-0.1126	-0.0002	-0.0000	-0.0000	-0.0000	-0.0000
5	-0.0000	-0.0000	-0.0001	-0.1126	-92.7182	-0.1126	-0.0001	-0.0000	-0.0000	-0.0000
6	-0.0000	-0.0000	-0.0000	-0.0002	-0.1126	-0.0002	-0.0000	-0.0000	-0.0000	-0.0000
7	-0.0000	-0.0000	-0.0000	-0.0000	-0.0001	-0.0000	-0.0000	-0.0000	-0.0000	-0.0000
8	-0.0000	-0.0000	-0.0000	-0.0000	-0.0000	-0.0000	-0.0000	-0.0000	-0.0000	-0.0000
9	-0.0000	-0.0000	-0.0000	-0.0000	-0.0000	-0.0000	-0.0000	-0.0000	-0.0000	-0.0000
10	-0.0000	-0.0000	-0.0000	-0.0000	-0.0000	-0.0000	-0.0000	-0.0000	-0.0000	-0.0000

2time= 25.96

0.6887317e-02 1

Table 18. Input Parameters (T = 1.0 Ft^2/Hour) and Resultant Output

INPUT	5	10 10 5	1.0 10 1.0	$^{2.0}$ 1.0 1.0	12e2 12e2	6.0 0.0	9.0 4307.				
1	-0.0000	-0.0000	-0.0000	-0.0000	-0.0000	-0.0000	-0.0000	-0.0000	-0.0000	-0.0000	
2	-0.0000	-0.0000	-0.0000	-0.0000	-0.0000	-0.0000	-0.0000	-0.0000	-0.0000	-0.0000	
3	-0.0000	-0.0000	-0.0000	-0.0000	-0.0000	-0.0000	-0.0000	-0.0000	-0.0000	-0.0000	
4	-0.0000	-0.0000	-0.0000	-0.0000	-0.0030	-0.0000	-0.0000	-0.0000	-0.0000	-0.0000	
5	-0.0000	-0.0000	-0.0000	-0.0030	-3.5773	-0.0030	-0.0000	-0.0000	-0.0000	-0.0000	
6	-0.0000	-0.0000	-0.0000	-0.0000	-0.0030	-0.0000	-0.0000	-0.0000	-0.0000	-0.0000	
7	-0.0000	-0.0000	-0.0000	-0.0000	-0.0000	-0.0000	-0.0000	-0.0000	-0.0000	-0.0000	
8	-0.0000	-0.0000	-0.0000	-0.0000	-0.0000	-0.0000	-0.0000	-0.0000	-0.0000	-0.0000	
9	-0.0000	-0.0000	-0.0000	-0.0000	-0.0000	-0.0000	-0.0000	-0.0000	-0.0000	-0.0000	
10	-0.0000	-0.0000	-0.0000	-0.0000	-0.0000	-0.0000	-0.0000	-0.0000	-0.0000	-0.0000	
1	-0.0000	-0.0000	-0.0000	-0.0000	-0.0000	-0.0000	-0.0000	-0.0000	-0.0000	-0.0000	
2	-0.0000	-0.0000	-0.0000	-0.0000	-0.0000	-0.0000	-0.0000	-0.0000	-0.0000	-0.0000	
3	-0.0000	-0.0000	-0.0000	-0.0000	-0.0000	-0.0000	-0.0000	-0.0000	-0.0000	-0.0000	
4	-0.0000	-0.0000	-0.0000	-0.0000	-0.0108	-0.0000	-0.0000	-0.0000	-0.0000	-0.0000	
5	-0.0000	-0.0000	-0.0000	-0.0108	-7.3529	-0.0108	-0.0000	-0.0000	-0.0000	-0.0000	
6	-0.0000	-0.0000	-0.0000	-0.0000	-0.0108	-0.0000	-0.0000	-0.0000	-0.0000	-0.0000	
7	-0.0000	-0.0000	-0.0000	-0.0000	-0.0000	-0.0000	-0.0000	-0.0000	-0.0000	-0.0000	
8	-0.0000	-0.0000	-0.0000	-0.0000	-0.0000	-0.0000	-0.0000	-0.0000	-0.0000	-0.0000	
9	-0.0000	-0.0000	-0.0000	-0.0000	-0.0000	-0.0000	-0.0000	-0.0000	-0.0000	-0.0000	
10	-0.0000	-0.0000	-0.0000	-0.0000	-0.0000	-0.0000	-0.0000	-0.0000	-0.0000	-0.0000	
1	-0.0000	-0.0000	-0.0000	-0.0000	-0.0000	-0.0000	-0.0000	-0.0000	-0.0000	-0.0000	
2	-0.0000	-0.0000	-0.0000	-0.0000	-0.0000	-0.0000	-0.0000	-0.0000	-0.0000	-0.0000	
3	-0.0000	-0.0000	-0.0000	-0.0000	-0.0000	-0.0000	-0.0000	-0.0000	-0.0000	-0.0000	
4	-0.0000	-0.0000	-0.0000	-0.0001	-0.0262	-0.0001	-0.0000	-0.0000	-0.0000	-0.0000	
5	-0.0000	-0.0000	-0.0000	-0.0262	-12.9592	-0.0262	-0.0000	-0.0000	-0.0000	-0.0000	
6	-0.0000	-0.0000	-0.0000	-0.0001	-0.0262	-0.0001	-0.0000	-0.0000	-0.0000	-0.0000	
7	-0.0000	-0.0000	-0.0000	-0.0000	-0.0000	-0.0000	-0.0000	-0.0000	-0.0000	-0.0000	
8	-0.0000	-0.0000	-0.0000	-0.0000	-0.0000	-0.0000	-0.0000	-0.0000	-0.0000	-0.0000	
9	-0.0000	-0.0000	-0.0000	-0.0000	-0.0000	-0.0000	-0.0000	-0.0000	-0.0000	-0.0000	
10	-0.0000	-0.0000	-0.0000	-0.0000	-0.0000	-0.0000	-0.0000	-0.0000	-0.0000	-0.0000	
1	-0.0000	-0.0000	-0.0000	-0.0000	-0.0000	-0.0000	-0.0000	-0.0000	-0.0000	-0.0000	

(continued)

Table 18. Input Parameters (T = 1.0 Ft^2/Hour) and Resultant Output (continued)

2	-0.0000	-0.0000	-0.0000	-0.0000	-0.0000	-0.0000	-0.0000	-0.0000	-0.0000	-0.0000
3	-0.0000	-0.0000	-0.0000	-0.0000	-0.0001	-0.0000	-0.0000	-0.0000	-0.0000	-0.0000
4	-0.0000	-0.0000	-0.0000	-0.0002	-0.0533	-0.0002	-0.0000	-0.0000	-0.0000	-0.0000
5	-0.0000	-0.0000	-0.0001	-0.0533	-19.0519	-0.0533	-0.0001	-0.0000	-0.0000	-0.0000
6	-0.0000	-0.0000	-0.0000	-0.0002	-0.0533	-0.0002	-0.0000	-0.0000	-0.0000	-0.0000
7	-0.0000	-0.0000	-0.0000	-0.0000	-0.0001	-0.0000	-0.0000	-0.0000	-0.0000	-0.0000
8	-0.0000	-0.0000	-0.0000	-0.0000	-0.0000	-0.0000	-0.0000	-0.0000	-0.0000	-0.0000
9	-0.0000	-0.0000	-0.0000	-0.0000	-0.0000	-0.0000	-0.0000	-0.0000	-0.0000	-0.0000
10	-0.0000	-0.0000	-0.0000	-0.0000	-0.0000	-0.0000	-0.0000	-0.0000	-0.0000	-0.0000
1	-0.0000	-0.0000	-0.0000	-0.0000	-0.0000	-0.0000	-0.0000	-0.0000	-0.0000	-0.0000
2	-0.0000	-0.0000	-0.0000	-0.0000	-0.0000	-0.0000	-0.0000	-0.0000	-0.0000	-0.0000
3	-0.0000	-0.0000	-0.0000	-0.0000	-0.0003	-0.0000	-0.0000	-0.0000	-0.0000	-0.0000
4	-0.0000	-0.0000	-0.0000	-0.0006	-0.0981	-0.0006	-0.0000	-0.0000	-0.0000	-0.0000
5	-0.0000	-0.0000	-0.0003	-0.0981	-26.3132	-0.0981	-0.0003	-0.0000	-0.0000	-0.0000
6	-0.0000	-0.0000	-0.0000	-0.0006	-0.0981	-0.0006	-0.0000	-0.0000	-0.0000	-0.0000
7	-0.0000	-0.0000	-0.0000	-0.0000	-0.0003	-0.0000	-0.0000	-0.0000	-0.0000	-0.0000
8	-0.0000	-0.0000	-0.0000	-0.0000	-0.0000	-0.0000	-0.0000	-0.0000	-0.0000	-0.0000
9	-0.0000	-0.0000	-0.0000	-0.0000	-0.0000	-0.0000	-0.0000	-0.0000	-0.0000	-0.0000
10	-0.0000	-0.0000	-0.0000	-0.0000	-0.0000	-0.0000	-0.0000	-0.0000	-0.0000	-0.0000
1	-0.0000	-0.0000	-0.0000	-0.0000	-0.0000	-0.0000	-0.0000	-0.0000	-0.0000	-0.0000
2	-0.0000	-0.0000	-0.0000	-0.0000	-0.0000	-0.0000	-0.0000	-0.0000	-0.0000	-0.0000
3	-0.0000	-0.0000	-0.0000	-0.0000	-0.0006	-0.0000	-0.0000	-0.0000	-0.0000	-0.0000
4	-0.0000	-0.0000	-0.0000	-0.0013	-0.1692	-0.0013	-0.0000	-0.0000	-0.0000	-0.0000
5	-0.0000	-0.0000	-0.0006	-0.1692	-34.9556	-0.1692	-0.0006	-0.0000	-0.0000	-0.0000
6	-0.0000	-0.0000	-0.0000	-0.0013	-0.1692	-0.0013	-0.0000	-0.0000	-0.0000	-0.0000
7	-0.0000	-0.0000	-0.0000	-0.0000	-0.0006	-0.0000	-0.0000	-0.0000	-0.0000	-0.0000
8	-0.0000	-0.0000	-0.0000	-0.0000	-0.0000	-0.0000	-0.0000	-0.0000	-0.0000	-0.0000
9	-0.0000	-0.0000	-0.0000	-0.0000	-0.0000	-0.0000	-0.0000	-0.0000	-0.0000	-0.0000
10	-0.0000	-0.0000	-0.0000	-0.0000	-0.0000	-0.0000	-0.0000	-0.0000	-0.0000	-0.0000
1	-0.0000	-0.0000	-0.0000	-0.0000	-0.0000	-0.0000	-0.0000	-0.0000	-0.0000	-0.0000
2	-0.0000	-0.0000	-0.0000	-0.0000	-0.0000	-0.0000	-0.0000	-0.0000	-0.0000	-0.0000

(continued)

Table 18. Input Parameters (T = 1.0 Ft^2/Hour) and Resultant Output (continued)

5	-0.0000	-0.0000	-0.0000	-0.0000	-0.0013	-0.0000	-0.0000	-0.0000	-0.0000	-0.0000
4	-0.0000	-0.0000	-0.0000	-0.0026	-0.2790	-0.0026	-0.0000	-0.0000	-0.0000	-0.0000
5	-0.0000	-0.0000	-0.0013	-0.2790	-45.2255	-0.2790	-0.0013	-0.0000	-0.0000	-0.0000
6	-0.0000	-0.0000	-0.0000	-0.0026	-0.2790	-0.0026	-0.0000	-0.0000	-0.0000	-0.0000
7	-0.0000	-0.0000	-0.0000	-0.0000	-0.0013	-0.0000	-0.0000	-0.0000	-0.0000	-0.0000
8	-0.0000	-0.0000	-0.0000	-0.0000	-0.0000	-0.0000	-0.0000	-0.0000	-0.0000	-0.0000
9	-0.0000	-0.0000	-0.0000	-0.0000	-0.0000	-0.0000	-0.0000	-0.0000	-0.0000	-0.0000
10	-0.0000	-0.0000	-0.0000	-0.0000	-0.0000	-0.0000	-0.0000	-0.0000	-0.0000	-0.0000
1	-0.0000	-0.0000	-0.0000	-0.0000	-0.0000	-0.0000	-0.0000	-0.0000	-0.0000	-0.0000
2	-0.0000	-0.0000	-0.0000	-0.0000	-0.0000	-0.0000	-0.0000	-0.0000	-0.0000	-0.0000
3	-0.0000	-0.0000	-0.0000	-0.0000	-0.0026	-0.0000	-0.0000	-0.0000	-0.0000	-0.0000
4	-0.0000	-0.0000	-0.0000	-0.0052	-0.4451	-0.0052	-0.0000	-0.0000	-0.0000	-0.0000
5	-0.0000	-0.0000	-0.0026	-0.4451	-57.4058	-0.4451	-0.0026	-0.0000	-0.0000	-0.0000
6	-0.0000	-0.0000	-0.0000	-0.0052	-0.4451	-0.0052	-0.0000	-0.0000	-0.0000	-0.0000
7	-0.0000	-0.0000	-0.0000	-0.0000	-0.0026	-0.0000	-0.0000	-0.0000	-0.0000	-0.0000
8	-0.0000	-0.0000	-0.0000	-0.0000	-0.0000	-0.0000	-0.0000	-0.0000	-0.0000	-0.0000
9	-0.0000	-0.0000	-0.0000	-0.0000	-0.0000	-0.0000	-0.0000	-0.0000	-0.0000	-0.0000
10	-0.0000	-0.0000	-0.0000	-0.0000	-0.0000	-0.0000	-0.0000	-0.0000	-0.0000	-0.0000
1	-0.0000	-0.0000	-0.0000	-0.0000	-0.0000	-0.0000	-0.0000	-0.0000	-0.0000	-0.0000
2	-0.0000	-0.0000	-0.0000	-0.0000	-0.0000	-0.0000	-0.0000	-0.0000	-0.0000	-0.0000
3	-0.0000	-0.0000	-0.0000	-0.0001	-0.0050	-0.0001	-0.0000	-0.0000	-0.0000	-0.0000
4	-0.0000	-0.0000	-0.0001	-0.0100	-0.6926	-0.0100	-0.0001	-0.0000	-0.0000	-0.0000
5	-0.0000	-0.0000	-0.0050	-0.6926	-71.8191	-0.6926	-0.0050	-0.0000	-0.0000	-0.0000
6	-0.0000	-0.0000	-0.0001	-0.0100	-0.6926	-0.0100	-0.0001	-0.0000	-0.0000	-0.0000
7	-0.0000	-0.0000	-0.0000	-0.0001	-0.0050	-0.0001	-0.0000	-0.0000	-0.0000	-0.0000
8	-0.0000	-0.0000	-0.0000	-0.0000	-0.0000	-0.0000	-0.0000	-0.0000	-0.0000	-0.0000
9	-0.0000	-0.0000	-0.0000	-0.0000	-0.0000	-0.0000	-0.0000	-0.0000	-0.0000	-0.0000
10	-0.0000	-0.0000	-0.0000	-0.0000	-0.0000	-0.0000	-0.0000	-0.0000	-0.0000	-0.0000
1	-0.0000	-0.0000	-0.0000	-0.0000	-0.0000	-0.0000	-0.0000	-0.0000	-0.0000	-0.0000
2	-0.0000	-0.0000	-0.0000	-0.0000	-0.0001	-0.0000	-0.0000	-0.0000	-0.0000	-0.0000
3	-0.0000	-0.0000	-0.0000	-0.0002	-0.0094	-0.0002	-0.0000	-0.0000	-0.0000	-0.0000

(continued)

Table 18. Input Parameters (T = 1.0 Ft^2/Hour) and Resultant Output (continued)

4	-0.0000	-0.0000	-0.0002	-0.0183	-1.0566	-0.0188	-0.0002	-0.0000	-0.0000	-0.0000
5	-0.0000	-0.0001	-0.0094	-1.0566	-86.8288	-1.0566	-0.0094	-0.0001	-0.0000	-0.0000
6	-0.0000	-0.0000	-0.0002	-0.0183	-1.0566	-0.0188	-0.0002	-0.0000	-0.0000	-0.0000
7	-0.0000	-0.0000	-0.0000	-0.0002	-0.0094	-0.0002	-0.0000	-0.0000	-0.0000	-0.0000
8	-0.0000	-0.0000	-0.0000	-0.0000	-0.0001	-0.0000	-0.0000	-0.0000	-0.0000	-0.0000
9	-0.0000	-0.0000	-0.0000	-0.0000	-0.0000	-0.0000	-0.0000	-0.0000	-0.0000	-0.0000
10	-0.0000	-0.0000	-0.0000	-0.0000	-0.0000	-0.0000	-0.0000	-0.0000	-0.0000	-0.0000

2time= 25.96

0.6617422e-01 1

Average hydraulic conductivity can be estimated for the open length of the well bore (510 ft), by using the expression T = Kh'. Values for hydraulic conductivity range from 4.7×10^{-3} ft/day to 4.7×10^{-2} ft/day. In addition, specific capacity of the well was determined to be 6.3 gallons per minute per foot of drawdown.

Questionable results were obtained for the determination of storage coefficient of a confined aquifer due to meteorological phenomena. The strip charts from the water-level recorders at each observation well and the microbarograph (for the month of January, 1985) were analyzed for water level fluctuations h (feet), and barometric pressure changes P_a (inches of Hg), respectively, for the same time periods. Water level fluctuations recorded on the strip chart (15-19 January, 1985) for the East Observation Well were used (Figure 38). However, there appears to be very little correlation between water level fluctuations and barometric pressure changes for the West Observation Well (Figure 39). As a result, data from the West well was not used. Also, barometric pressures were scrutinized for the time period 15-19 January, 1985 (Figure 40). Finally, the data from both strip charts were synthesized and listed in Table 19. Values from Table 19, ΔP_a versus Δh (vertical) axis were plotted (Figure 41). The plot is extremely scattered, but a best 'eye' fit resulted in a value of .47 for barometric effi-

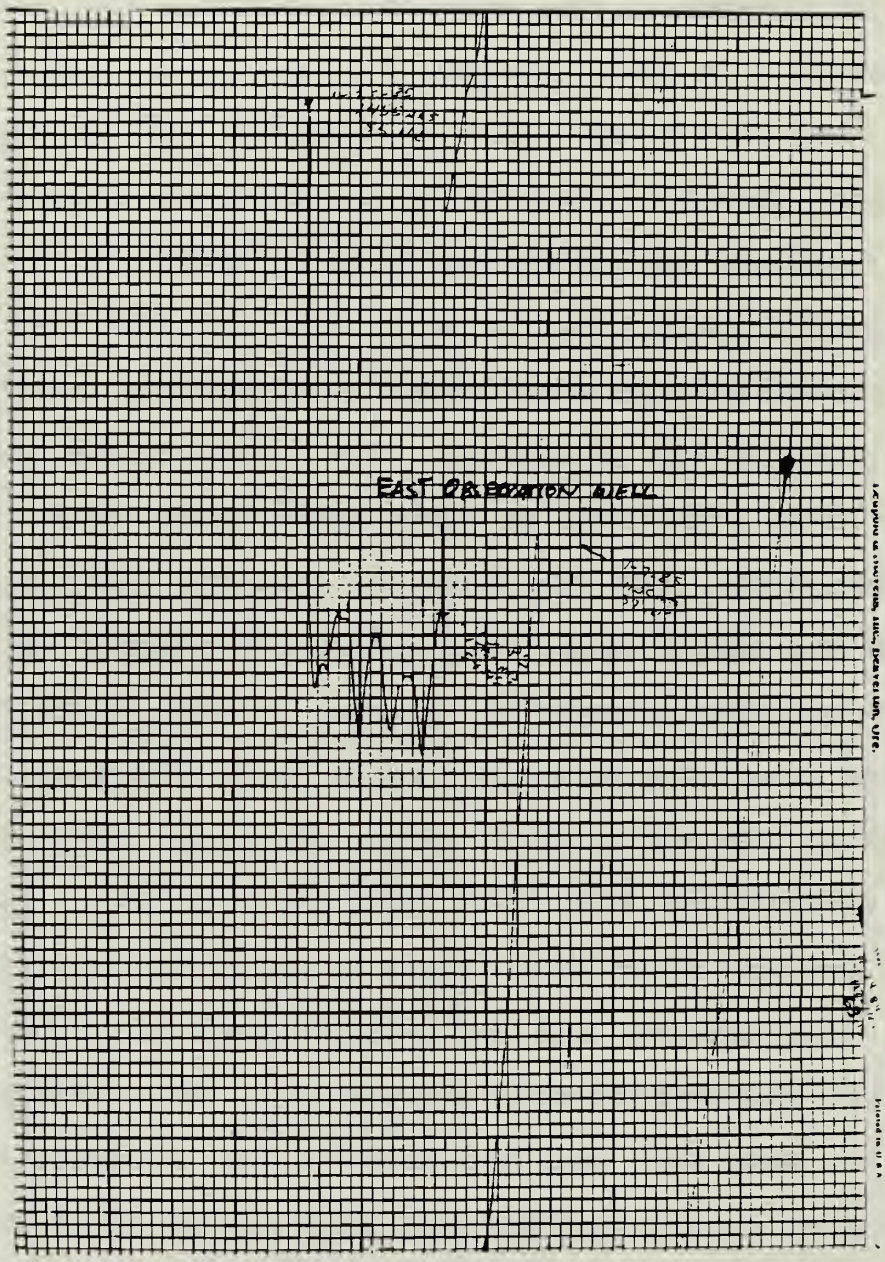

Figure 38. Strip chart from a Stevens'Water Level Recorder positioned at the East Observation Well, depicting continuous monitoring of water level fluctuations, h (feet).

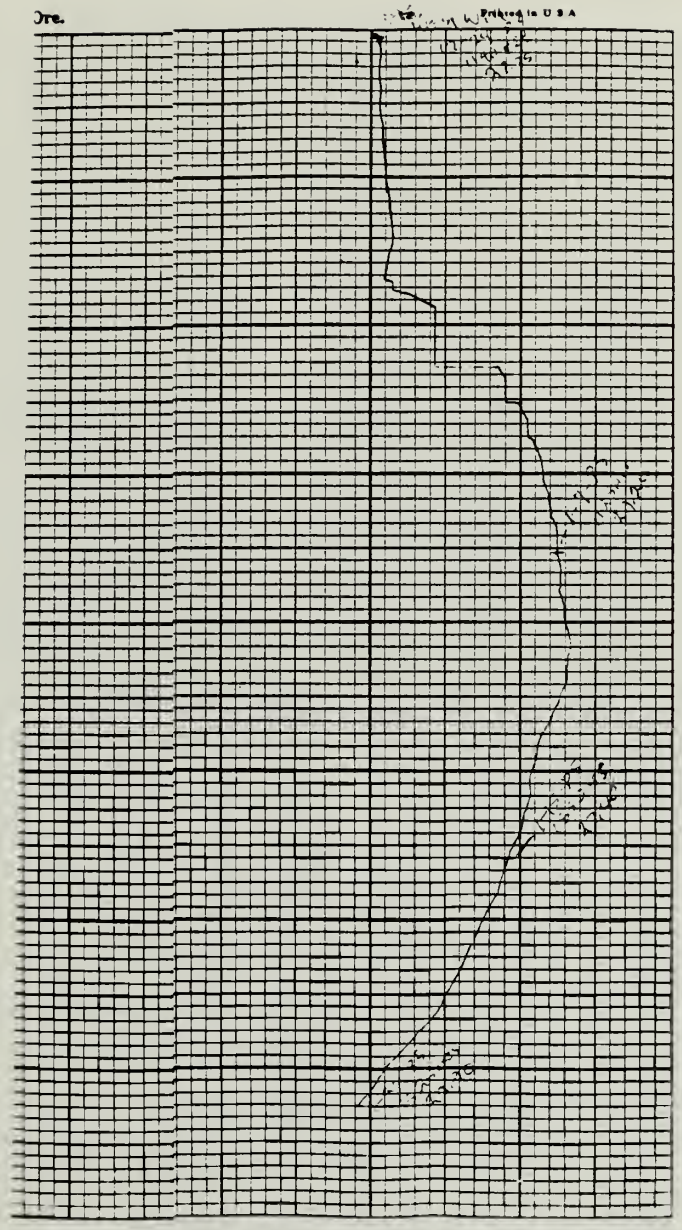

Figure 39. Strip chart from a Stevens' Water Level Recorder positioned at the West Observation Well, depicting continuous monitoring of water-level fluctuations, h (feet).

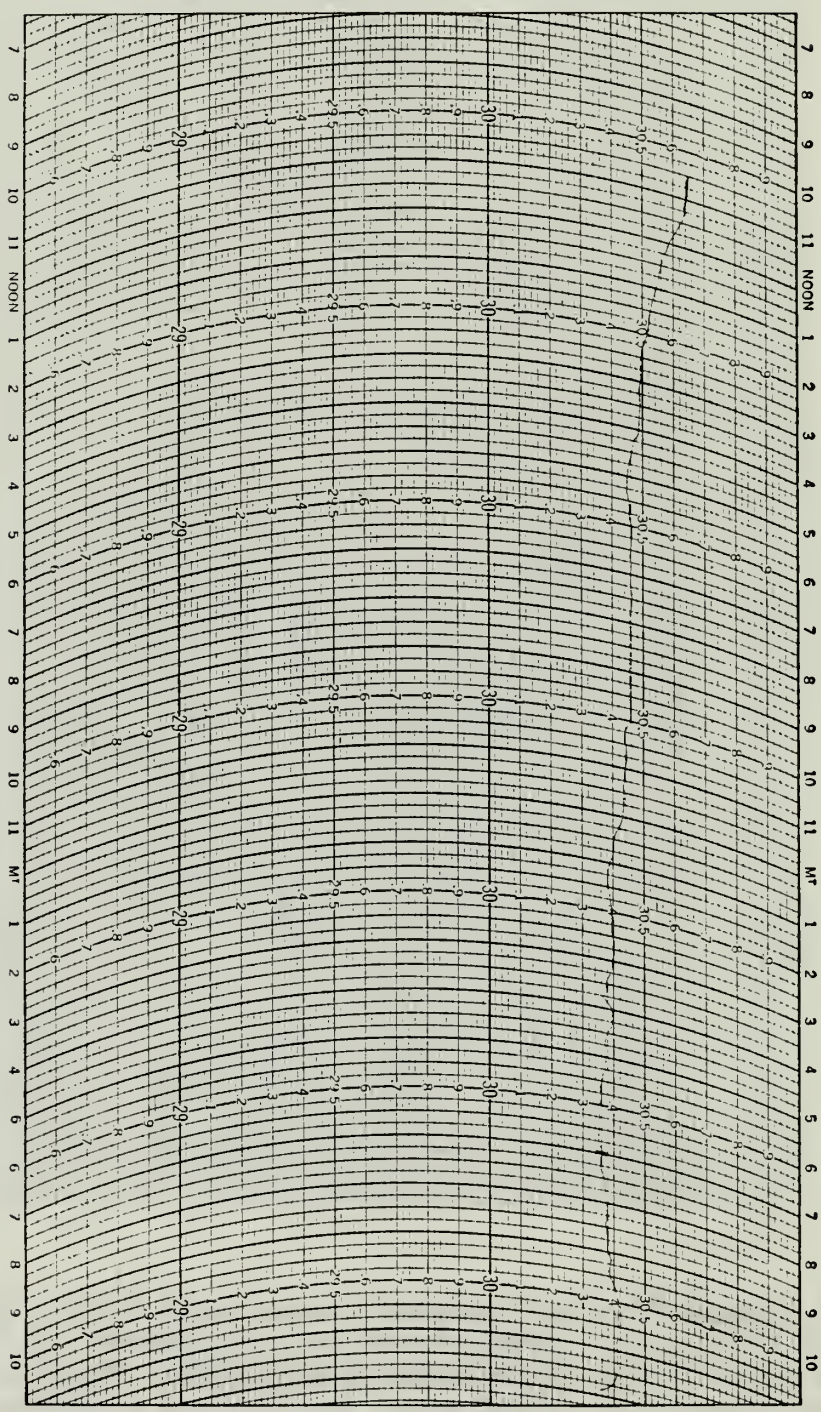

(continued)

Figure 40. Strip charts from a microbarograph positioned at the Travertine Nature Center, depicting continuous readings of barometric pressure, P_a (inches of H_g).

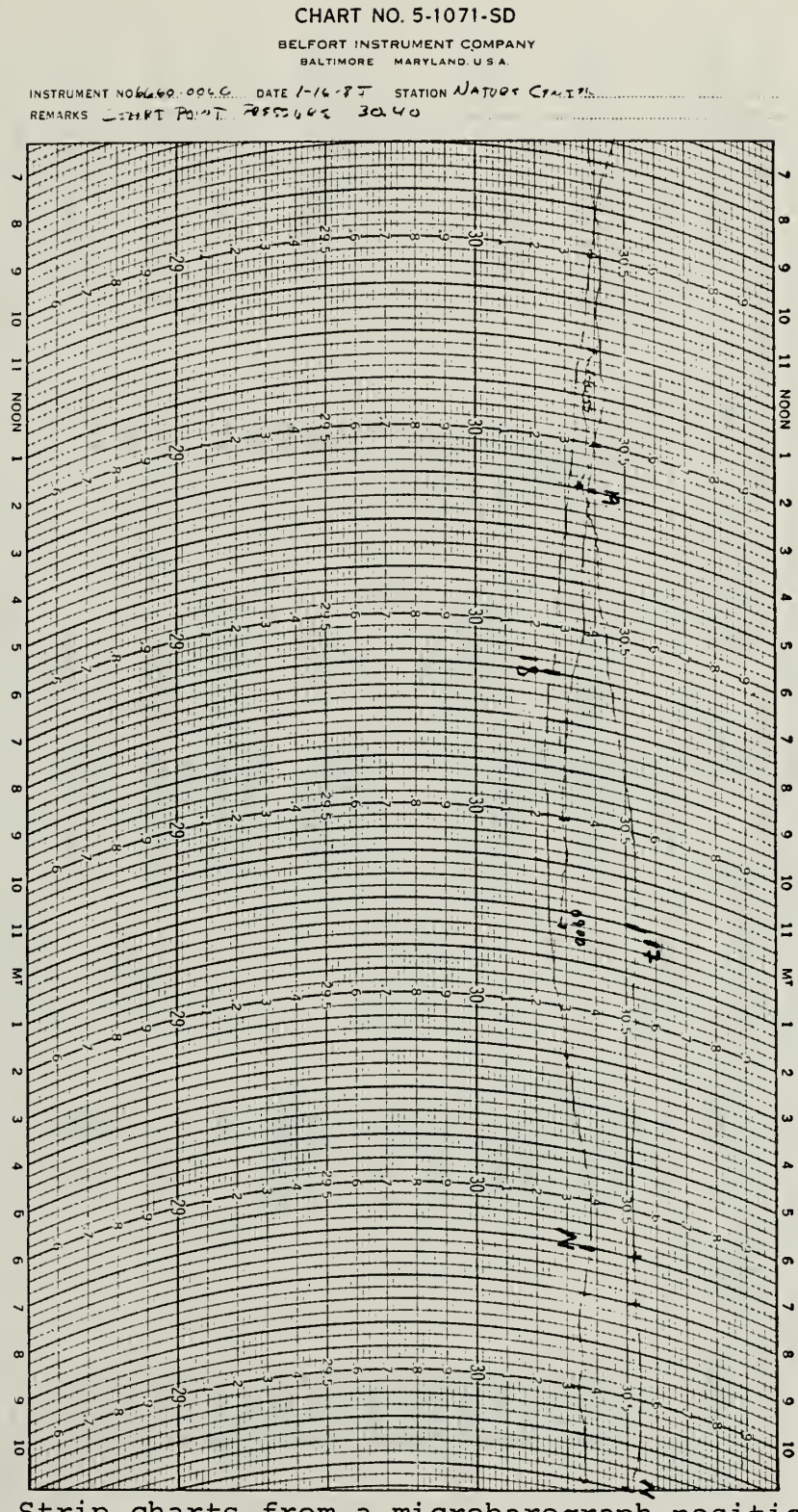

Figure 40. Strip charts from a microbarograph positioned at the Travertine Nature Center, depicting continuous readings of barometric pressure P_a (inches of H_g)(continued).

Table 19. Water Level Fluctuations and Barometric Pressure Changes

Day	Hour	+Water Level Fluctuations h (ft)	Δh (ft)	Barometric Pressure P_a (in. of Hg)	*ΔPa (feet of H_2O)
15	1500	54.45	.08	30.49	.14
16	0700	54.33	(151500-160700)	30.36	(151500-160700)
	1100			30.41	
	1200	54.36	.40	30.41	.04
	1500	54.40	(161200-161500)	30.36	(161200-161500)
	2100			30.5	
	2300	54.40		30.53	
17	0700			30.52	
	0800	54.36		30.53	
	1100		.08	30.52	.23
	1700	54.44	(170800-171700)	30.33	(170800-171700)
	2100	54.44		30.30	
	2300		.08	30.29	.02
18	0700	54.36	(172100-180700)	30.28	(172100-180700)
	1100		.09	30.38	.07
	1500	54.45	(180700-181500)	30.34	(180700-181500)
	2200			30.43	
	2300	54.45	.04	30.40	.12
19	0700	54.41	(182300-190700)		(182300-190700)

Note: Δh and ΔP_a represent changes in water level (feet) and barometric pressure (feet of H_2O) respectively, for a period of time. The period of time, in parenthesis, is listed under the values.

\+ Depth of water level readings of the East Observation Well

* ΔP_a (feet of H_2O) = (Pa_1 - Pa_2) inches of Hg x (specific gravity of Hg) x 1ft/12inches.

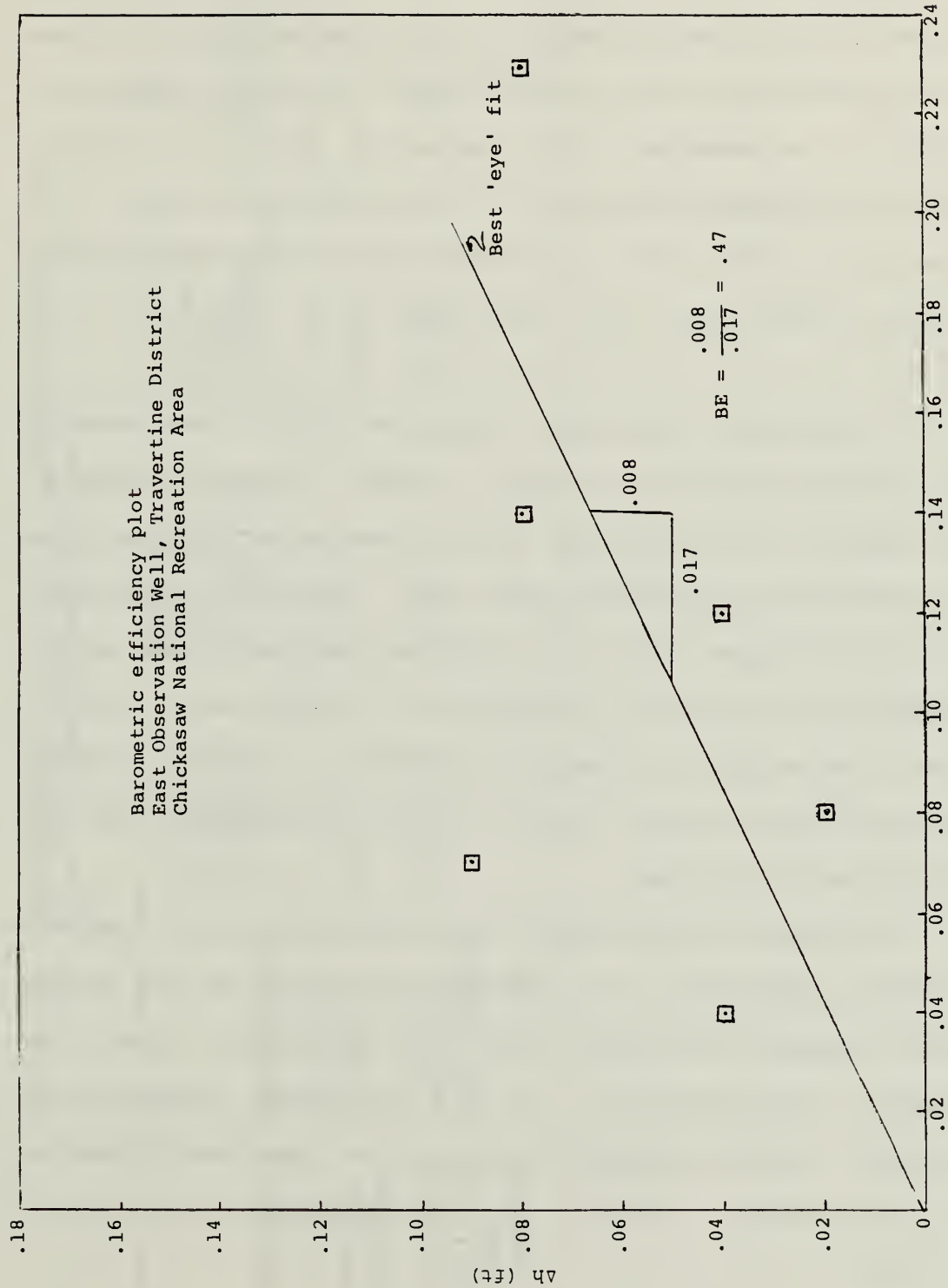

Figure 41. Graphical solution to obtain the barometric efficiency, BE.

ciency, BE.

Assumptions that were made in determining the value of the storage coefficient are: (1) saturated thickness of the Arbuckle Group is 3,500 feet; (2) water compressibility β, is constant with a value of $.25 \times 10^{-7}$ ft^2/lb; and (3) average porosity n, of the Arbuckle Group is .1. Equations (3.6) and (3.7) were used in determining the storage coefficient S_c, resulting in a value of 1.2×10^{-3}.

A regional technique, Equation (3.10), was used in the determination of average aquifer transmissivity T, for combined discharge Q_D, of the freshwater springs, and the mixed-water springs (Table 20). Estimates of average spring discharge coincided with the period of the potentiometric survey (25 January to 08 February, 1985). Also, the average hydraulic gradient I, and the average contributing aquifer width W, were extracted from the potentiometric survey.

Average transmissivity of the unconfined Arbuckle Aquifer responsible for combined discharge of the freshwater springs is about 43×10^3 ft^2/day. Also, the average transmissivity of the confined Simpson and Arbuckle Aquifers responsible for the combined discharge of mixed-water springs is approximately 3.9×10^2 ft^2/day.

Table 20. Determination of Average Aquifer Transmissivity as a Function of Spring Discharge

Springs	Aquifer(s)	Average Hydraulic Gradient I (ft/ft)	Average Width of Contributing Aquifer(s), W (ft)	Combined Spring Discharge Q_D (ft^3/day)	*Average Transmissivity, T (ft^2/day)
Buffalo Antelope	Arbuckle	10/5280	5280	432,000	4.3×10^4
Hillside Pavillion Black Sulphur	Arbuckle and Simpson	50/5280	5280	19,250	3.9×10^2

* $T = \frac{Q_D}{IW}$

4.4 Wells and Springs

East and West Observation Wells, completed in the Arbuckle Group, are located in close proximity to the artesian, freshwater springs (Plate III). The original intent of these wells were to monitor deprivation effects of adjacent production wells outside the confines of the park and establish a relationship of spring discharge versus piezometric level in the wells (Moore, 1972). Depth to water table measurements for the beginning of each month (since January 1974) for each observation well are listed in Tables 21 and 22.

Monthly-average stage data for Buffalo and Antelope are listed in Tables 23 and 24, respectively. As determined by previous investigators, flow of both springs can be approximated by modified weir equations. Monthly flow averages are calculated from stage data (in Tables 23 and 24) and are listed for both springs in Tables 25 and 26.

Hydrographs of East and West Observation Wells, and of Buffalo and Antelope Springs are depicted in Figure 42. Monthly precipitation histogram, long-term trend of hydrographs, and no-flow periods of Buffalo and Antelope are also included. Figure 42 graphically demonstrates spring discharge as a function of precipitation events and water table elevations of the East Observation Well.

The slope of the long-term trend of hydrograph for

Table 21. Ground Water Levels East Observation Well

Chickasaw National Recreation Area
Sulphur, Okla.
(Approximate Surface Elevation = 1150')

Depth to water, below land surface datum

(Beginning of Month Readings)

Year	Jan	Feb	Mar	Apr	May	June	July	Aug	Sept	Oct	Nov	Dec
1974*	38.5	44.5	47.0	49.5	51.0	51.0	54.0	58.0	61.0	59.0	56.0	44.0
1975*	49.0	51.0	42.0	39.0	41.0	40.5	44.5	50.0	56.0	59.5	62.0	64.0
1976*	66.0	67.5	69.5	68.0	67.0	64.5	65.0	63.5	69.5	71.0	71.0	73.0
1977*	74.5	76.5	75.5	67.0	64.0+	63.0	64.5	66.0	57.0	59.0	60.5	61.5
1978*	63.0	66.0	76.0	73.5	71.0	67.5	61.0	64.5	66.0	68.5	71.0	73.0
1979*	75.0	76.0	77.0	71.0	67.0	63.5	62.0	63.5	66.5	68.5	70.0	71.5
1980*	--	--	76.5	76.5	81.0	82.5	81.5	83.5	87.0	86.0	86.0	87.0
1981	86.5*	88.0*	89.0*	86.5*	86.5*	85.5*	75.5*	76.8	78.1	80.2	59.2	58.1
1982	61.6	59.8	57.2+	58.7	60.5	48.0+	44.2	47.9	53.2	57.0	61.2	64.8
1983	66.8	66.7+	62.0	61.5	60.8	45.2	49.7	56.1	60.9	63.1	65.5	66.3
1984	70.0	70.9	71.9+	70.0	68.9	70.5	71.4	73.3	75.8	77.7	74.2	69.5

NOTE: Flow at both Antelope and Buffalo Springs cease when this well reaches a depth of between 68 and 72 feet below the ground surface.

* Data taken from graph - original data unavailable

+ Denotes questionable value

(after Harp, 1984)

Table 22. Ground Water Levels West Observation Well

Chickasaw National Recreation Area
Sulphur, Okla.
(Approximate Surface Elevation = 1080')

Depth to water, below land surface datum

(Beginning of Month Readings)

Year	Jan	Feb	Mar	Apr	May	June	July	Aug	Sept	Oct	Nov	Dec
1974*	23.0	24.5	23.5	24.0	23.0	25.0	26.5	27.0	28.5	25.5	23.0	23.0
1975*	24.5	23.5	23.0	20.5	21.0	20.5	23.5	23.5	26.0	27.0	27.0	27.0
1976*	26.5	27.5	29.0	28.0	28.0	26.5	29.0	29.0	30.5	30.5	31.0	31.0
1977*	31.5	31.0	30.0	29.0	29.0	28.0	28.5	29.5	30.5	30.5	30.5	30.5
1978*	30.5	30.5	29.5	29.5	29.5	29.0	29.0	29.0	29.0	29.0	29.0	29.0
1979*	29.5	29.5	29.0	29.0	28.5	25.0	26.0	31.0	31.0	31.5	32.5	33.0
1980*	--	--	32.0	32.0	33.0	33.0	33.0	34.5	34.5	33.0	34.0	33.5
1981	32.0*	32.5*	32.5*	31.5*	32.5*	30.8	31.8	33.0	33.0	33.5	28.8	28.6
1982	32.2	28.5	28.3+	29.4	30.2	26.3	27.3	29.1	29.8	29.0	29.5	30.5
1983	--	28.7+	28.3	28.1	28.6	27.2	28.1	29.2	30.3	30.6	29.3	29.5
1984	29.2	29.2	30.1	29.0	28.8	30.9	31.4	32.1	32.4	32.7	30.2	29.6

* Data taken from graph - original data unavailable

+ Denotes questionable data

(after Harp, 1984)

Table 23. Stage Data Buffalo Springs

Chickasaw National Recreation Area
Sulphur, Okla.
(Approximate Surface Elevation = 1078')

Year	Jan	Feb	Mar	Apr	May	June	July	Aug	Sept	Oct	Nov	Dec
1972	-	-	-	-	-	1.95	1.91	1.99	1.49	1.06	2.00	-
1973	2.08	2.10	2.15	2.18	2.16	2.13	2.10	2.08	2.08	2.12	2.18	2.17
1974	2.15	2.12	2.08	2.08	2.08	2.09	2.02	2.01	2.03	2.07	2.13	2.11
1975	2.10	2.13	2.15	2.13	2.13	2.10	1.00	2.05	2.05	2.01	1.99	2.00
1976	1.97	1.94	1.96	1.96	1.99	1.98	1.94	1.90	1.86	1.56	1.33	0.52
1977	Dry	Dry	Dry	1.99	2.00	1.99	1.97	1.95	1.92	1.82	1.54	1.00+
1978	0.46+	Dry	Dry	1.79	1.93	2.01	2.01	1.95	1.90	1.76	1.36	Dry
1979	Dry	Dry	1.93	1.97	2.00	2.01	1.02	1.07	1.92	1.90	1.59	0.93
1980	Dry	Dry	Dry	Dry	Dry	Dry	Dry	Dry	Dry	Dry	Dry	Dry
1981	Dry	Dry	Dry	Dry	Dry	Dry	Dry	Dry	Dry	2.20	2.25	2.22
1982	2.23	2.22+	2.22+	2.22	2.26+	2.26	2.21	2.21	--	2.15+	2.13+	2.14+
1983	2.16	2.29	2.20	2.20	2.28	2.23	2.21	2.20	2.16+	2.70	2.10	1.49
1984	1.78	1.54	1.66	2.06	2.03	1.83	1.17	.05	Dry	Dry	1.73	2.18

\+ Denotes questionable data

Monthly average as derived from field data collected during the month

(after Harp, 1984)

Table 24. Stage Data Antelope Springs

Chickasaw National Recreation Area
Sulphur, Okla.
(Approximate Surface Elevation = 1080')

Year	Jan	Feb	Mar	Apr	May	June	July	Aug	Sept	Oct	Nov	Dec
1969	-	-	-	-	-	0.95	0.92	0.88	0.87	0.88	0.88	0.89+
1970	0.87	0.86	0.89	0.92	0.93	0.86	0.83	0.79	0.82	0.96	0.94	0.94
1971	0.91	0.89	0.87	0.83	0.80+	0.75	0.69	0.70	0.64	0.70	0.70	0.87
1972	0.88	0.87	0.85+	0.84	0.84	0.78	0.73	0.68	0.62+	0.54	0.87	0.89
1973	0.90	0.97	1.05	1.08	1.07	1.05	1.01	0.99	1.01	1.02	1.11	1.08
1974	1.06	1.05	1.05	1.06	1.03+	1.01	0.96	0.91	0.92+	1.04	1.03	1.02
1975	1.05	1.11	1.20	1.23	1.23	1.19	1.00	0.98	0.95	0.95	0.90	0.88
1976	0.76	0.84	0.86	0.86	0.96	0.94	0.84	0.80	0.73	0.65	Dry	Dry
1977	Dry	Dry	0.84	0.92	0.91	0.90	0.87	0.83	0.80	0.77	0.70	Dry
1978	Dry	Dry	Dry	0.71	0.80	0.88	0.84	0.81	0.76	0.68	0.65	Dry
1979	Dry	Dry	0.78	0.78	0.88	0.90	0.84	0.80	0.75	0.74	0.68+	Dry
1980	Dry	Dry	Dry	Dry	Dry	Dry	Dry	Dry	Dry	Dry	Dry	Dry
1981	Dry	Dry	Dry	Dry	Dry	Dry	Dry	Dry	Dry	0.95	0.99	0.99+
1982	0.94+	0.96+	0.98+	-	0.94	1.02	0.93	1.91+	1.74+	1.29+	0.83+	0.83+
1983	0.79	0.87	0.90	0.88	1.00	0.94	0.92	0.84+	0.87+	0.81	0.79	0.78
1984	0.65	.50	.56	.73	.69	.63	.12	Dry	Dry	Dry	.47	.83

+ Denotes approximate value

Monthly average as derived from field data collected during the month

(after Harp, 1984)

Table 25. Spring Flow in Cubic Feet Per Second
Buffalo Springs

Chickasaw National Recreation Area
Sulphur, Okla.

For the Years 1972 - 1983

Year	Jan	Feb	Mar	Apr	May	June	July	Aug	Sept	Oct	Nov	Dec
1972	-	-	-	-	-	0.49	0.28	0.73	0.00	0.00	0.80	0.00
1973	1.38	1.55	1.98	2.26	2.07	1.80	1.55	1.38	1.38	1.72	2.26	2.16
1974	1.98	1.72	1.38	1.38	1.38	1.46	0.93	0.86	1.00	1.31	1.80	1.63
1975	1.55	1.80	1.98	1.80	1.80	1.55	0.73	1.15	1.15	0.86	0.73	0.80
1976	0.61	0.43	0.55	0.55	0.73	0.67	0.43	0.24	0.08	0.00	0.00	0.00
1977	0.00	0.00	0.00	0.73	0.80	0.73	0.61	0.49	0.33	0.00	0.00	0.00
1978	0.00	0.00	0.00	0.00	0.38	0.86	0.86	0.49	0.24	0.00	0.00	0.00
1979	0.00	0.00	0.38	0.61	0.80	0.86	0.33	0.55	0.33	0.24	0.00	0.00
1980	0.00	0.00	0.00	0.00	0.00	0.00	0.00	0.00	0.00	0.00	0.00	0.00
1981	0.00	0.00	0.00	0.00	0.00	0.00	0.00	0.00	0.00	1.15+	1.55	1.30
1982	1.38	1.30	1.30	1.30	1.63	1.63	1.23	1.23	1.02	0.80	0.67	0.73
1983	0.86	1.89	1.15	1.15	1.80	1.38	1.23	1.15	0.86	.65	0.49	0.0
1984	0.00	0.00	0.00	.28	.15	0.00	0.00	0.00	0.00	0.00	0.00	1.00

All flows calculated using the equation: (for data thru October of 1981)

$$Q = 10.44(P.R.-1.82)^{1.5}$$

After October of 1981, the equation was changed to:

$$Q = 10.44(P.R.-1.97)^{1.5}$$

where: Q = flow in cfs,
P.R. = pin reading (stage of spring, in feet

+ Pin reset, approx. 0.15' lower than original setting

Monthly mean flow as derived from data of Table 22.

(after Harp, 1984)

Table 26. Spring Flow in Cubic Feet Per Second
Antelope Springs

Chickasaw National Recreation Area
Sulphur, Okla.

For the Years 1969 - 1983

Year	Jan	Feb	Mar	Apr	May	June	July	Aug	Sept	Oct	Nov	Dec
1969	-	-	-	-	-	1.80	1.57	1.29	1.22	1.29	1.29	1.36
1970	1.22	1.15	1.36	1.57	1.65	1.15	0.96	0.72	0.90	1.88	1.72	1.72
1971	1.50	1.36	1.22	0.96	0.78	0.50	0.23	0.27	0.07	0.27	0.27	1.22
1972	1.29	1.22	1.09	1.02	1.02	0.66	0.41	0.20	0.02	0.00	1.22	1.36
1973	1.43	1.96	2.62	2.89	2.80	2.62	2.28	2.12	2.28	2.37	3.17	2.89
1974	2.71	2.62	2.62	2.71	2.45	2.28	1.88	1.50	1.50	2.54	2.45	2.37
1975	2.62	3.17	4.04	4.35	4.35	3.94	2.20	2.04	1.80	1.80	1.43	1.29
1976	0.56	1.02	1.15	1.15	1.88	1.72	1.02	0.78	0.41	0.10	0.00	0.00
1977	0.00	0.00	1.02	1.57	1.50	1.43	1.22	0.96	0.78	0.61	0.27	0.00
1978	0.00	0.00	0.00	0.32	0.78	1.29	1.02	0.84	0.56	0.20	0.10	0.00
1979	0.00	0.00	0.66	0.66	1.29	1.43	1.02	0.89	0.50	0.46	0.20	0.00
1980	0.00	0.00	0.00	0.00	0.00	0.00	0.00	0.00	0.00	0.00	0.00	0.00
1981	0.00	0.00	0.00	0.00	0.00	0.00	0.00	0.00	0.00	1.80	2.12	2.12
1982	1.72	1.88	2.04	1.88	1.72	2.37	1.65	1.30	1.06	1.01	0.96	0.96
1983	0.72	1.22	1.43	1.29	2.20	1.72	1.57	1.02	1.22	0.84	0.72	0.66
1984	0.10	0.00	0.00	0.41	0.24	0.05	0.00	0.00	0.00	0.00	0.00	0.96

All Flows calculated using the equation:

$$Q = 8.69(P.R.-0.6)^{1.5}$$

where Q = flow in cfs
P.R. = pin reading (stage of spring, in feet)

Monthly mean flow as derived from data of Table 23.

(after Harp, 1984)

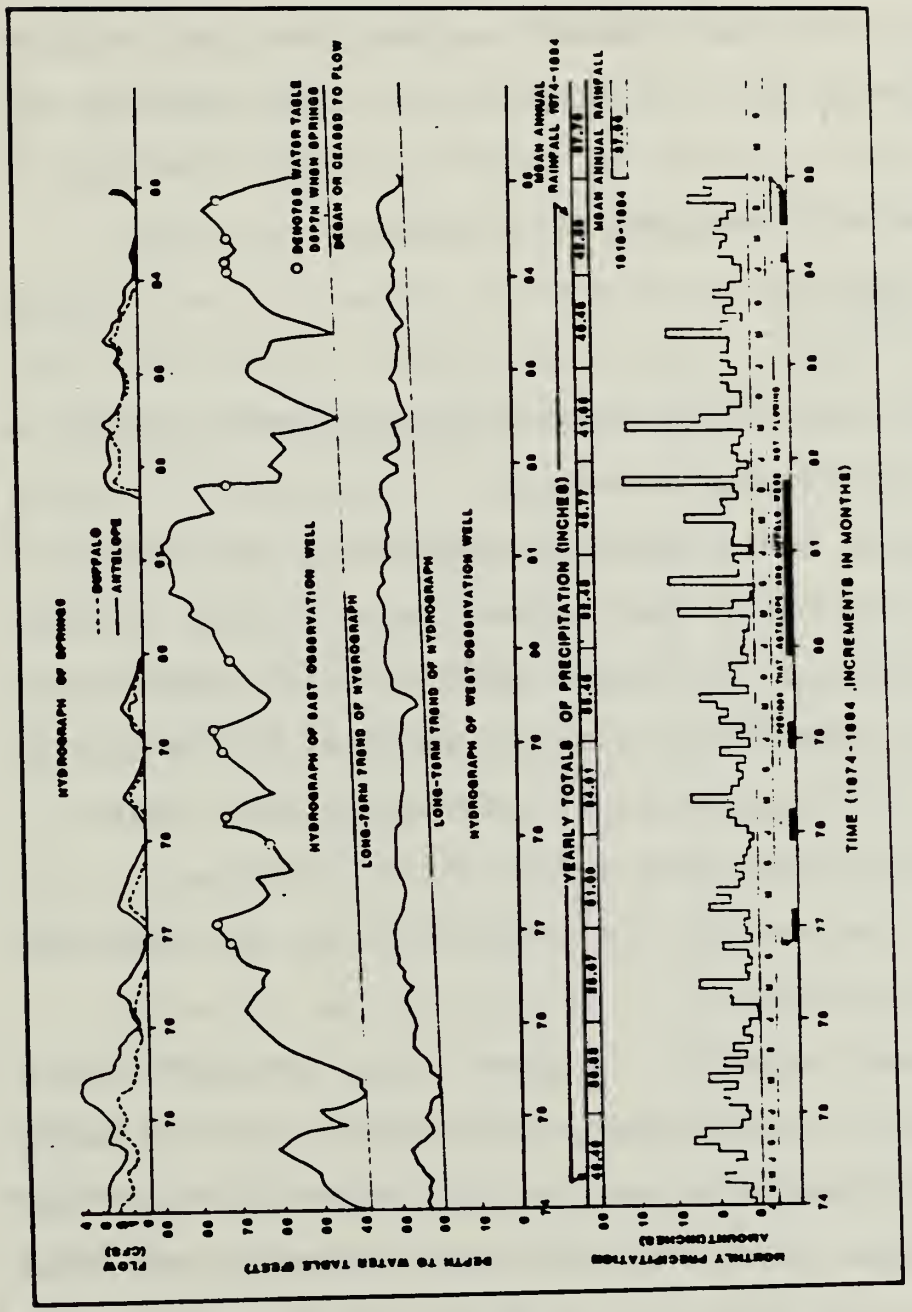

Figure 42. Well and spring hydrograph. Note: surface elevations of East and West Observation Wells are 1150 feet and 1080 feet, respectively. Piezometric elevation can be obtained by subtracting depth to water table from surface elevation.

East and West Observation wells is increasing (piezometric level is decreasing) at a rate of .65 ft/year (Figure 42). The depth to water table is approximately 72 feet in the East Observation Well when springs commence or cease to flow (Figure 42). The following expression can be used to forecast total cessation of spring flow with reasonable certainty:

$$X = \frac{Y_{NF} - Y_T}{b_h} \qquad (4.1)$$

where X = number of years when springs cease flowing from some time T,

Y_{NF} = 72 feet = depth to water table in an observation well when springs cease flowing (feet),

$Y_T = Y_{1984}$ = 45 feet = depth to water table obtained from long-term trend of hydrograph of an observation well at some time T (feet),

b_h = .65 feet/year = deprivation slope as determined from long-term trend of hydrograph (ft/year).

Thus, in approximately 40 years from the submittal of this report, a strong possibility exists that the springs will cease flowing unless certain conservation measures are undertaken. The long-term trend of hydrograph can be attributed to deprivational effects of adjacent sinks and not to a lack of precipitation for the time period 1974 to 1984 (Figure 42).

Peak discharge, minimum depth to water table, and maximum precipitation during the calendar year occur in either middle spring or early fall (Figure 42). Conversely, minimum discharge, maximum depth to water table, and minimum precipitation generally occur in late summer or early winter.

Spring hydrographs of Antelope and Buffalo demonstrate that both eminate from the same aquifer. In addition, the East Observation Well, 1,000 feet east-northeast of Antelope and 1,000 feet north-northeast of Buffalo, fluctuates in response to precipitation events in a very similar manner to that of wells located in the Arbuckle Group outcrop, 1-mile east of the park boundary. The piezometric level of Crawford's Well, located in the outcrop area, rose nearly 38.5 feet for the time period, 15 October 1984 to 25 January 1985 (Table 27). Likewise, the piezometric level of the East Observation Well rose 23.3 feet for the same period of time.

Figure 43 depicts periods of no flow of Antelope and Buffalo springs with respect to annual precipitation amounts, from 1919 to 1984. Particularly noteworthy, for the first time in 66 years of recorded observations, the cessation of spring flow occurred in 1984 when 3 years of above-average annual precipitation preceded it (Figure 43). This anomalous behavior is indicative of long-term deprivation effects of free flowing wells and production

Table 27. Piezometric Levels of Selected Wells in the Arbuckle Group

Date	East Observation Well Piezometric Elevation (feet)	+Crawford's Well Piezometric Elevation (feet)
10/15/84	1071.7	1073.0
10/27/84	1079.0	1082.0
11/10/84	1076.3	1085.7
11/16/84	--	1083.8
11/19/84	1078.9	--
11/21/84	--	1089.2
1/25/85	1095.0	1111.5

+ Location of Crawford's Well - C NE¼ SE¼ of Sec. 31, T1N, R4E.

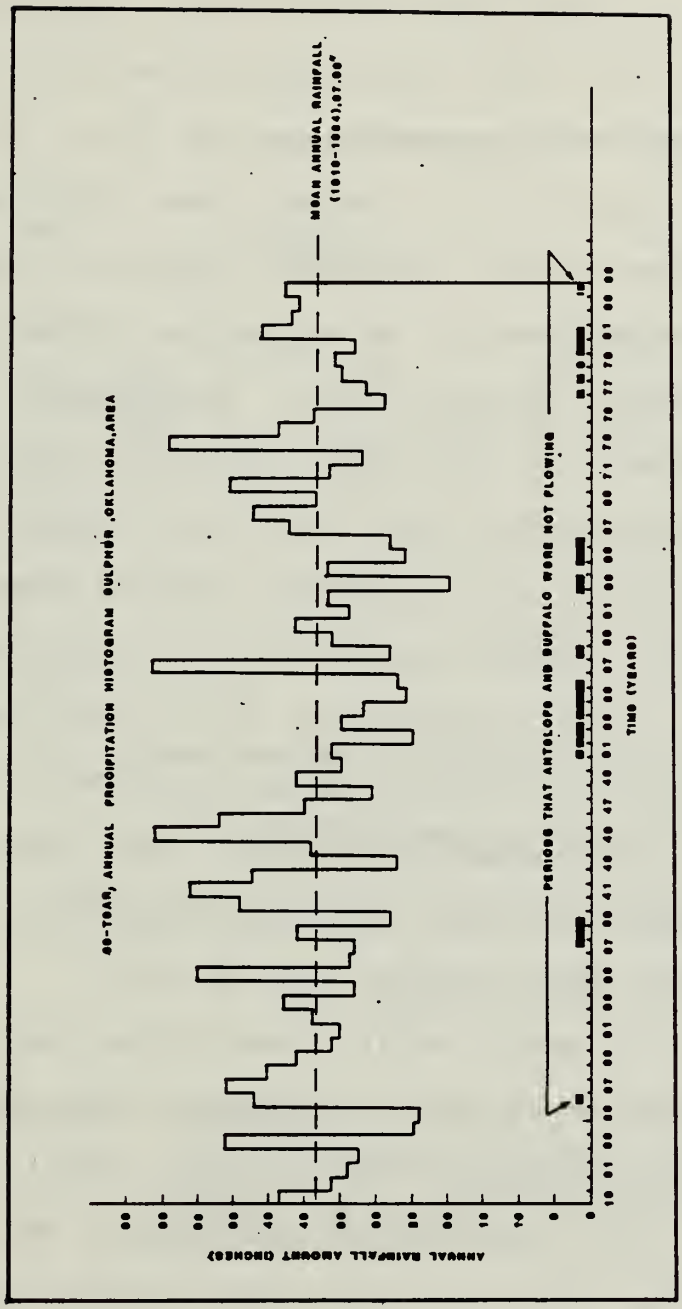

Figure 43. Long-term precipitation histogram versus periods of no flow of the fresh water springs.

wells that are gradually lowering the piezometric level in the Sulphur artesian basin.

The inch-year, time bar chart, Figure 44, portrays the summation of rainfall that falls above (positive) or below (negative) the mean annual precipitation of 37.96 inches (1919-1984) for a specified period (i.e., 15 or 20 years). Inside each bar is a number that indicates the total no-flow time of the freshwater springs. Deprivation caused by withdrawal of water can be firmly established by the use of this bar chart. For example, a total no-flow period of .58 years occurred during the 15-year span from 1919 to 1934. The total amount of inch years is +12.0 (Figure 44). However, for the time period, 1964-1984, the no-flow period is 5.08 years and the inch years is a +30.0. Comparison of the two time intervals reveals that the total amount of cessation is approximately 10 times longer during the time frame 1964-1984; even though,the total inch years of 1964 to 1984 exceeded the total inch years of 1919 to 1934.

Locations of flowing wells, observation wells, and springs are shown on Plate III. Pumpage data of major production wells in close vicinity to the park is listed in Table 28. The investigator was unable to obtain pumpage data from O.G.E. for the time periods: 1973 to 1979, and 1983 to 1984 (Table 27).

The major artesian well in close proximity to the

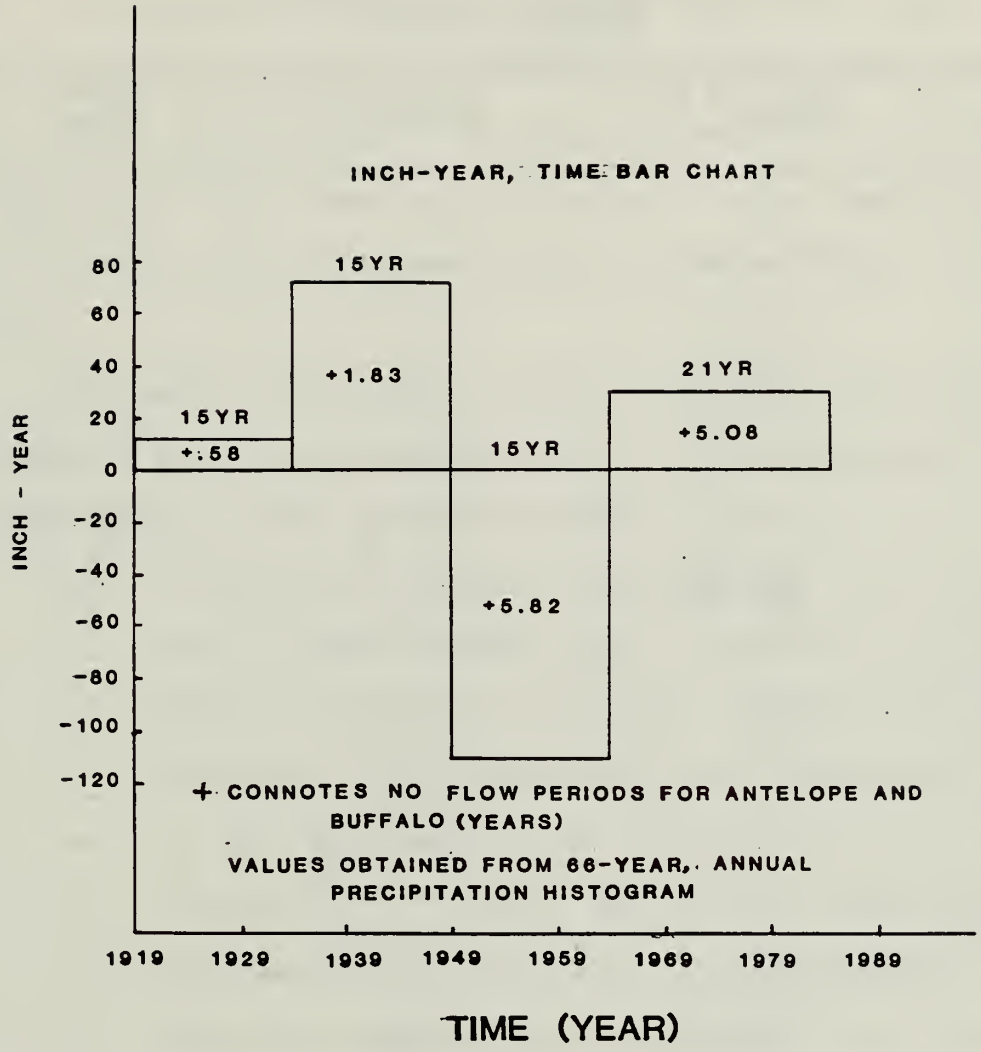

Figure 44. Inch-year, time bar chart that depicts above- or below-normal precipitation amounts for a specified period, in relation to no-flow periods of Antelope and Buffalo.

Table 28. Well Pumpage Data,Area Well Fields

Chickasaw National Recreation Area
Sulphur, Okla.

Year	O.G. & E Wells	City of Sulphur	Roos Ranch
1964	--	--	169.44
1965	348.66	240.14	102.97
1966	296.52	364.95	--
1967	291.31	300.11	--
1968	302.39	210.83	162.93
1969	328.46	211.80	173.68
1970	440.55	228.10	173.68
1971	334.98	235.26	217.34
1972	348.66	271.43	--
1973	--	361.56	--
1974	--	340.45	--
1975	--	274.71	--
1976	--	298.73	--
1977	--	336.00	--
1978	--	--	--
1979	--	438.20	--
1980	472.39	371.47	--
1981	466.97	224.82	--
1982	480.88	400.75	--
1983	--	376.02	--
1984	--	392.01	--

(All data in million gallons)

(after Harp, 1984)

park, the Vendome Well, was estimated to flow at approximately 2 ft^3/sec or 472 x 10^6 gallons per year (Appendix IV). Currently, the total combined amount of water that is extracted by O.G.E., Sulphur Well Field, and Vendome Well on an annual basis, is approximately 1.4 x 10^9 gallons. The total combined discharge of the remainder of the flowing wells in the Sulphur artesian basin is unknown.

The major findings of the two downhole TV surveys conducted during the calendar year 1980 on selected wells in the project area are as follows:

(1) A downhole TV survey was completed on 20 August 1980 of the Vendome Well, located at NE¼ NE¼ NW¼ NE¼ of Sec. 3 T1S, R3E; surface elevation, 945 feet. The Vendome Well is cased to a depth of 300 feet below the surface, with an inner diameter of .5 feet. The overall condition of the casing is fair, but it is extremely corroded at depths between 250 and 300 feet. A fairly uniform conglomerate formation consisting of boulders and cobbles is exposed in the open well from 300 to 320 feet. A large cavity, 3 feet in thickness, was observed between 320 and 323 feet. A distinctly different formation, massive in appearance, appears between a depth of 323 and 324 feet.

The total depth of the well is 324 feet. The original depth of the well, completed in 1922, was 364 feet.

(2) A downhole TV survey was conducted on 13 and 14 March 1980, of the Horseman Well, located NE¼ NW¼ NE¼ NW¼ of Sec. 1, T1S, R3E; approximate surface elevation, 1,075 feet. The condition of casing is good and extends to a depth of 101 feet, with a .5 feet inner diameter. Open well bore extends from 101 feet to 632 feet below the surface. Water was extremely murky to a depth of 380 feet, and as a result, visibility was poor. The open well bore penetrated only the West Spring Formation of the Arbuckle Group. Near-vertical fractures, solution cavities, and vugs were observed at all depths in the open well bore. At times, the well bore periphery resembled a swiss cheese texture. Less frequently, smooth sections of 5-20 feet thick of the open well bore were observed. This would indicate a change in lithology within the West Spring Formation, Arbuckle Group.

Mean annual flow (cfs) and one standard deviation is tabulated for both freshwater springs in Table 29. Included in Table 29 is the annual rainfall amount. Also,

Table 29. Mean Annual Flow of Antelope and Buffalo Springs, and Annual Precipitation

Year	Antelope Spring Mean Flow and *S.D. (cfs)	Buffalo Spring Mean Flow and S.D. (cfs)	Annual Precipitation (inches)
1970	1.33 ± .37	--	50.07
1971	.72 ± .512	--	36.35
1972	.79 ± .51	--	31.85
1973	2.45 ± .48	1.79 ± .35	58.93
1974	2.3 ± .44	1.40 ± .35	43.48
1975	2.75 ± 1.16	1.32 ± .47	38.33
1976	.81 ± .63	.36 ± .28	28.67
1977	.78 ± .6	.31 ± .34	31.09
1978	.43 ± .46	.24 ± .34	34.91
1979	.58 ± .49	.34 ± .31	35.43
1980	0.00	0.00	32.98
1981	.50 ± .91	.33 ± .61	45.77
1982	1.54 ± .48	1.19 ± .32	41.65
1983	1.21 ± .47	1.05 ± .53	40.48
1984	.15 ± .29	.12 ± .29	42.59

* S.D. - one standard deviation

mean precipitation and mean flow of the springs on a monthly basis are listed in Table 30. Data entered in Table 30 demonstrates that the maximum average discharge of the springs occurs in May and the minimum discharge occurs in August, for the time period of 1969 to 1984.

Spring variance V'_a (Equation 3.13), for Antelope Spring is 430% for the time period of June 1969 to December 1984 (Table 31). Also, the spring variance V'_a, for Buffalo Spring is 390% for the time period of June 1972 to December 1984 (Table 31). The values of spring variance V'_a for both springs are fairly close. The relatively high variance values indicate that the Arbuckle Aquifer has a low storage capacity.

Exhaustion coefficients ε, or diffusivity constants K_d (are used interchangeably), and response times t_r, are listed in Table 32. Recession limbs selected for analysis are from calendar years 1976 to 1979. The exhaustion coefficients ranged from .49 to .60 mos^{-1} and the response times varied from 50 to 61 days.

Finally, on-site reconnoiter of Buffalo Spring, when flow resumed, revealed that there is additional water welling up in the creek bed in close proximity to Buffalo Spring. Total discharge of water is unknown at this vicinity, but shouldn't exceed the flow at Antelope by more than 50%. This was based on visual comparison of the streams that flow from the spring areas.

Table 30. Mean Precipitation and Mean Flow of the Springs on a Monthly Basis

Month	(1969-1984) Mean Precipitation and *S.D. (in.)	(June 1969-1984) Antelope Spring Mean Flow and S.D. (cfs)	(June 1972-1984 Buffalo Spring Mean Flow and S.D. (cfs)
Jan.	1.38 ± .89	.92 ± .95	.65 ± .76
Feb.	2.07 ± 1.10	1.04 ± 1.04	.72 ± .84
March	3.16 ± 1.85	1.28 ± 1.12	.73 ± .79
April	3.48 ± 1.45	1.39 ± 1.08	.84 ± .74
May	6.29 ± 3.65	1.51 ± 1.16	.96 ± .75
June	3.83 ± 1.83	1.44 ± 1.07	.88 ± .65
July	2.38 ± 1.33	1.06 ± .77	.64 ± .49
August	2.29 ± 1.49	.87 ± .67	.64 ± .49
Sept.	4.29 ± 3.80	.77 ± .70	.49 ± .51
October	5.98 ± 4.68	.95 ± .89	.52 ± .60
Nov.	2.50 ± 1.79	1.00 ± .98	.64 ± .78
Dec.	1.79 ± 1.59	1.06 ± .54	.59 ± .75

*S.D. = one standard deviation

Table 31. Input Variables and Resultant Values of Spring Variance for Antelope and Buffalo Springs

Spring	Time Period	Maximum Discharge Q_{max} (cfs)	Minimum Discharge Q_{min} (cfs)	*Median Discharge Q_{med} (cfs)	+Spring Variance V'_a %
Buffalo	June 1972 to Dec. 1984	2.26	0.	.575	390
Antelope	June 1969 to Dec. 1984	4.35	0.	1.013	430

* Median discharge was determined by statistical analysis, interval is .25 cfs.

+ Spring Variance = $V'_a = \frac{Q_{max} - Q_{min}}{Q_{med}}$ (100%)

Table 32. Data Input and Resultant Values of Exhaustion Coefficient and Response Time of Antelope Spring

Calendar Year	Base Flow Q (cfs)	Inflection Point Flow Q_o (cfs)	Time t(mos)	*Exhaustion Coefficient ε (mos^{-1})	+Response Time t_r (day)
1976	.1	1.0	4.0	.60	50
1977	.1	1.5	5.5	.49	61
1978	.1	1.0	4.0	.57	53
1979	.1	1.0	4.5	.51	59

* Exhaustion coefficient = $\varepsilon = K_d = \frac{\ln (Q_o/Q)}{t}$

+ Response time = $t_r = \frac{30}{\varepsilon}$

4.5 Recharge Areas Responsible for Spring Flow in the Travertine District, Chickasaw National Recreation Area

As stated previously, a potentiometric survey of the Arbuckle Mountain area was completed by Fairchild et al. (1983), in the winter of 1976-1977 (Plate II). This map was used to define the project area.

The potentiometric survey for this investigation was conducted from 25 January to 8 February 1985. Results of the survey are listed in Table 33. Depth to water table readings were rounded off to the nearest foot, and surface elevations of wells were estimated from topographic maps (Table 33).

A potentiometric map, Figure 45, was constructed from piezometric elevations of the Simpson and Arbuckle Groups. Also, equipotential lines were inferred from surface elevations of flowing wells in the city of Sulphur and surface elevations of springs in the central and western portion of the Travertine District, Chickasaw National Recreation Area.

Recharge areas were primarily determined from the potentiometric survey conducted by Fairchild et al. (Winter, 1976-1977), and the survey for this study. Geologic control, primarily fractures and faults, were considered also. The areas of recharge are shown on the geologic and hydrogeologic map, Figure 30.

The recharge area for Antelope and Buffalo is ap-

Table 33. Results of the Potentiometric Survey (25 January to 08 February 1985)

Well No.	Surface Elevation (ft)	Depth to Water-table (ft)	Piezometric Level (ft)	Location	Remarks
1	1050.0	0.	1050.0	SE¼ NE¼ SE¼ SE¼ Sec. 35, T1N, R3E	Sulphur Well Field, Arbuckle
2	1175.0	64.0	1111.0	SE¼ NE¼ SE¼ SE¼ Sec. 31, T1N R4E	Crawford's Well, Arbuckle
3	1175.0	71.0	1104.0	NW¼ NW¼ NE¼ SE¼ Sec. 32, T1N, R4E	Powell's Well #1, Arbuckle
4	1185.0	80.0	1105.0	SW¼ SE¼ SW¼ SW¼ Sec. 28, T1N, R4E	Powell's Well #2, Arbuckle
5	1080.0	28.0	1052.0	NW¼ NW¼ NW¼ Sec. 1, T1S, R3E	West Observation Well, Arbuckle
6	1150.0	55.0	1095.0	NE¼ NW¼ NE¼ Sec. 1, T1S, R3E	East Obervation Well, Arbuckle
7	1258.0	5.0	1253.0	SE¼ SE¼ SE¼ NE¼ Sec. 14, T1N, R4E	Griffis' Well, Simpson
8	1210.0	80.0	1130.0	SW¼ SE¼ SE¼ SW¼ Sec. 22, T1N, R4E	Chitwood's Well, Arbuckle

(continued)

Table 33. Results of the Potentiometric Survey (continued)
(25 January to 08 February 1985)

Well No.	Surface Elevation (ft)	Depth to Water-table (ft)	Piezometric Level (ft)	Location	Remarks
9	1210.0	80.0	1130.0	SW¼ SE¼ SW¼ SW¼ Sec. 25, T1N, R4E	Roos' Well #1, Arbuckle
10	1210.0	78.0	1132.0	SW¼ SW¼ NW¼ SE¼ Sec. 25, T1N, R4E	Roos' Well #2, Arbuckle
11	1240.0	116.0	1124.0	SE¼ NE¼ NW¼ SE¼ Sec. 24, T1N, R4E	Roos' Well #3, Arbuckle
12	1175.0	65.0	1110.0	SW¼ SE¼ SE¼ SE¼ Sec. 32, R5E, T1N	Davison's Windmill, Arbuckle
13	1240.0	72.0	1168.0	SW¼ SE¼ SE¼ SE¼ Sec. 34, R4E, T2N	Chicken Farm Well, Arbuckle
14	1192.0	5.0	1187.0	SW¼ NE¼ NE¼ SE¼ Sec. 15, T1N, R4E	Pauls' Well, Simpson
15	1215.0	7.0	1208.0	SW¼ SE¼ SW¼ NW¼ Sec. 14, T1N, R4E	Abandoned House Well, Simpson
16	1220.0	122.0	1098.0	SW¼ SW¼ SW¼ SW¼ Sec. 11, T1N, R4E	Dr. Easley's Well, Simpson-Arbuckle

(continued)

Table 33. Results of the Potentiometric Survey (continued)
(25 January to 08 February 1985)

Well No.	Surface Elevation (ft)	Depth to Water-table (ft)	Piezometric Level (ft)	Location	Remarks
17	1220.0	103.0	1117.0	C SW¼ SW¼ SW¼ Sec. 35, T1N, R4E	Y-Intersection Well, Arbuckle
18	1135.0	25.0	1110.0	NE¼ NE¼ SE¼ NE¼ Sec. 12, T1S, R4E	Sparks' Well #1, Arbuckle
19	1190.0	45.0	1145.0	SE¼ SE¼ SE¼ SE¼ Sec. 11, T1S, R4E	Sparks' Well #2, Arbuckle
20	1150.0	20.0	1130.0	SW¼ SW¼ SE¼ SE¼ Sec. 3, T1S, R4E	Freeze's Windmill, Arbuckle
21	1165.0	25.0	1140.0	SE¼ NE¼ SE¼ NE¼ Sec. 8, T1S, R4E	Kirby's Well, Simpson
22	1150.0	64.0	1086.0	NW¼ NW¼ NE¼ SE¼ Sec. 8, T1S, R4E	Runyon's Well, Simpson
23	1145.0	65.0	1080.0	NW¼ NW¼ NW¼ SW¼ Sec. 9, T1S, R4E	Long's Well #1, Simpson
24	1175.0	73.0	1102.0	SW¼ SE¼ SE¼ SW¼ Sec. 33, T1N, R4E	Long's Well #2, Arbuckle

(continued)

Table 33. Results of the Potentiometric Survey (continued)
(25 January to 08 February 1985)

Well No.	Surface Elevation (ft)	Depth to Water-table (ft)	Piezometric Level (ft)	Location	Remarks
25	1140.0	26.0	1114.0	SW¼ SE¼ SE¼ SW¼ Sec. 32, T1N, R4E	Wood's Windmill, Arbuckle
26	1205.0	103.0	1102.0	NW¼ NW¼ SW¼ NE¼ Sec. 6, T1S, R3E	Collin's Well #1, Arbuckle
27	1160.0	30.0	1130.0	SE¼ NE¼ NE¼ SE¼ Sec. 6, T1S, R3E	Collin's Well #2, Simpson
28	1215.0	125.0	1090.0	SW¼ NW¼ NW¼ SW¼ Sec. 6, T1S, R4E	Mushinski's Well, Simpson
29	1175.0	68.0	1107.0	SW¼ NW¼ SW¼ SW¼ Sec. 17, T1S, R4E	Ranch Well, Simpson
30	1170.0	33.0	1137.0	SW¼ SW¼ SE¼ SE¼ Sec. 11, T1S, R3E	Wade's Well, Simpson-Arbuckle
31	1155.0	27.0	1128.0	SW¼ SE¼ NE¼ SW¼ Sec. 11, T1S, R3E	Horse Ranch Well #1, Simpson
32	1135.0	7.0	1128.0	NE¼ SW¼ NE¼ NW¼ Sec. 11, T1S, R3E	Horse Ranch Well #2, Simpson

(continued)

Table 33. Results of the Potentiometric Survey (continued)
(25 January to 08 February 1985)

Well No.	Surface Elevation (ft)	Depth to Water-table (ft)	Piezometric Level (ft)	Location	Remarks
33	1105.0	8.0	1097.0	NE¼ NW¼ SW¼ SW¼ Sec. 11, T1S, R3E	Horse Ranch Well #3, Simpson
34	1180.0	5.0	1175.0	NW¼ NE¼ NE¼ NW¼ Sec. 18, T1S, R3E	Neal's Well #1, Simpson
35	1160.0	6.0	1154.0	NW¼ NE¼ NW¼ NW¼ Sec. 18, T1S, R3E	Neal's Well #2, Simpson
36	1205.0	44.0	1161.0	NW¼ NE¼ NE¼ NE¼ Sec. 29, T1N, R4E	Standerfer's Well, Simpson

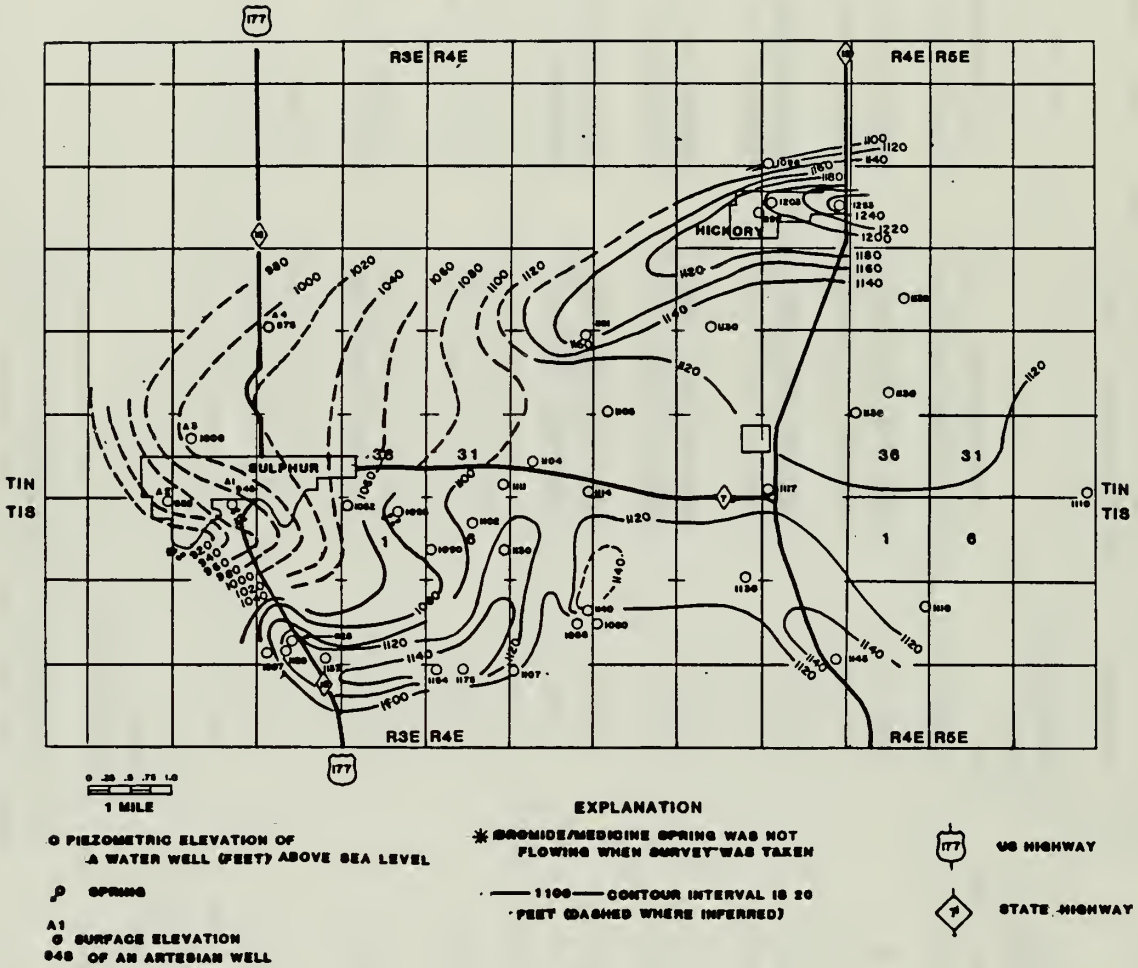

Figure 45. Potentiometric map (Jan. and Feb., 1985) of the Simpson-Arbuckle Aquifer, Sulphur, Oklahoma, area.

proximately 5 mi.^{2}, located north of the west-northwest trending Sulphur Fault (Figure 30). The primary recharge area for the remainder of the springs in the park is approximately 2 mi.^{2}, located south of the Sulphur Fault, along the periphery of the Sulphur Syncline (Figure 30).

4.6 Concise Nomenclature and Origin of the Fresh Water Springs, Buffalo and Antelope.

Buffalo and Antelope are third-magnitude, intermediate-response, freshwater artesian springs; that derive their waters from the Arbuckle Group.

The springs occur as a result of fractures that become solution cavities in the confining layer of the Pontotoc that extend to the surface top of the pressurized water of the Arbuckle Group, just north of the Sulphur Fault. Both springs are topographically low, compared to the surrounding area. If the Arbuckle Group receives sufficient recharge in the outcrop area, the piezometric level will rise above the surface elevation of the springs, and discharge will result.

Groundwater flow to the springs is controlled by the Sulphur Fault. The elevated Arbuckle dolomite on the upthrown side of the fault is extensively fractured and contains solution cavities and small caverns. Third-magnitude springs normally eminate from a highly permeable aquifer. Low hydraulic gradients (10 ft. per mile) in the outcrop area of the Arbuckle Group, east of

Sulphur, indicate high regional transmissivity. Conversely, high hydraulic gradients (20 to 100 ft. per mile) of the Simpson Group, south of the Sulphur Fault, indicate lower transmissivities.

4.7 Hydrologic Budget of the Sulphur Area

The piezometric level of the Simpson-Arbuckle aquifer should remain constant if inflow equals outflow. However, the piezometric level of the Sulphur artesian basin is declining at an average annual rate of .65 ft per year. Hence, outflow exceeds inflow for the area.

As previously discussed, the total amount of water that is currently withdrawn from the Sulphur area, is in excess of 1.4×10^9 gallons per year. The total recharge area for the Sulphur artesian basin is approximately 15 mi^2 (Figure 30). Assuming a long-term annual recharge rate of 4.6 inches per year (Fairchild et al., 1983), the total amount of inflow on a yearly basis is approximately 1.2×10^9 gallons per year. Since outflow is equivalent to withdrawal, and withdrawal exceeds outflow; it becomes quite evident as to why the piezometric level is declining in the Sulphur area.

CHAPTER V

DISCUSSION OF FINDINGS

5.1 Geologic Control of Groundwater

Macrostructure and fractures heavily influence groundwater occurrence and flow in the study area. In particular, the Sulphur Fault combined with the regional dip to the northwest on the upthrown side of the same fault, greatly influences general groundwater flow direction to freshwater springs.

The Sulphur Fault invokes high permeability in the fine-grained Arbuckle dolomite on the upthrown side, and creates an impermeable boundary in the Simpson clastics and calcarenites (Figures 32, 33) on the downthrown side. This statement generally agrees with the literature (Davis and DeWiest 1966). Also, Ham (1945) observed small pinnacles of orthoquartzite of the usually friable and permeable basal sands of the McLish and the Oil Creek formations, adjacent to the Sulphur Fault.

Fine-grained dolomites (Figure 38) are more likely to fracture than deform (Stearns, 1967). Dips greater than 20° in the Arbuckle were not observed by this

investigator. Field reconnaissance of the fractures in the Arbuckle Group substantiate brittle deformation. Conversely, dips of the Simpson beds in the grabens of the Sulphur and Hickory Synclines easily surpass 20°. This is indicative of the ductile and cataclastic behavior of the Simpson Group.

The potentiometric map, Figure 44, shows good correlation with formations and structure (Figures 29 and 30). Fairchild et al. (1983), concluded that the structural geology of the area heavily influences groundwater flow and occurrence.

The relatively high regional transmissivity of the Arbuckle Group can be attributed to solution activities of the bedding planes and fractures. A landowner, Mr. Woods, informed this investigator that drillers on his property encountered a 20-foot thick cavern, in the Arbuckle Group, at SW¼ NW¼ SW¼ SE¼ of Sec. 32, T1N, R4E. This location is 2 miles east-northeast of the freshwater springs and 3/4 mile north of the Sulphur Fault. Fairly numerous sinks and swallow shafts in and along stream valleys of the Arbuckle Group were observed. Rapid rise in water levels to intense precipitation events during the fall and spring can be attributed to fractures and swallow shafts at the surface, (high vertical permeability), and the low storage coefficient of the Arbuckle Group. In addition, the relatively flat water table of

the Arbuckle Group (Figure 44) could conceivably suggest karst hydrology (Fetter, 1980).

Finally, an inferrence of the Sulphur Fault through the park and the city of Sulphur was accomplished (Figures 29, 30). Exact location is not known, but the inferrence of fault is quite close in the author's opinion. The fault's trend was determined by: (1) the geomorphology of the park, (2) spring occurrence, (3) the newly-mapped formation, (4) lithology of the observation wells, (5) piezometric levels and hydraulic gradients from the potentiometric survey, (6) high discharge of the Vendome Well relative to the springs in the park, (7) water quality analysis, (8) downhole TV logs of the Vendome Well and the Horseman Well, and (9) surface elevation tops of the Arbuckle Group from well completion report and well logs.

5.2 Aquifer Properties

Simulation of drawdown at a sink node demonstrated that drawdown at the wellbore is a function of storage coefficient, and to a lesser degree, transmissivity. Transmissivity values obtained from the simulation, 2.4 ft^2/day to 24 ft^2/day, are fairly low; yet drawdown at the West Observation Well, approximately .5 mile from the production well, experienced negligible drawdown. However, caution must be exercised, as pump tests conducted

by Gringarten (1982) in a karst aquifer demonstrated anisotropic behavior. Hence, transmissivity valves for this simulation are fairly reliable between the observation well and the production well, but not suitable for transmissivity in other directions.

Also, Fairchild et al. (1983), conducted pump tests in the Arbuckle aquifer and observed no drawdown in observation wells at distances of a 1/2 mile from the sink point. The value of storage coefficient, 1.7×10^{-4}, as determined by the simulation, is reasonable, and compares favorably with a storage coefficient of 1.2×10^{-3} at the East Observation Well.

The major limitations to this simulation are: (1) that the Prickett Lonnquist model (1975) assumes a fully penetrating well in a confined aquifer at some specified sink node; (2) insufficient data from the pump test, (i.e., rate of drawdown); and (3) homogeneous aquifer in close proximity to the well bore.

The hydraulic conductivity value of 1.6 ft. per day, obtained from the slug test on Crawford's Well, is indicative of the high transmissivity at this locale. The regional hydraulic conductivity, as determined by regional techniques (Fairchild et al., 1983) of this area, is one order of magnitude larger than that determined by the slug test. This is generally the case, as hydraulic conductivity determined from slug tests are generally one

order of magnitude less than hydraulic conductivity determined by pump tests that stress the aquifer on a much larger scale.* In addition, this slug test was performed in an area that was determined to be responsible for recharge to the freshwater springs (Figure 30).

The storage coefficient value of approximately 1 x 10^{-3}, that was determined for the East Observation Well, is not entirely adequate. The lack of data combined with inoperative water-level recorders, hindered a close approximation of the barometric efficiency. Under the circumstances, a fairly reasonable value was determine because of the following: (1) a relatively thin, confining layer of 120 ft. thick lies unconformably upon the Arbuckle Group; and (2) the East Observation Well is located in close proximity to the recharge area that has an overall storage coefficient of 8 x 10^{-3} (Fairchild et al., 1983).

The average aquifer transmissivity value of 43,000 ft^2/day, as determined by a regional technique as a function of spring discharge, is fairly accurate in terms of order of magnitude (Fairchild, et al., 1983). The regional technique, a modified form of Darcy's Law, assumes that Laplacian conditions prevail; which is probably not the case for the Arbuckle aquifer.

---

* Investigator's personal experience of data analysis of slug tests and pump tests on the same well.

However, Basmaci et al. (1977), assert that on a regional basis, karst aquifers behave like granular media. Then, Basaci et al. (1977), maintain that Darcy's Law is applicable with the assumption that some error (12-24%) is committed by the linear flow assumption throughout the fractured karst system.

A comparison of the aquifer transmissivity responsible for the spring discharge of mixed waters in the central portion of the park, to that of the freshwater springs, is two orders of magnitude less. This is confirmed by comparatively high hydraulic gradients and much smaller discharge amounts. These findings agree quite favorably with the commentary of Davis and DeWiest (1966) on spring discharge amount as a function of aquifer permeability.

5.3 Data Analysis of Wells and Springs

Well hydrographs firmly establish a relationship between spring discharge and piezometric elevation (Figure 42). Variations of piezometric levels in the East Observation Well are very similar to water-level fluctuations in the outcrop area of the Arbuckle Group, east of Sulphur (Table 26). Previous investigators, Hart (1972) and Harp et al. (1976), also concur with these observations.

The West Observation Well hydrograph is considerably dampened with respect to the hydrograph of the East

Observation Well (Figure 42). This can be attributed to decreased permeability or increased storativity of the Arbuckle Group. The hydraulic gradient increases to 40 ft. per mile, down dip from the East Observation Well; which indicates decreasing permeability in the direction of the West Observation Well.

Also, the slug test that was performed on the West Observation Well, revealed an extremely slow rate of rise after the probe was withdrawn. This provides additional substantiation that the permeability of the Arbuckle Aquifer is considerably reduced in the vicinity of the West Observation Well.

The long-term trend of the hydrograph can be used to ascertain deprivation effects of adjacent production wells (Figure 42). The deprivation slope or the slope of the long-term trend of the hydrograph was determined to be .65 ft/year for both observation wells (Figure 42). It was also established by the use of the inch-year time bar chart, that the primary cause of increasing cessation of spring flow is attributed to nearby production wells. Finally, assuming that the deprivation slope remains constant, cessation of all spring flow will occur in 40 years (Equation 4.1).

The variability of Antelope and Buffalo Springs is high; indicating that both derive their waters from the Arbuckle Group (Table 30). The source of the freshwater

springs can be further correlated by well hydrographs that vary as much as 50 feet per year in the outcrop area of the Arbuckle Group, east of Sulphur (Fairchild et al., 1983). Conversely, the variance of water levels in the Simpson Group is less than 10 feet per year (Fairchild et al., 1983).

The exhaustion coefficient ε, indicates whether conduit or diffuse flow predominates in a carbonate aquifer (White et al., 1974). Another variable, response time t_r, can also be utilized to assess conduit or diffuse flow. White (1977) asserts that conduit flow prevails when the recession limb of a spring hydrograph is similar to a recession limb of a stream hydrograph. Visual inspection of the recession limbs of the well hydrographs and spring hydrographs, Figure 42, indicates a predominately diffuse-flow system. Values of response time t_r, listed in Table 30, most nearly coincides with the values for intermediate-response springs listed in Table 4 (White, 1974).

Statistical analysis revealed that the peak discharge of Buffalo and Antelope Springs closely coincides with the peak precipitation events in spring and fall (Table 29). White et al. (1974) maintains that peak discharges of diffuse-flow springs will coincide with the mean spacing of maximum precipitation events on a seasonal basis. White's preceding statement agrees favorably

with these findings, and lends further credibility that the Arbuckle Group is primarily a diffuse-flow system.

5.4 Analysis of Spring Flow Occurrence and the Recharge Areas

The freshwater, artesian springs, Antelope and Buffalo, discharge from orifices of the Pontotoc Group. The source of water for both springs is from fractures and joints in the Pontotoc Group that extend downward to the top of the pressurized Arbuckle Aquifer. The thickness of the confining layer, the Pontotoc Group is believed to be less than 50 feet in the vicinity of Buffalo and Antelope Springs. This thickness was deduced from a lithologic log of the East Observation Well (Moore, 1972).

The Sulphur Fault is inferred with virtual certainty just south of Buffalo Spring (Figure 30). This can be readily justified by the following: (1) lithology of the East Observation Well; (2) water quality analysis conducted by Hart (1972) and Harp et al. (1976); (3) the newly mapped outcrop of the Simpson; (4) spring discharge as a function of aquifer transmissivity; and (5) orientation of fracture sets in the Pontotoc Group that trend in a westerly direction, located just east of the park boundary (Table 9). This is also in agreement with Hart (1972), who previously inferred the Sulphur Fault to Buffalo Spring.

The freshwater springs evolved as a result of intense fracturing and subsequent solution of the brittle Arbuckle dolomites in close proximity to the Sulphur Fault. In addition, the permeable Arbuckle Group on the upthrown side of the Sulphur Fault is offset next to the less permeable Simpson Group on the downthrown side.

The recharge area for Buffalo and Antelope springs is in the outcrop of the Arbuckle Group, east of Sulphur (Figure 30). In addition, some recharge probably occurs from the Pontotoc that overlays the Arbuckle Group, located between the springs and the surface contact of the two geologic units to the east.

The recharge area was determined by general flow directions from the potentiometric map and structural geology of the project area. It is believed that the groundwater flow is highly anisotropic along the Sulphur Fault. The dip of the Arbuckle Group is to the west and northwest in the study area, which also impacts on groundwater flow direction to the artesian springs.

The recharge area is approximately 5 mi^2 for Antelope and Buffalo Springs. This estimate agrees favorably with the nomograph devised by Davis and DeWiest (1966), Figure 46; for values of 3 cfs and 4.6 inches of annual recharge. Also, the primary recharge area for the remainder of the springs in the park is estimated to be less than 2 mi^2; in the outcrop of the Simpson Group

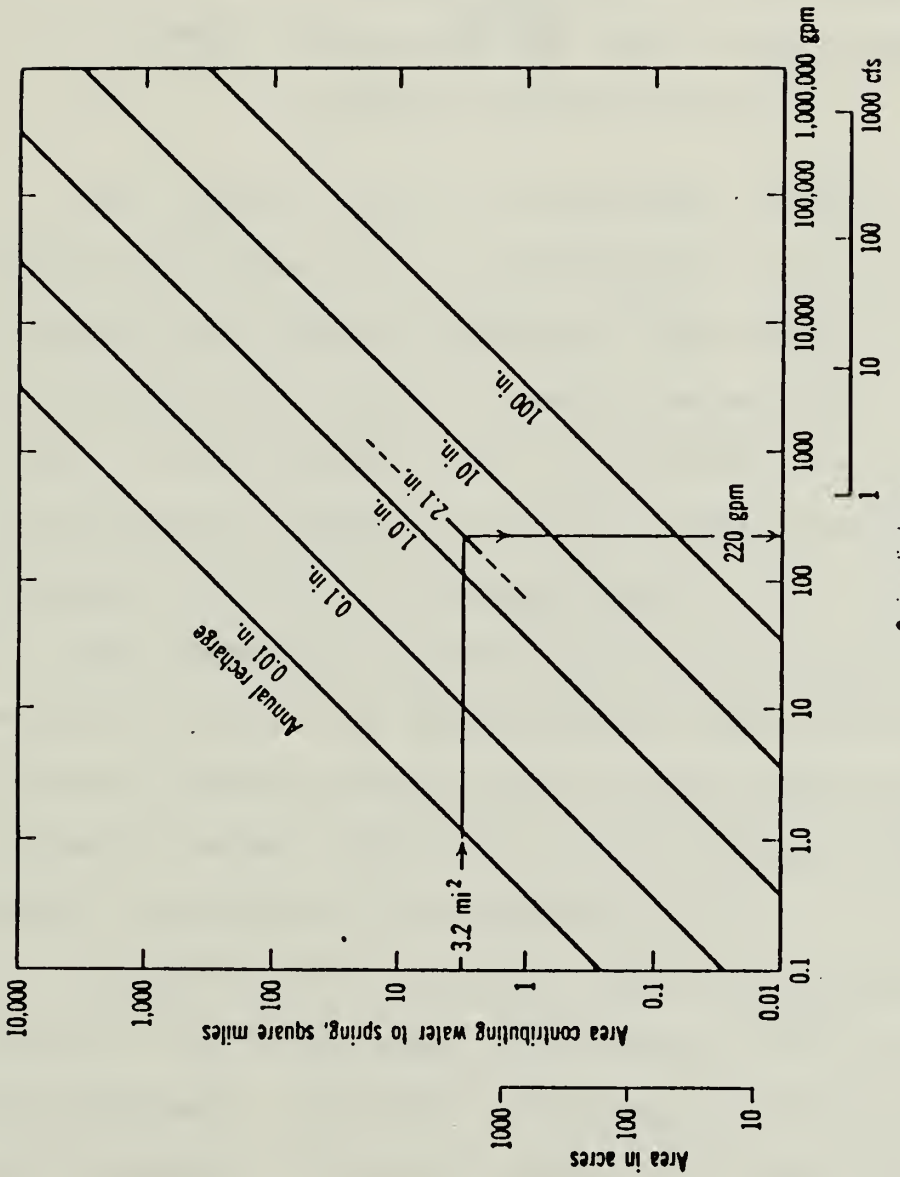

Figure 46. Nomograph that correlates recharge area to spring discharge by annual recharge amount (After Davis and DeWiest, 1966).

along the periphery of the Sulphur Syncline, south and southeast of the park. Finally, the estimate of the total recharge area responsible for spring flow in the park is considerably less than originally believed by previous investigators, Hart (1972) and Harp et al. (1976).

CHAPTER VI

SUMMARY AND CONCLUSIONS

The origin of the freshwater artesian springs, Buffalo and Antelope, is attributed to the Sulphur Fault crossing hard, brittle dolomite of the Arbuckle Group and thereby creating zones of greater permeability. In addition, it is believed that the fault has offset the fractured and permeable Arbuckle Group against the less permeable rocks of the Simpson Group.

The freshwater springs eminate from orifices of the Pontotoc Group. The springs derive their water from the confined Arbuckle Aquifer that flows upward by pressure through fissures and joints in the Pontotoc Group, ultimately discharging at the surface.

Structure and lithology govern groundwater occurrence in the study area. The Sulphur Fault that trends west-northwest separates groundwater flow to the park. The freshwater artesian springs, Antelope and Buffalo, receive recharge in the form of precipitation that falls on the outcrop of the Arbuckle Group east of Sulphur, then infiltrates to the water table, and moves downdip to

the springs (Figure 30). The remainder of the mineralized spring in the park, receive recharge primarily from the outcrop of the Simpson along the periphery of the Sulphur Syncline (Figure 30). The area of recharge is approximately 5 $mi.^2$ for Antelope and Buffalo Springs. Also, the recharge area for the mineralized springs is estimated to be 2 $mi.^2$.

Geological reconnaissance of the Arbuckle Group, east of Sulphur, revealed intensely fractured microcrystalline dolomite, with a fair amount of sinks and swallow shafts in the stream valleys. The Arbuckle Group is relatively flat, gently dipping to the northwest. In addition, the inferrence of the Sulphur Fault into the park boundary was greatly enhanced by the discovery of a small outcrop of the Simpson Group, east-southeast of Buffalo Spring.

Regional transmissivity of the Arbuckle Aquifer responsible for groundwater flow to Antelope and Buffalo Springs was determined to be approximately 43,000 ft^2/day. Hydraulic conductivity of 1.6 ft/day was determined from results of a slug test on a selected well in the outcrop area of the Arbuckle Group. The values of storage coefficient ranged from about 1.2×10^{-3} to 1.7×10^{-4} for the confined Arbuckle Aquifer in close vicinity to the springs.

Well and spring hydrographs provided additional

insight to the subsurface hydrology of the Sulphur area. The peak discharge of the springs coincided with the maximum precipitation event, and the maximum piezometric elevation in the observation wells. The slope of the long-term trend of the hydrograph was ascertained to be .65 ft/year. This slope indicates that the piezometric elevation of the Sulphur area is declining at a yearly rate of .65 ft. If this slope value remains constant, permanent cessation of flow of the freshwater springs will occur in 40 years.

Variance values of the freshwater artesian springs are in excess of 390% for at least a period of 12 years. Thus, confirming that both springs derive their waters from the Arbuckle Group, an aquifer of low storativity. Also statistical analysis revealed that the peak discharge occurs in May and the minimum discharge in August. The exhaustion coefficient values ranged from .49 to .6 $mos.^{-1}$ for Antelope Spring. These values are typical for intermediate response, diffuse-flow springs that originate from carbonate aquifers.

The annual hydrologic budget for the Sulphur area is based on 15 $mi.^2$ of recharge area with an average annual recharge rate of 4.6 inches per year. The total amount of water available for use on a average yearly basis is approximately 1.2×10^9 gallons. Current analysis of production wells and flowing wells in the Sulphur area,

reveals that withdrawal of water exceeds 1.4×10^9 gallons per year.

NOMENCLATURE

L = length

T = time

F = force

M = mass

h = head [L]

A = area [L^2]

P = pressure [FL^{-2}]

q = specific discharge [LT^{-1}]

γ = specific weight [FL^{-3}]

ρ = density [ML^{-3}]

v = velocity [LT^{-1}]

K = hydraulic conductivity [LT^{-1}]

μ = dynamic viscosity [$ML^{-1}T^{-1}$]

g = gravitational acceleration constant [LT^{-2}]

h_p = pressure head [L]

z = elevation head [L]

V_p = volume of the pores [L^3]

V_B = bulk volume [L^3]

d = diameter [L]

n = porosity [L^3L^{-3}]

K_r = recession coefficient [$L^3T^{-1}L^{-3}T^1$]

NOMENCLATURE (continued)

V_s = volume of solids $[L^3]$

I' = Inflow $[L^3]$

O' = Outflow $[L^3]$

S' = Storage $[L^3]$

S_c = storage coefficient $[LL^{-1}]$

S_s = specific storage $[L^{-1}]$

Φ = force potential $[L^2T^{-2}]$

T = transmissivity $[L^2T^{-1}]$

P = pressure $[FL^{-2}]$

β = water compressibility $[F^{-1}L^2]$

α = aquifer compressibility $[F^{-1}L^2]$

b = aperture width of fracture $[L]$

K_f = hydraulic conductivity of a single fracture $[LT^{-1}]$

K_{ij} = intrinsic permeability $[L^2]$

q_j = fracture-flux vector per unit width of conduit $[L^3T^{-1}]$

V_a = volume of sample chamber $[L^3]$

V_b = volume of evacuated chamber $[L^3]$

BE = barometric efficiency $[FL^{-2}F^{-1}L^2]$

r = radius $[L]$

x = coordinate in the horizontal axis $[L]$

y = coordinate in the vertical axis $[L]$

R = radius of influence $[L]$

NOMENCLATURE (continued)

α' = constant aquifer characteristic $[TL^{-2}]$

Q' = total average annual runoff [L]

ET = average annual evapotranspiration [L]

P' = average annual precipitation [L]

ΔP_a = change in barometric pressure [L]

b' = thickness of a confined aquifer [L]

h' = saturated thickness of an aquifer [L]

E_{tv} = total energy per incremental volume $[FLL^{-3}]$

t = time [T]

Q_n = (-) recharge or (+) withdrawal $[LT^{-1}]$

S_y = specific yield $[L^3L^{-3}]$

K_n = normal stiffness factor $[L^2T^{-1}F^{-1}]$

S_f = fracture spacing [L]

I = hydraulic gradient $[LL^{-1}]$

t_r = response time [T]

q_{2s} = space-averaged velocity of the fracture relative to the matrix $[LT^{-1}]$

Γ = mass flow rate from block to fracture $[MT^{-1}]$

ε = exhaustion coefficient $[T^{-1}]$

k_d = diffusivity constant $[T^{-1}]$

V'_a = variability or spring variance $[L^3T^{-1}L^{-3}T^1]$

K_1 = intrinsic permeability of the matrix $[L^2]$

K_2 = intrinsic permeability of the fracture $[L^2]$

s = drawdown [L]

NOMENCLATURE (continued)

b_w = width of weir [L]

H = depth of pool at a specified point [L]

k' = weir constant, unitless

BIBLIOGRAPHY

Barker, B.M., and W.C. Jameson, 1975, Platt National Park, Chickasaw National Recreation Area: Norman, University of Oklahoma, 127 pp.

Basmaci, Y., and L.V.A. Sendlein, Model analysis of closed systems in karstic aquifers: Hydrologic Problems in Karst Regions, pp. 202-213.

Boulton, N.S., and T.D. Streltsova, 1977, Flow to a well in an unconfined fractured aquifer: Hydrologic Problems in Karst Regions, pp. 214-227.

Bouwer, H., 1978, Groundwater hydrology: New York, McGraw-Hill Book Co., 480 pp.

Briz-Kishore, B.H., and V.L.S. Bhimasankaram, 1982, A comprehensive study and analysis of groundwater in a typical fractured environment: AWRC Conference Groundwater in Fractured Rock, pp. 13-23.

Chilingarian, G.V., 1975, Compaction of coarse-grained sediments, I: Developments in Sedimentology 18A, New York, Elsevier Scientific Publishing Co., 552 pp.

Collins, R.E., 1961 and 1976, Fluid flow through porous media (1st ed.): U.S.A., Reinhold Company, 1961, 2nd Printing, Tulsa, Penn Well Publishing Co., 1976, 270 pp.

Davis, S.N., and R.J.M. DeWiest, 1966, Hydrogeology: New York, Wiley & Sons, 463 pp.

Dreiss, S., 1974, Lithologic controls on solution of carbonate rocks in Christian County, Missouri: Karst Geology and Hydrology Proceedings, pp. 145-152.

Duquid, J.O., and P.Y.C. Lee, 1977, Flow in fractured porous media: Water Resources Research, Vol. 13, No. 3, pp. 558-566.

BIBLIOGRAPHY (continued)

Fairchild, R.W., and R.L. Hanson, and R.E. Davis, 1983, Hydrology of the Arbuckle Mountain area, south-central Oklahoma: U.S.G.S. Open File Report 83-775, 156 pp.

Fairchild, R.W., 1984, Oklahoma geology notes: Oklahoma Geological Survey, Vol. 44, No. 1, pp. 4-11.

Fetter Jr., C.W., 1980, Applied hydrogeology: Columbus, Merrill Co., 488 pp.

Gale, J.E., 1982, Assessing the permeability characteristics of fractured rock: Geological Society of America Special Paper 189, pp. 163-179.

Gould, C.N., 1906, Report on springs: Department of Interior Report, 11 pp.

Gould, C.N., and S.L. Schoff, 1939, Geological report on water conditions of Platt National Park Oklahoma: National Park Service Region II and U.S.G.S., 38 pp.

Gringarten, A.C., 1982, Flow-test evaluation of fractured reservoirs: Geological Society of America Special Paper 189, pp. 237-263.

Ham, W.E., 1945, Geology and glass sand resources, central Arbuckle Mountains, Oklahoma: Oklahoma Geological Survey Bull. No. 65, 103 pp.

Ham, W.E., and M.E. McKinley, 1954, Geologic map and sections of the Arbuckle Mountains, Oklahoma: Oklahoma Geological Survey, one map.

Ham, W.E., and R.E. Denison, and C.A. Merrit, 1964, Basement rocks and structural evolution southern Oklahoma: Oklahoma Geological Survey Bulletin No. 95, 302 pp.

Ham, W.C. (Deceased), 1973 and 1978, Regional geology of the Arbuckle Mountains, Oklahoma: Oklahoma Geological Survey Special Publication 73-3, 2nd Printing, 1978, 61 pp.

Hanson, B.C., 1973, A fracture pattern analysis employing small scale photography with emphasis on groundwater movement in northwest Arkansas: Thesis, Unpublished, University of Arkansas, 66 pp.

BIBLIOGRAPHY (continued)

Harp, J.F., and J.G. Laguros, 1975, Deprivation contribution and interference effects of multiple wells in a common aquifer: Groundwater, Vol. 13, No. 3, pp. 251-253.

Harp, J.F., and H.M. Schornick, and J.G. Laguros, 1976, Subsurface and surface water flows at Platt National Park, Sulphur, Oklahoma: Final Report, Unpublished, University of Oklahoma, 49 pp.

Harp, J.F., and J.G. Laguros, and S.G. McLin, and L.B. West, 1984, A hydrologic study of the Sulphur artesian groundwater system and associated waters at the Chickasaw National Recreational Area, Sulphur, Oklahoma: Interim Report, Unpublished, University of Oklahoma, 17 pp.

Hart Jr., D.L., 1972, Hydrology of the Platt National Park area, Murray County, Oklahoma: USGS Administrative Report, 14 pp.

_____, 1974 and 1983, Reconnaissance of the water resources of the Ardmore and Sherman quadrangle, southern Oklahoma: Oklahoma Geological Survey, Hydrologic Atlas 3, 1983, maps.

Hensch, D.A., 1984, Subsurface and surface water flows at Platt National Park, Sulphur, Oklahoma: An Update, Unpublished, University of Oklahoma, 10 pp.

Houstin, W.N., and A.G. Kasim, 1982, Physical properties of porous geologic materials: Geological Society of America Special Paper 189, pp. 143-162.

Jakucks, L., 1977, Morphogenetics of karst regions: Budapest, Adam Hilger Ltd., 284 pp.

Johnson, K.S., 1984, Guidebook for Arbuckle Mountain field trip, southern Oklahoma: Oklahoma Geological Survey Special Publication 84-1, 21 pp.

Kastning, E.H., 1977, Faults as positive and negative influences on ground-water flow and conduit enlargement: Hydrologic Problems in Karst Regions, pp. 193-201.

BIBLIOGRAPHY (continued)

Klinkenburg, L.J., 1941, The permeability of porous media to liquid and gases: Drilling and Production Practice, New York, American Petroleum Institute, pp. 200-214.

Marine, I.W., 1967, The use of a tracer test to verify an estimate of the groundwater velocity in fractured crystalline rock at the Savannah River Plant near Aiken, South Carolina: American Geophysical Union, Vol. 11, pp. 171-179.

Moore, G., 1972, USGS report on Observation Wells A and B, Platt: Memorandum, Unpublished, National Park Service, 2 pp.

Morris, H.M., 1972, Applied hydraulics in engineering: New York, John Wiley and Sons, 616 pp.

Narasimhan, T.N., 1982, Physics of saturated - unsaturated subsurface flow: Geological Society of America Special Paper 189, pp. 3-23.

Prickett, T.A., and C.G. Lonnquist, 1971, Selected digital computer techniques for groundwater resource evaluation: Illinois State Water Survey Bulletin 55, 62 pp.

Stearns, D.W., 1967, Certain aspects of fracture in naturally deformed rocks: Manuscript, Unpublished, Texas A & M University, 9 pp.

Sabins Jr., F.F., 1978, Remote sensing principles and interpretation: San Francisco, W.H. Freeman and Co., 426 pp.

Todd, D.K., 1959, Groundwater hydrology: New York, Wiley & Sons, 336 pp.

Tuttle, S.D., 1970 and 1975, Landforms and landscapes (2nd ed.): Dubuque, W.C. Brown Co., 1975, 152 pp.

Walton, W.C., 1970, Groundwater resource evaluation: New York, McGraw-Hill Book Co., 664 pp.

Wang, H.F., and M.P. Anderson, 1982, Introduction to groundwater modeling: San Francisco, W.H. Freeman and Co., 224 pp.

BIBLIOGRAPHY (continued)

White, E.L., and W.B. White, Analysis of spring hydrographs as a characterization tool for karst aquifers: Karst Geology and Hydrology Proceedings, pp. 103-106.

White, W.B., 1977, Conceptual models for carbonate aquifers revisited: Hydrologic Problems in Karst Regions, pp. 176-187.

William, H., and F. J. Turner, and C.M. Gilbert, 1954, Petrography and introduction to the study of rocks in thin sections: San Francisco, W.H. Freeman and Co., 406 pp.

APPENDIX I

CONTINUITY PRINCIPLE

(Fetter, 1980)

APPENDIX I

CONTINUITY PRINCIPLE
(Fetter, 1980)

Fluid moves in only one direction through the elemental volume. The fluid movement can be subdivided in three component flows aligned with the three principal axes (refer to Figure 13). Flux along the x axis in the elemental cube is $\rho_w q_x$ dydz (units in FTL^{-1}). Mass flux (along the x axis) out is $\rho_w q_x$ dydz + $\frac{\partial}{\partial x}(\rho_w q_x)$dxdydz. The net, accumulated mass flux is influx-outflux, $-\frac{\partial}{\partial x}(\rho_w q_x)$dxdydz. It follows that the other two net fluxes, y and z components of flux, are identical in derivation: (1) y axis, $-\frac{\partial}{\partial y}(\rho_w q_z)$dxdydz; and (2) z axis, $-\frac{\partial}{\partial z}(\rho_w q_z)$dxdydz. Combining all three terms yields the following equation:

$$-\left(\frac{\partial}{\partial x}\rho_w q_x + \frac{\partial}{\partial y}\rho_w q_y + \frac{\partial}{\partial z}\rho_w q_z\right)dxdydz \qquad (I\text{-}1)$$

The volume of water in storage (fully saturated) is equal to ndxdydz, and the mass of water in storage is $\rho_w n$ dxdydz. The mass of the matrix of the elemental volume is (1-n)dxdydz. Change of the mass of water with respect to time is:

$$\frac{\partial M}{\partial t} = \frac{\partial}{\partial t} (\rho_w n \, dxdydz) \tag{I-2}$$

The fluid density and porosity will change when pressure changes occur in the elemental volume. The compressibility of water, β, is the rate of change in density with a corresponding change in pressure, P:

$$\beta dP = d\rho_w / \rho_w \tag{I-3}$$

In addition, changes in volume occur when pressure varies. Due to lateral constraining forces, changes in volume will primarily occur in the z direction. The aquifer compressibility, α, is:

$$\alpha dP = \frac{d(dz)}{dz} \tag{I-4}$$

Expansion and contraction of the aquifer changes porosity, but the volume of the matrix remains constant. If deformation is in the z axis only, then differentiation of the matrix volume with respect to time yields:

$$dzdn = (1-n)d(dz) \tag{I-5}$$

and

$$dn = \frac{(1-n)d(dz)}{dz} \tag{I-6}$$

The pressure, P, at some point in the aquifer is equal to $P_o + \rho_w gh$, where P_o is equal to atmospheric pressure (a constant), and h is the height of the column of water above that point. Thus, $dP = \rho_w gdh$, and substituting equations (I-3) and (I-4), respectively, into

the preceding equation yields the following equations:

$$d\rho_w = \rho_w \beta (\rho_w g dh) \tag{I-7}$$

and

$$d(dz) = -dz\alpha(\rho_w g dh) \tag{I-8}$$

Equation (I-5) can be rearranged by substituting the equivalent of d(dz) of Equation (I-8):

$$dn = (n-1)\alpha\rho_w g dh \tag{I-9}$$

The change of mass with respect to time (dx and dy are constant) yields another version of Equation (I-2) (carrying out the differentiation).

$$\frac{\partial M}{\partial t} = \{\rho_w n \frac{\partial (dz)}{\partial t} + \rho_w dz \frac{\partial n}{\partial t} + ndz \frac{\partial \rho_w}{\partial t}\} dxdy \tag{I-10}$$

Substitution of Equations (I-7) through (I-9) into Equation (I-10) with some algebraic manipulation yields:

$$\frac{\partial M}{\partial t} = (\alpha\rho_w g + n\beta\rho_w g)\ \rho_w dxdydz \frac{\partial h}{\partial t} \tag{I-11}$$

Set Equation (I-2) equal to Equation (I-11); where Equation (I-2) is net accumulation of material, and Equation (I-11) is the change in mass with time:

$$-\{\frac{\partial (q_x)}{\partial x} + \frac{\partial (q_y)}{\partial y} + \frac{\partial (q_z)}{\partial z}\}\ \rho_w dxdydz$$

$$(\alpha\rho_w g + n\beta\rho_w g)\rho_w\ dxdydz\ \partial h/_{\partial t} \tag{I-12}$$

From Darcy's Law:

$$q_x = -K \frac{\partial h}{\partial x} \tag{I-13}$$

$$q_y = -K \frac{\partial h}{\partial y} \tag{I-14}$$

and

$$q_z = -K \frac{\partial h}{\partial z} \tag{I-15}$$

Substituting Equations (I-13) through (I-15) into Equation (I-12) yields:

$$K \left(\frac{\partial^2 h}{\partial x^2} + \frac{\partial^2 h}{\partial y^2} + \frac{\partial^2 h}{\partial z^2} \right) = (\alpha \rho_w g + n\beta \rho_w g) \frac{\partial h}{\partial t} \tag{I-16}$$

which is the governing, three-dimensional flow equation for an isotropic, homogeneous confined aquifer. For two-dimensional flow with no vertical flow component and the storage coefficient, $S_c = m(\alpha \rho_w g + n\beta \rho_w g)$, and Transmissivity $T = Km$ where m is a constant saturated aquifer thickness; Equation (I-16) can be rearranged as follows:

$$\frac{\partial^2 h}{\partial x^2} + \frac{\partial^2 h}{\partial y^2} = \frac{S_c}{T} \frac{\partial h}{\partial t} \tag{I-17}$$

Another equation that is used when steady-state conditions prevail in a homogeneous porous media is the LaPlace equation:

$$\frac{\partial^2 h}{\partial x^2} + \frac{\partial^2 h}{\partial y^2} + \frac{\partial^2 h}{\partial z^2} = 0 \tag{I-18}$$

or

$$\nabla^2 h = 0 \tag{I-19}$$

APPENDIX II

PRICKETT-LONNQUIST MODEL

APPENDIX II

PRICKETT-LONNQUIST MODEL

Prickett and Lonnquist (1971) devised a finite difference model capable of handling transient, two-dimensional flow equation for homogeneous or nonhomogeneous, isotropic, non-leaky confined aquifer (Figure A.1). Also, Prickett and Lonnquist (1971) outlined other modifications to the model that are capable of solving phreatic aquifer behavior, leaky confined aquifer, confined aquifer goes to phreatic aquifer, and evaporation of groundwater.

The model requires certain input parameters, such as initial conditions of head at each node, and boundary conditions (if applicable), such as no flow or constant head. Additional input parameters include recharge, discharge, storage factor (storage coefficient x incremental area ($\Delta x \Delta y$)), and transmissivity in the x and y direction for each node. Parameter data and data array are also required.

Data array is simply the number of columns and the number of rows. The model is designed for a 50 x 50 array or less. The parameter input includes: the number

```
                                                                    IO
                                                                  NUMBER
C     ILLINOIS STATE WATER SURVEY                                
C     BASIC AQUIFER SIMULATION PROGRAM                            0001
C                                                                 0002
C                                                                 0003
C     DEFINITION OF VARIABLES                                     0004
C                                                                 0005
C     HO(I,J)-----HEADS AT START OF TIME                          0006
C               INCREMENT (I,J)                                   0007
C     H(I,J)------HEADS AT END OF TIME                            0008
C               INCREMENT (FT)                                    0009
C     SF1(I,J)----STORAGE FACTOR FOR                              0010
C               ARTESIAN CONDITIONS                               0011
C               (GAL/FT)                                          0012
C     Q(I,J)------CONSTANT WITHDRAWAL                             0013
C               RATES (GPD)                                       0014
C     T(I,J,1)----AQUIFER TRANSMISSIVITY                          0015
C               BETWEEN I,J AND I+1,J                             0016
C               (GAL/DAY/FT)                                      0017
C     T(I,J,2)----AQUIFER TRANSMISSIVITY                          0018
C               BETWEEN I,J AND I+1,J                             0019
C               (GAL/DAY/FT)                                      0020
C     AA,BB,CC,DD-COEFFICIENTS IN WATER                           0021
C               BALANCE EQUATIONS                                 0022
C     NR----------NO. OF ROWS IN MODEL                            0023
C     NC----------NO. OF COLUMNS IN MODEL                         0024
C     NSTEPS------NO. OF TIME INCREMENTS                          0025
C     DELTA-------TIME INCREMENTS (DAYS)                          0026
C     HH,SI,QQ,TT-DEFAULT VALUES                                  0027
C     I----------MODEL COLUMN NUMBER                              0028
C     J----------MODEL ROW NUMBER                                 0029
C                                                                 0030
C                                                                 0031
C                                                                 0032
C                                                                 0033
      DIMENSION H(50,50),HO(50,50),
     1SF1(50,50),Q(50,50),T(50,50,2),
     2B(50),G(50),DL(50,50)                                       0034
C                                                                 0035
C     TURN OFF UNDERFLOW TRAP                                     0036
C                                                                 0037
      CALL ERRSET(208,256,-1,1)                                   0038
C                                                                 0039
C     DEFINE INPUT AND OUTPUT DEVICE NUMBERS                      0040
C                                                                 0041
      INTEGER OUT                                                 0042
      IN=5                                                        0043
      OUT=6                                                       0044
C                                                                 0045
C     READ PARAMETER CARD AND                                     0046
C     DEFAULT VALUE CARD                                          0047
C                                                                 0048
      READ(IN,10)NSTEPS,DELTA,ERROR,
     INC,NR,TT,SI,HH,QQ                                           0049
10    FORMAT(I6,2F6.0/2I6,4F6.0)                                  0050
C                                                                 0051
C     FILL ARRAYS WITH DEFAULT VALUES                             0052
C                                                                 0053
      DO 20 I=1,NC                                                0054
      DO 20 J=1,NR                                                0055
      T(I,J,1)=TT                                                 0056
      T(I,J,2)=TT                                                 0057
      SF1(I,J)=SI                                                 0058
      H(I,J)=HH                                                   0059
      HO(I,J)=HH                                                  0060
20    Q(I,J)=QQ                                                   0061
C                                                                 0062
C     READ NODE CARDS                                             0063
C                                                                 0064
30    READ(IN,40,END=50)I,J,T(I,J,1),
     1T(I,J,2),SF1(I,J),H(I,J),Q(I,J)                             0065
40    FORMAT(2I3,2F6.0,2F4.0,1F6.0)                               0066
      GO TO 30                                                    0067
C                                                                 0068
C     START OF SIMULATION                                         0069
C                                                                 0070
50    TIME=0                                                      0071
      DO 420 ISTEP=1,NSTEPS                                       0072
      TIME=TIME+DELTA                                             0073
C                                                                 0074
C     PROJECT HEADS FOR NEXT                                      0075
C     TIME INCREMENT                                              0076
C                                                                 0077
      DO 70 I=1,NC                                                0078
      DO 70 J=1,NR                                                0079
      D=H(I,J)-HO(I,J)                                            0080
      HO(I,J)=H(I,J)                                              0081
      F=1.0                                                       0082
      IF(Q(I,J).EQ.0.0)GO TO 60                                   0083
      IF(ISTEP.GT.2)F=D/DL(I,J)                                   0084
      IF(F.GT.5)F=5.0                                             0085
      IF(F.LT.0.0)F=0.0                                           0086
60    DL(I,J)=D                                                   0087
70    H(I,J)=H(I,J)+D*F                                           0088
C                                                                 0089
```

```
                                                                    IO
                                                                  NUMBER
C     REFINE ESTIMATES OF HEADS BY IADI METHOD                    0090
C                                                                 0091
      ITER=0                                                      0092
80    E=0.0                                                       0093
      ITER=ITER+1                                                 0094
C                                                                 0095
C     COLUMN CALCULATIONS                                         0096
C                                                                 0097
      DO 190 I=1,NC                                               0098
      I=I                                                         0099
      IF(MOD(ISTEP+ITER,2).EQ.1) I=NC-I+1                         0100
      DO 170 J=1,NR                                               0101
C                                                                 0102
C     CALCULATE B AND G ARRAYS                                    0103
C                                                                 0104
      BB=SF1(I,J)/DELTA                                           0105
      DD=HO(I,J)*SF1(I,J)/DELTA-Q(I,J)                            0106
      AA=0.0                                                      0107
      CC=0.0                                                      0108
      IF(J-1)90,100,90                                            0109
90    AA=-T(I,J-1,1)                                              0110
      BB=BB+T(I,J-1,1)                                            0111
100   IF(J-NR)110,120,110                                         0112
110   CC=-T(I,J,1)                                                0113
      BB=BB+T(I,J,1)                                              0114
120   IF(I-1)130,140,130                                          0115
130   BB=BB+T(I-1,J,2)                                            0116
      DD=DD+H(I-1,J)*T(I-1,J,2)                                   0117
140   IF(I-NC)150,160,150                                         0118
150   BB=BB+T(I,J,2)                                              0119
      DD=DD+H(I+1,J)*T(I,J,2)                                     0120
160   W=BB-AA*B(J-1)                                              0121
      B(J)=CC/W                                                   0122
170   G(J)=(DD-AA*G(J-1))/W                                       0123
C                                                                 0124
C     RE-ESTIMATE HEADS                                           0125
C                                                                 0126
      E=E+ABS(H(I,NR)-G(NR))                                      0127
      H(I,NR)=G(NR)                                               0128
      N=NR-1                                                      0129
180   HA=G(N)-B(N)*H(I,N+1)                                       0130
      E=E+ABS(HA-H(I,N))                                          0131
      H(I,N)=HA                                                   0132
      N=N-1                                                       0133
      IF(N)190,190,180                                            0134
190   CONTINUE                                                    0135
C                                                                 0136
C     ROW CALCULATIONS                                            0137
C                                                                 0138
      DO 300 JJ=1,NR                                              0139
      J=JJ                                                        0140
      IF(MOD(ISTEP+ITER,2).EQ.1) J=NR-J+1                         0141
      DO 280 I=1,NC                                               0142
      BB=SF1(I,J)/DELTA                                           0143
      DD=HO(I,J)*SF1(I,J)/DELTA-Q(I,J)                            0144
      AA=0.0                                                      0145
      CC=0.0                                                      0146
      IF(J-1)200,210,200                                          0147
200   BB=BB+T(I,J-1,1)                                            0148
      DD=DD+H(I,J-1)*T(I,J-1,1)                                   0149
210   IF(J-NR)220,230,220                                         0150
220   DD=DD+H(I,J+1)*T(I,J,1)                                     0151
      BB=BB+T(I,J,1)                                              0152
230   IF(I-1)240,250,240                                          0153
240   BB=BB+T(I-1,J,2)                                            0154
      AA=-T(I-1,J,2)                                              0155
250   IF(I-NC)260,270,260                                         0156
260   BB=BB+T(I,J,2)                                              0157
      CC=-T(I,J,2)                                                0158
270   W=BB-AA*B(I-1)                                              0159
      B(I)=CC/W                                                   0160
280   G(I)=(DD-AA*G(I-1))/W                                       0161
C                                                                 0162
C     RE-ESTIMATE HEADS                                           0163
C                                                                 0164
      E=E+ABS(H(NC,J)-G(NC))                                      0165
      H(NC,J)=G(NC)                                               0166
      N=NC-1                                                      0167
290   HA=G(N)-B(N)*H(N+1,J)                                       0168
      E=E+ABS(H(N,J)-HA)                                          0169
      H(N,J)=HA                                                   0170
      N=N-1                                                       0171
      IF(N)300,300,290                                            0172
300   CONTINUE                                                    0173
      IF(E.GT.ERROR) GO TO 80                                     0174
C                                                                 0175
C     PRINT RESULTS                                               0176
C                                                                 0177
      WRITE(OUT,310)TIME,E,ITER                                   0178
310   FORMAT(16H2TIME=,F6.2///,E20.7,I5)                          0179
      DELTA=DELTA*1.2                                             0180
      DO 320 J=1,NR                                               0181
320   WRITE(OUT,330)J,(H(I,J),I=1,NC)                             0182
330   FORMAT(I5,5X,10F10.4/(12X10F10.4))                          0183
C                                                                 0184
      STOP                                                        0185
      END                                                         0186
```

Figure A.1. Prickett-Lonnquist Model for an isotropic, nonleaky, confined aquifer (After Prickett and Lonnquist, 1971).

of increments NSTEP, the time increments DELTA, and the ERROR value for closure. The model is designed for incremental time increases as depicted in Table A.1. For example, an NSTEP value of 10 which is equivalent to ISTEP value of 10 in Table A.1; time = ISTEP = 25.96 hours or 25.96 days for a DELTA value of 1 hour or 1 day. If one chooses to model to the exact time, line 184 can be deleted. NSTEP and DELTA would be specified, resulting in data output for head at a constant increment of time to the desired time.

The flow chart for the confined aquifer simulation model is shown in Figure A.2. The program basically consists of (1) variable explanation in lines 1 through 33; (2) parameter data stored, and data array filled with default values and node values in lines 34 through 72; (3) computation of data in lines 73 through 178; and (4) print out of results in lines 180 through 187.

Finally the preceding discussion is just a brief overview of the Prickett-Lonnquist model. For an in-depth explanation of the simulation model, the reader is referred to the original article put forth by Prickett and Lonnquist (1971).

Table A.1. ISTEP Function Values

ISTEP	ISTEP Function	ISTEP	ISTEP Function
1	1.00	26	567.37
2	2.20	27	681.84
3	3.64	28	819.21
4	5.37	29	984.05
5	7.44	30	1181.87
6	9.93	31	1419.24
7	12.92	32	1704.08
8	16.50	33	2045.90
9	20.80	34	2456.08
10	25.96	35	2948.29
11	32.15	36	3538.95
12	39.58	37	4247.74
13	48.50	38	5098.28
14	59.20	39	6118.93
15	72.03	40	7343.71
16	87.44	41	8813.45
17	105.93	42	10577.14
18	128.12	43	12693.57
19	154.74	44	15233.28
20	186.69	45	18280.93
21	225.02	46	21938.11
22	271.03	47	26326.73
23	326.23	48	31593.07
24	392.48	49	37912.68
25	471.98	50	45496.21

(after Prickett and Lonnquist, 1971)

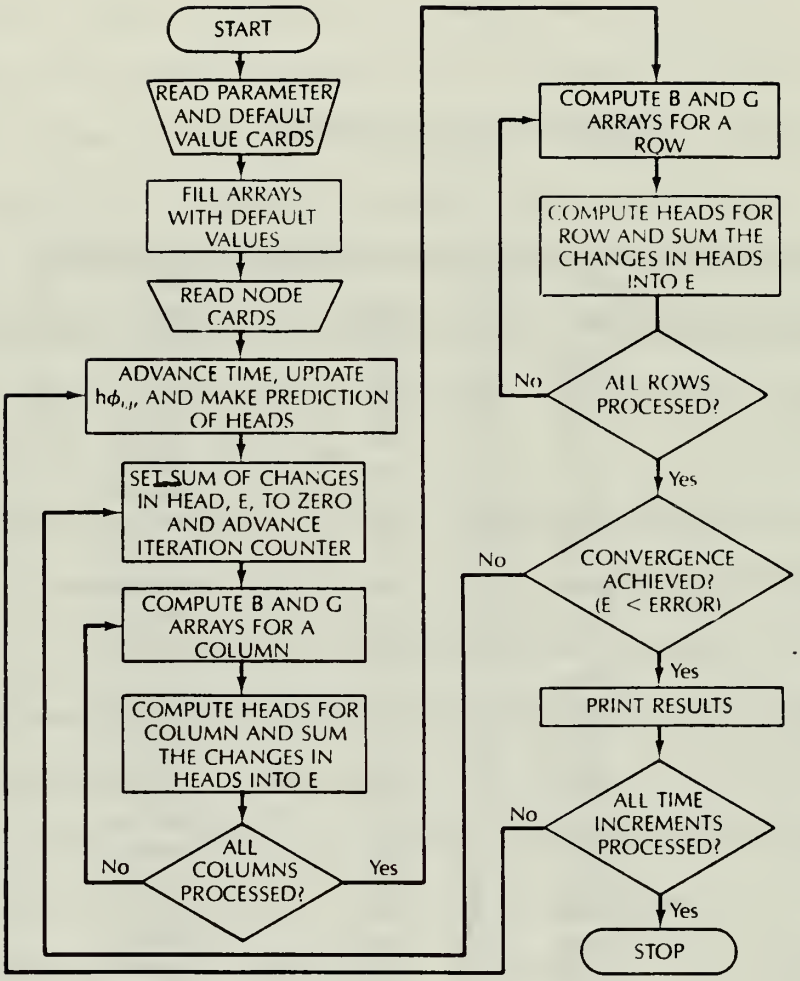

Figure A.2. Simplified flowchart of the Prickett-Lonnquist Model (After Prickett and Lonnquist, 1971).

APPENDIX III

LITHOLOGY AND STRUCTURE OF THE SIMPSON GROUP OUTCROP

APPENDIX III

LITHOLOGY AND STRUCTURE OF THE SIMPSON GROUP OUTCROP

Station 1. Location - NW¼ NW¼ NW¼ SW¼ of Sec. 6, T1S, R4E; on a ridge near a primitive trail. Detected basal conglomerate of the Pontotoc Group lying adjacent to a carbonate unit. Attitude of the carbonate unit is, N40°W strike with 30° SE dip. Broken specimens revealed a brown, coarse-crystalline dolomitic lime with some silica. Rocks weathered to a light-buff color, and contain numerous microfractures. The well-cemented conglomerate consists of lime cobbles and boulders.

Station 2. Location - SW¼ SW¼ SW¼ NW¼ of Sec. 6, T1S, R4E; in a ravine. Attitude is N60°W strike with 16° NE dip. Brown, sandy dolomite and lime with rounded and subrounded fine-grained quartz and chert particles. Shaley limes outcrop just south of this location on a east-trending ridge.

Station 3. Location - NW¼ NW¼ SW¼ NW¼ of Sec. 6, T1S, R4E. Resistant formation, thickness of approximately 12 feet, outcrops in a ravine. The bottom half of the section consists of a light tan (streaks of red) to a light brown (small amounts of silica) dolomitic limes.

The top half of the section contains light-brown, crystalline dolomite; and pinkish-colored, silica-cemented, fine to medium grained, subrounded to rounded quartz sand. Bedding planes of dolomitic limes are easily discerned. The attitude of beds strike N60°E with a N25°W dip. Two swallow shafts and one small sink hole were found in and along this ravine.

The outcrop was mapped with the use of aerial photographs, and then transferred to a topographic map. The dip of the beds in this outcrop area are extremely erratic, suggesting complex geologic structure.

APPENDIX IV

ESTIMATE OF DISCHARGE OF THE VENDOME WELL

APPENDIX IV

ESTIMATE OF DISCHARGE OF THE VENDOME WELL

Determination of the discharge from Vendome Well using the Mannings equation for open channel flow can be expressed as (Morris, 1972):

$$Q = VA = \frac{1.49\ R^{2/3}\ S^{1/2}\ A}{n'} \qquad \text{(IV.1)}$$

where Q = discharge from the well into an open channel (ft^3/sec),

V = average velocity (ft/sec),

n' = channel coefficient,

S = gradient of channel (ft/ft),

$R = A/P$ = hydraulic radius (ft),

A = area of channel (ft^2),

P = perimeter of channel (ft).

Given:

(1) V = average surface velocity = 3.3 ft/sec

(2) n' = .02, channel coefficient for concrete

(3) A = configuration of channel is rectangular

$= bh\ (44/12\ ft)(2/12\ ft) = .611\ ft^2$

(4) $R = bh/(b+h) = .61\ ft^2/(48/12)\ ft. = .153\ ft.$

Solving for $S^{1/2}$ yields,

$$S^{1/2} = \frac{n'V}{1.49\ R^{2/3}} = .155 \qquad \text{(IV.2)}$$

Then Q can be obtained by using Equation (IV.1)

$$Q = \frac{1.49\ A\ S^{1/2}\ A}{n'} = 2\ ft^3/sec.$$

or

$$Q = 472 \times 10^6 \text{ gallons/year.}$$